

Investigation of early endosomal sorting and budding

PhD Thesis

in partial fulfilment of the requirements for the degree
“**Doctor of Natural Sciences (Dr. rer. nat.)**”
in the Molecular Biology Program at the
Georg August University Göttingen, Faculty of Biology

submitted by
Sina-Victoria Barysch

born in
Wolfen, Germany

September 2009

I hereby declare that I prepared the PhD thesis “Investigation of early endosomal sorting and budding” on my own and with no other sources and aids than quoted.

Sina-Victoria Barysch

Publications

Parts of the work presented in this thesis are based on the following publications. I want to thank all co-authors and all people acknowledged therein for the successful collaboration.

U Geumann, **SV Barysch**, P Hoopmann, R Jahn, SO Rizzoli.

SNARE function is not involved in early endosome docking.

Mol Biol Cell, 2008 Dec;19(12):5327-37. Epub 2008 Oct 8.

SV Barysch, S Aggarwal, R Jahn, SO Rizzoli.

Sorting in early endosomes reveals connections to docking- and fusion-associated factors.

Proc Natl Acad Sci U S A, 2009 Jun 16;106(24):9697-702. Epub 2009 Jun 1.

SV Barysch, R Jahn, SO Rizzoli.

***In vitro* microscopy investigation of endosome dynamics.**

Nat Protoc, invited, manuscript in preparation.

Contents

Publications	V
Contents	VII
Abstract	XI
Abbreviations	XIII
List of Figures	XV
List of Tables	XVII
1 Introduction	1
1.1 Membrane Traffic	1
1.2 The Endocytic Pathway	3
1.2.1 Internalization: Different Modes of Endocytosis	3
1.2.2 Organelles in the Endocytic Pathway	6
1.3 Membrane Docking and Fusion	9
1.3.1 Docking machineries	9
1.3.2 SNARE Proteins as Mediators of Membrane Fusion	11
1.3.3 Early Endosome Docking and Fusion	13
1.4 Sorting and Membrane Budding	16
1.4.1 Vesicle Budding	17
1.4.2 Cargo Selection and Sorting	19
1.4.3 Early Endosome Sorting and Budding	21
1.5 Aims of this Work	23

2	Materials and Methods	25
2.1	Materials	25
2.1.1	Antibodies	25
2.1.2	Chemicals, Enzymes and Kits	27
2.1.3	Mammalian Cell Lines and Bacterial Strains	28
2.1.4	Recombinant Proteins and Peptides	30
2.1.5	DNA Constructs	30
2.2	Methods	30
2.2.1	Molecular Biology and Biochemical Standard methods	30
2.2.2	Protein Expression and Purification	33
2.2.3	Preparation of Rat Brain Cytosol	36
2.2.4	Cell Culture	37
2.2.5	Transient Transfection	38
2.2.6	Preparation of Postnuclear Supernatants	39
2.2.7	<i>In vitro</i> Endosomal Docking/Fusion and Sorting/Budding Assays	40
2.2.8	Endosomal Sorting/Budding Assays in Intact Cells	46
3	Results	49
3.1	An Assay for Early Endosomal Sorting	49
3.2	Verification of the Assay	51
3.2.1	The Assay is not Affected by De-Aggregation, Cargo Degradation or Organelle Leakage	51
3.2.2	Determination of Double Labeled Early Endosomes	52
3.2.3	Quantification of the Sorting Reaction	56
3.2.4	Endosomal Sorting of Different Cargoes	59
3.2.5	<i>In vitro</i> Sorting Results in the Formation of Small Transferrin-Containing Vesicles	62
3.3	Characterization of Early Endosomal Sorting and Budding	69
3.3.1	Basic Requirements of Endosomal Sorting and Budding	69

3.3.2	EEA1 and Rab Proteins Are Required for Early Endosomal Sorting	70
3.3.3	SNARE Disassembly but not SNARE Function is Required for Early Endosomal Sorting	71
3.3.4	Cholera Toxin Subunit B Sorting also Depends on EEA1 and NSF	75
3.4	Vesiculation and Maturation in Cargo Sorting	78
3.5	Analysis of Early Endosomal Sorting in Intact Cells	81
3.6	The Role of Rab Proteins in Sorting and Budding	85
3.6.1	Function of Rab GTPases Studied <i>in vivo</i>	85
3.6.2	Function of Rab GTPases Studied <i>in vitro</i>	88
4	Discussion	91
4.1	A Novel <i>in vitro</i> Sorting Assay	91
4.2	Docking and Fusion Factors in Endosomal Sorting	96
4.2.1	The Role of SNARE-disassembly in Sorting and Budding	96
4.2.2	The Role of PI(3)-kinase, Rab Proteins and EEA1 in Sorting and Budding	98
4.2.3	Possible Links Between Budding and Fusion	102
4.3	Factors Required for Budding of Transferrin and Cholera Toxin	103
4.4	The Cell-based Sorting Assay	105
4.5	Conclusions	106
5	Summary and Outlook	107
	Bibliography	111
	Acknowledgements	145
	Curriculum Vitae	147

Abstract

Early endosomes constitute a major sorting platform of eukaryotic cells. They receive endocytic carrier vesicles from the plasma membrane and trafficking vesicles from the Golgi complex and distribute both membrane-bound and soluble cargo, via vesicular carriers, to different intracellular destinations. Thus, the elementary steps underlying endosome function are fusion with incoming vesicles, cargo sorting and budding of new vesicles. While endosomal fusion is well understood, sorting is less characterized; the two processes are generally thought to be effected by different, unrelated machineries. I developed a novel cell free assay for sorting and budding from early endosomes, by taking advantage of their ability to segregate different cargoes (such as transferrin, cholera toxin subunit B, and low-density-lipoprotein, LDL). Cargo separation required both carrier vesicle formation and active maturation of the endosomes. Sorting and budding were insensitive to reagents perturbing clathrin coats, COPI coats, dynamin, and actin, but were inhibited by anti-retromer subunit antibodies. In addition, the process required the endosomal proteins Rab5, phosphatidylinositol-3-phosphate, and, surprisingly, the docking factor EEA1. It also required the function of the *N*-ethylmaleimide-sensitive factor (NSF), a well-known fusion co-factor, while it did not depend on preceding fusion of endosomes. I therefore conclude that fusion, docking and sorting/budding, although serving different purposes, are strongly interconnected at the molecular level.

Abbreviations

ab	antibody
ABTS	2,2'-Azino-bis(3-ethylbenzothiazoline-6-sulfonic acid)
BAPTA	1,2-bis(o-aminophenoxy)ethane-N,N,N',N'-tetraacetic acid
BHK	baby hamster kidney
BSA	bovine serum albumine
DMSO	dimethyl sulfoxide
DNA	deoxyribonucleic acid
DTT	dithiothreitol
<i>E.coli</i>	<i>Escherichia coli</i>
EDTA	ethylene diamine tetraacetic acid
EEA1	early endosomal autoantigen 1
EGTA	ethylene glycol tetraacetic acid
FCCP	carbonyl cyanide 4-(trifluoromethoxy)phenylhydrazone
FPLC	fast protein liquid chromatography
FYVE	Fab1p, YOTB, Vac1p, EEA1 domain
GDI	GDP-dissociation inhibitor
GEF	GDP-exchange factor
GMP-P(NH)P	guanosine-5'-[β , γ -imido]triphosphate
GTP γ S	guanosine 5'-[γ -thio]triphosphate
HEPES	4-(2-Hydroxyethyl)piperazine-1-ethanesulfonic acid
HPLC	high pressure/performance liquid chromatography
HRP	horseradish peroxidase
IPTG	isopropyl β -D-thiogalactopyranoside
kDa	kilo-dalton

LDL	low-density lipoprotein
LY 294,002	2-(4-morpholinyl)-8-phenylchromone
NEM	<i>N</i> -Ethylmaleimide
NSF	NEM-sensitive factor
PBS	phosphate buffered saline
PFA	paraformaldehyde
PI3K/PI(3)K	phosphatidyl-inositol-(3)-kinase
PI3P/PI(3)P	phosphatidyl-inositol-(3)-phosphate
PMSF	phenylmethanesulfonyl fluoride
PNS	post-nuclear supernatant
Rab	Ras-like protein in brain or Ras-abundant in brain
rpm	rotations per minute
RT	room temperature
SDS	sodium dodecyl sulfate
SEM	standard error mean
SNAP	soluble NSF attachment protein
SNAP-25	synaptosomal-associated protein of 25 kDa
SNARE	soluble NSF attachment protein receptor
STED	stimulated emission depletion
Sx	syntaxin
Syb	synaptobrevin
Tf/Tfn	transferrin
TGN	<i>trans</i> -Golgi network
Tris	tris(hydroxymethyl)aminomethane
u	units (enzyme activity)
v/v	volume/volume
VAMP	vesicle-associated membrane protein
W-7	N-(6-aminohexyl)-5-chloro-1-naphthalenesulfonamide
w/v	weight/volume
wt	wildtype

List of Figures

1.1	Membrane traffic in eukaryotic cells	2
1.2	The early endosomal docking machinery	15
1.3	Homotypic early endosomal fusion assay	16
3.1	Trafficking of transferrin and LDL in PC12 cells	50
3.2	The microscopic assay <i>in vitro</i> for early endosomal sorting	51
3.3	The <i>in vitro</i> sorting assay is not affected by de-aggregation	52
3.4	The <i>in vitro</i> sorting assay is not affected by cargo degradation or leakage	53
3.5	Distances of transferrin- and LDL-containing endosomes	54
3.6	Distances for different types of beads	55
3.7	Docking and fusion in early endosomes	57
3.8	Basic characterization of the sorting reaction	58
3.9	Endosomal sorting of different endocytic markers	61
3.10	Fusion of early endosomes containing different endocytic markers	61
3.11	Dextran-, transferrin- and cholera toxin-containing organelles become dimmer with sorting and budding.	62
3.12	Size analysis of labeled endosomes using STED microscopy	65
3.13	Size analysis of labeled endosomes using electron microscopy	66
3.14	Budding investigated by a biochemical assay	67
3.15	Formation of small transferrin-containing vesicles visualized by time- lapse imaging	68
3.16	Basic requirements for endosomal sorting	69
3.17	Wortmannin and 3-Methyladenine inhibit of early endosomal sorting.	71
3.18	Docking factors are required for early endosomal sorting	72

3.19 Fusion factors, but not the fusion step itself, are essential for sorting in early endosomes.	74
3.20 The SNARE composition changes in transferrin-containing endosomes	75
3.21 Fusion and docking factors are also required for the segregation of cholera toxin and LDL.	76
3.22 Dynasore inhibits synaptic vesicle recycling.	79
3.23 Carrier vesicle formation and endosome maturation in cargo sorting. .	80
3.24 Transferrin-, LDL- and cholera toxin recycling <i>in vivo</i>	82
3.25 Use of COS-7 cells for cargo sorting <i>in vivo</i>	83
3.26 Identification of double labeled endosomes in COS-7 cells	84
3.27 Cargo sorting in COS-7 cells <i>in vivo</i>	86
3.28 Rab5 is required for cargo sorting in intact cells	87
3.29 Rab5 is required for cargo sorting <i>in vitro</i>	89
4.1 Schematic on endosomal fusion and sorting	95

List of Tables

2.1	Antibodies used in this study	26
2.2	Enzymes used in this study	28
2.3	Commercial kits used in this study	29
2.4	Mammalian cell lines and bacterial strains used in this study	29
2.5	DNA constructs used in this study	31

“It is theory that decides what can
be observed.”

(Albert Einstein)

1

Introduction

1.1 Membrane Traffic

All eukaryotic cells are comprised of different organelles, which exhibit relatively defined localizations within the cell and serve specific functions. Within the secretory pathway, the Endoplasmic Reticulum (ER), for example, is responsible for protein biosynthesis and quality control; the Golgi apparatus deals with posttranslationally modifying and processing the proteins, as well as their proper sorting to different target destinations. The endosomes and lysosomes of the endocytic pathway are required for sorting and processing of molecules that were internalized by the cell.

Despite their functional separation, which demands a specific lipid and protein composition, the organelles from the secretory and endocytic pathway communicate with each other and exchange material extensively (see arrows in **Figure 1.1**). The work by (Palade, 1975) led to the hypothesis that this exchange and transport between organelles is mediated by small trafficking vesicles, which bud from the donor compartment, travel to the correct acceptor compartment, and then dock and fuse with it. These processes are mediated by specific soluble and membrane resident proteins and are subject to high degrees of regulation. First, budding of trafficking vesicles requires the selective incorporation of cargo into the newly forming vesicle (cargo sorting) and is mediated by coat proteins (Bonifacino and Lippincott-Schwartz, 2003; Kirchhausen, 2000). The coat components are recruited from the cytosol to the membranes, form large assemblies and deform flat membrane patches into round

buds, finally leading to the release of vesicles. Second, fusion with the acceptor compartment requires the function of so-called SNARE (soluble *N*-ethylmaleimide-sensitive factor attachment protein receptor) proteins, which are present on the two opposing membranes, interact with each other and bring the two membranes in close apposition, finally leading to their lipid- and content-mixing (Jahn et al., 2003; Jahn and Scheller, 2006).

The concept of membrane trafficking, with the basic reactions of docking/fusion and sorting/budding, was the subject of several detailed review articles in the past years (Bonifacino and Glick, 2004; Pfeffer, 2007) and will be discussed in greater detail in the sections 1.3 and 1.4, with a focus on endosomal trafficking.

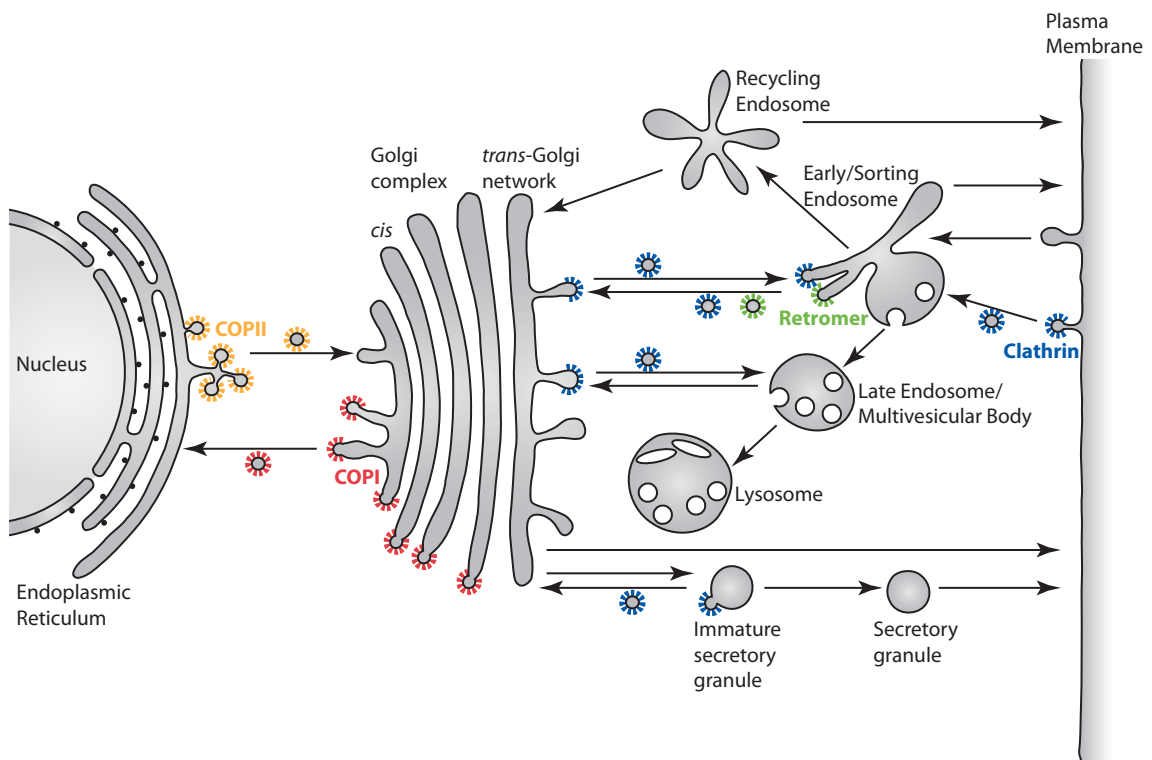


Figure 1.1: The key events in membrane traffic are cargo sorting, budding of trafficking vesicles from a donor compartment, transport, and fusion of the vesicles with the acceptor compartment.

1.2 The Endocytic Pathway

The endocytic pathway processes material that is taken up by the cell via different modes of endocytosis. It involves a variety of different organelles, such as early (or sorting) endosomes, recycling endosomes, multivesicular bodies (MVBs, or late endosomes) and lysosomes. They are in constant exchange with each other and additionally interact with the *trans*-Golgi network (TGN) as one part of the secretory pathway (Clague, 1998; Maxfield and McGraw, 2004).

1.2.1 Internalization: Different Modes of Endocytosis

Cells are shielded from the extracellular environment by the plasma membrane, which represents an efficient protective barrier for the chemically distinct cytoplasm within the cell. Small molecules such as ions, sugars or amino acids can cross this membrane mainly by using specialized transporters or channels. Macromolecules on the other hand need to be engulfed by the plasma membrane, leading to the formation of carrier vesicles that bud off from the inner side of the membrane. This process is referred to as endocytosis and is essential for the uptake of nutrients, maintenance of cellular homeostasis, signalling, intercellular communication, development, neurotransmission and immune responses, while being also used by different pathogens to enter into the host cells. Several modes of endocytosis have been described in the past (Conner and Schmid, 2003; Maxfield and McGraw, 2004), including clathrin-mediated endocytosis, caveolae-mediated endocytosis, macropinocytosis and phagocytosis.

Clathrin-Mediated Endocytosis

The best characterized internalization mode is the clathrin-mediated endocytosis (CME), which occurs constitutively in all mammalian cells [reviewed in detail in Kirchhausen (2000), McMahon and Mills (2004) and Ungewickell and Hinrichsen (2007)]. It carries out the continuous uptake of essential nutrients, such as the iron-

bound transferrin (Tfn) or the cholesterol-bound low-density lipoprotein (LDL), as well as the uptake of several growth hormones, such as the epidermal growth factor (EGF). These ligands bind to their receptors (the Tfn-, LDL- or EGF-receptor, respectively), which triggers a conformational change in their cytosolic part and thereby leads to the sequential recruitment of several factors, such as AP2, clathrin, dynamin and synaptojanin.

AP2 is a “classical” clathrin adaptor, which consists of four subunits that link the cargo to clathrin. With its different subunits it can simultaneously bind to special recognition motifs on the cargo receptor, to the plasma membrane-specific lipid PI(4,5)P₂ (and sometimes also PI(3,4,5)P₃), as well as to the coat protein clathrin. Another adaptor, the monomeric AP180, is not able to bind cargo. However, it seems to play an important role in neuronal endocytosis of synaptic vesicles, since its disruption leads to strong phenotypes in synaptic vesicle recycling ([Morgan et al., 1999](#); [Nonet et al., 1999](#); [Zhang et al., 1998](#)). The two adaptor molecules promote the recruitment and self-assembly of clathrin, which forms a triskelion shape that is composed of three clathrin heavy chains and three light chains. Upon interaction of the triskelia they form a polyhedral lattice which surrounds the forming vesicle. Both adaptors and clathrin are necessary but not sufficient to drive vesicle budding at the plasma membrane. In addition, a large number of accessory proteins have been described for CME, for example Eps15, epsin, endophilin and amphiphysin are proteins that can bind clathrin, dynamin (see below) and/or the lipid PI(4,5)P₂. They create membrane curvature in the newly forming vesicle and can partially accelerate the clathrin assembly. However, their exact spatial and temporal recruitment in CME is still under discussion, at least for several of the components ([Kirchhausen, 2000](#); [McMahon and Mills, 2004](#); [Ungewickell and Hinrichsen, 2007](#)). The protein that mediates the final budding step is the GTPase dynamin. As a clathrin-coated vesicle invaginates, dynamin forms a spiral around its neck. GTP-hydrolysis triggers a conformational change in dynamin, which leads to either constriction ([Sweitzer and Hinshaw, 1998](#)), helical expansion ([Stowell et al., 1999](#)) or twisting ([Roux et al., 2006](#)) of the neck, ultimately causing the vesicle to pinch off

from the donor membrane. Finally, the phosphatase synaptojanin together with auxilin and Hsc70 mediate the uncoating of the vesicle ([Rapoport et al., 2008](#)).

Caveolae-Mediated Endocytosis

Another entry mode into the cell uses caveolae, which are morphologically defined plasma membrane invagination that have a characteristic flask shape. In contrast to the clathrin-mediated endocytosis, they contain no obvious coat. Caveolae define cholesterol and sphingolipid-rich microdomains of the plasma membrane (also termed lipid rafts), in which different signalling molecules and membrane transporters are concentrated. The structure and shape of caveolae is provided by the protein caveolin, which exists in three different isoforms. Caveolin binds to cholesterol, inserts as a loop into the inner leaflet of the plasma membrane and self-associates, thereby stabilizing the invagination ([Lajoie et al., 2009](#); [Parton and Simons, 2007](#)). As in clathrin-mediated endocytosis, caveolae use dynamin for budding from the plasma membrane ([Henley et al., 1998](#); [Yao et al., 2005](#)). The resulting vesicles are then transported to the early endosome or to the so-called caveosome, a distinct organelle that has been described by Ari Helenius and coworkers ([Pelkmans et al., 2001](#)). In addition to their prominent role in signalling events, caveolae are exploited by viruses such as the simian virus 40 ([Norkin and Anderson, 1996](#)). Furthermore, the bacterial toxins cholera toxin and shiga toxin use this pathway as an entry into the cell [reviewed in [Pelkmans and Helenius \(2002\)](#)].

Other Modes of Endocytosis

Apart from clathrin- and caveolae-mediated endocytosis, there are other entries into the cell. Macropinocytosis (“cell-drinking”) is an endocytosis model which is accompanied by membrane ruffling. Fluid-phase markers such as dextran, horseradish-peroxidase (HRP) or other macromolecules which are functionally irrelevant to the cell can be taken up by this pathway, even though they may also enter the cell by the other above mentioned endocytosis pathways. Recent evidence suggests that

macropinocytosis can be triggered by the activation of the small GTPases Arf6 and Ras, or the kinase Src (Donaldson et al., 2009). Phagocytosis (“cell-eating”) is the process by which cells ingest large objects, such as bacteria, viruses or apoptotic cells. This pathway occurs mainly in specialized cells of the immune system.

1.2.2 Organelles in the Endocytic Pathway

After the uptake of several macromolecules by the different modes of endocytosis, these compounds are present in small vesicles inside the cell and are further processed within the endocytic pathways. There, the early endosome plays a central role: it is responsible for distributing the different macromolecules to other organelles of the endocytic and secretory pathway, such as the recycling endosome, multivesicular body/late endosome, as well as the *trans*-Golgi network.

Early Endosomes

Early endosomes are sorting stations and represent the first endocytic compartment on which the internalized molecules from almost all above mentioned endocytosis pathways converge. Depending on the cell type, these incoming vesicles fuse with the early endosomes a few minutes after internalization. Furthermore, they receive carrier vesicles from the Golgi complex. Initially, early endosomes have been described by Geuze et al. (1983) as the “compartment for the uncoupling of receptor and ligand” (CURL). This is due to the fact that at their acidic luminal pH (pH 6.0), internalized ligands dissociate from their receptors and are sorted and distributed separately to different destinations within the cell. Outgoing trafficking pathways include (a) direct and rapid recycling of transferrin and of receptors (e.g. those of Tf, LDL and EGF) to the plasma membrane by means of small vesicles, (b) transport of elongated tubulo-vesicular structures to the microtubule organizing center where they form a separate compartment, the recycling endosome, (c) delivery of vesicles to the Golgi apparatus (e.g. the viruses and toxins that are taken up by caveolae), and finally (d) maturation of early endosomes into multivesicu-

lar bodies/late endosomes that fuse with lysosomes as the final destination (e.g. LDL and EGF) [reviewed in [Maxfield and McGraw \(2004\)](#)]. In different cell types, receptors and other membrane proteins may also be targeted into specialized post-endosomal vesicles, e.g. synaptic vesicles in neuronal cells ([Faundez et al., 1998](#)), transcytotic vesicles in epithelial cells ([Mostov, 1993](#)), GLUT4 vesicles in adipocytes ([Karylowski et al., 2004](#)) and MHCII-containing vesicles in antigen-presenting cells ([Brachet et al., 1999](#)). Therefore, early endosomes are highly dynamic organelles which constantly undergo fusion, sorting and budding.

Due to this high membrane turnover it is a challenge to maintain the identity and integrity of the organelle. It is believed that this is achieved by several early endosomal factors, including the lipid phosphatidyl-inositol-(3)-phosphate (PI(3)P), the small GTPase Rab5 and the docking factor early endosomal autoantigen 1 (EEA1). These molecules will be discussed in the following section.

Recycling Endosomes

Apart from a fast recycling route, which connects the early endosomes directly with the plasma membrane via small trafficking vesicles, receptors can also be recycled via a slow pathway. This includes the recycling endosomes, organelles which are localized to the pericentriolar region in the cell. They are usually less acidic (pH 6.5) than the sorting endosomes (pH 6.0). While direct recycling takes only a few minutes, depending on the cell type, the half time for the indirect recycling via the recycling endosome is proposed to be approximately 14 min ([Maxfield and McGraw, 2004](#)). However, as it is experimentally difficult to distinguish between the two recycling pathways, it is not clear to which amount these two routes are used and most likely dependent on the cell type, as well as on the nature of the molecules that need to be recycled (membrane proteins, soluble proteins and lipids). Apart from a large amount of transferrin receptors, which seem to recycle steadily via the slow pathway, the small GTPases Rab4 and Rab11 are enriched in the recycling endosome and thus serve as markers for this organelle ([Clague, 1998](#)).

Late Endosomes/Multivesicular Bodies and Lysosomes

Late endosomes or multivesicular bodies (MVBs) are part of the degradative pathway. Soluble cargo such as LDL and EGF, as well as membrane proteins that are to be degraded can be found in MVBs before they fuse with the lysosome, the final degradative organelle. The internalized membrane proteins are sorted into microdomains on the MVBs, which are then invaginated as internal vesicles into the lumen of the MVB (from where the name multivesicular body is derived). Upon fusion with the lysosome these intraluminal vesicles are degraded by hydrolases. Both organelles of the degradative pathway have an acidic lumen (pH 5.0-6.0 for MVBs and 5.0-5.5 for lysosomes) and their identity is determined by Rab7 and Rab9.

The relationship between early and late endosomes is controversial, with two main views being proposed: (a) formation of endosomal carrier vesicles (ECVs) and (b) endosome maturation. The first model the early endosome would represent a relatively stable organelle which is maintained by a balance of incoming and outgoing material. The second model of endosome maturation has been favored over the past years. Here, early endosomes are formed *de novo* from incoming vesicles, while MVBs represent the residue of the early endosomes once all budding pathways (to the TGN or the plasma membrane) have been exhausted ([Clague, 1998](#)).

Trafficking in the endocytic pathway and delivery of material to the different organelles mentioned above is extremely efficient and occurs with almost no errors. This can only be achieved by regulating the selection of different cargo molecules, as well as efficiently recognizing the “correct” target compartment, which may be mediated by different docking/tethering and fusion factors.

1.3 Membrane Docking and Fusion

Membrane fusion occurs when two separate lipid membranes merge into a single continuous bilayer. The molecular machinery that mediates membrane fusion consists of a large variety of proteins, which mediate (a) the initial recognition of the two membranes (docking) and (b) the final lipid- and content-mixing (fusion). Despite the diversity of involved proteins, fusion reactions in eukaryotic cells share many common features, with a clear requirement for structurally distinct docking/tethering factors, Rab proteins and SNARE proteins. These proteins are described in more detail in this section, both in general terms, and in early endosomal trafficking.

1.3.1 Docking machineries

Docking or Tethering Factors

Two groups of docking or tethering factors can be distinguished, (a) large multi-subunit complexes and (b) long coiled-coil proteins. For the first group, eight large and conserved complexes have been proposed to have roles in vesicle tethering at distinct trafficking steps [summarized in [Cai et al. \(2007\)](#); [Markgraf et al. \(2007\)](#); [Whyte and Munro \(2002\)](#)]. Within the secretory pathway the exocyst complex mediates exocytosis, while the GARP, COG and TRAPP II complexes act as tethering factors at the Golgi apparatus in the retrograde intra Golgi and endosome-to-Golgi transport steps. Dsl1 functions in the retrograde Golgi-to-ER trafficking and TRAPP I mediates tethering in the anterograde ER-to-Golgi transport. Two class C Vps complexes, the HOPS and the CORVET complex, function in the endocytic pathway at endosomes and they seem to be able to undergo interconversion ([Peplowska et al., 2007](#)). The second group of docking/tethering factors has the potential to form homodimeric (or heterodimeric) coiled-coils with lengths up to several times the diameter of the vesicle. Crystallographic studies of the early endosomal autoantigen 1 (EEA1) ([Christoforidis et al., 1999a](#); [Simonsen et al., 1999](#)) suggest that this is indeed the case ([Dumas et al., 2001](#)). The same is true for another early

endosomal factor, Rabenosyn-5, and the Golgi tethering factors “golgins”, such as GM130, golgin-45, p115 (Barr and Short, 2003; Sonnichsen et al., 1998) or GCC185 (Burguete et al., 2008). Therefore, a model has been proposed in which the large coiled-coil proteins are anchored at one end to a membrane, while the other end “searches” the surrounding space for passing vesicles, a model which, however, remains to be confirmed.

The docking/tethering factors may perform their function independently, or through interactions with Rab proteins. For the long coiled-coil proteins such interactions appear to be a crucial recognition and targeting mechanism, while they seem less important for the different multi-subunit complexes, of which only the two TRAPP complexes and Dsl1 interact with Rab proteins.

Rab Proteins

Rab proteins constitute the largest family of monomeric small GTPases. While the yeast *Saccharomyces cerevisiae* has eleven Rab proteins (Ypt proteins), humans express at least 60 different isoforms (Bock et al., 2001). They contain a prenyl group (a lipid anchor) which allows them to bind to membranes. Several studies have suggested that Rab proteins are distributed to distinct intracellular compartments and regulate transport between organelles. Apart from vesicle docking, Rabs exhibit pleiotropic functions, which involve maintenance of organelle identity, vesicle budding, vesicle uncoating and vesicle motility through interactions with the cytoskeleton (Stenmark, 2009; Zerial and McBride, 2001). This functional diversity led to the hypothesis that Rab proteins are localized in distinct domains on their respective membranes (Gruenberg, 2001; Miaczynska and Zerial, 2002).

As in other small GTPases, the regulatory principle of Rab proteins lies in their ability to function as molecular switches that oscillate between GTP- and GDP-bound conformations. Even though the GTP-bound form represents the “active” state and the GDP-bound form the “inactive” one, the most important feature is their ability to cycle regularly between both states. This cycle imposes temporal and spatial regulation to membrane transport, in which the Rab proteins act like

timers, depending on the (intrinsic or catalyzed) rates of nucleotide exchange and hydrolysis. A guanine nucleotide exchange factor (GEF), which is present in the target membrane, catalyzes the conversion from GDP-bound to GTP-bound forms. It thereby activates the Rab protein, allowing it to interact with other proteins and exert different effects. The GTP hydrolysis is catalyzed by a GTPase-activating protein (GAP), leading to the inactivation of the Rab protein. Subsequently, the GDP dissociation inhibitor (GDI) binds the prenyl groups of the inactive, GDP-bound form of the Rab protein and thereby inhibits its reactivation [reviewed in [Stenmark \(2009\)](#)].

In each trafficking step, Rab proteins transduce various functions in their GTP-bound form. In this activated state, they are able to interact with different membrane-bound proteins and recruit soluble cytosolic factors which act as “Rab effectors”. Such interactions occur for example with the docking/tethering factors described in the previous section, as well as the fusion-mediating SNARE proteins (next section). Thus, Rab proteins may be seen as a molecular link between the docking and fusion machineries.

1.3.2 SNARE Proteins as Mediators of Membrane Fusion

The step that follows the docking of two membranes is their fusion, which is mediated by soluble *N*-ethylmaleimide-sensitive factor (NSF) attachment receptors (SNAREs). It is believed that special sets of SNAREs (“cognate SNAREs”) mediate distinct fusion events, despite the fact that many more other SNAREs (“non-cognate SNAREs”) may be present on the same organelle ([Bethani et al., 2007, 2009](#)).

SNARE Structure and Classification

SNAREs are a superfamily of small proteins, with around 100-300 amino acids in length, and consist of 25 known members in yeast and around 36 distinct isoforms in mammalian cells ([Bock et al., 2001](#)). They represent a highly conserved class of proteins that are comprised of several domains ([Kloepper et al., 2007, 2008](#)). One

hallmark of this conservation is the so-called SNARE motif, a sequence stretch of 60-70 amino acids in length, which defines all members of the family. It arranges in eight amphiphatic heptad repeats, which are prone to form coiled coil structures. At the C-terminus, adjacent to the SNARE motif, the majority of the SNAREs contain a hydrophobic transmembrane region. Those SNAREs lacking the transmembrane domain possess hydrophobic post-translational modifications for membrane binding instead. Additionally, many SNAREs contain independently folded domains which are positioned at the N-terminus, adjacent to the SNARE motif, and which have been used as a criterion for further classifications ([Jahn and Scheller, 2006](#)).

Initially, SNARE proteins were divided into two subclasses, depending on their compartment of residence: v-SNAREs (present on the vesicles) and t-SNAREs (present on the target membrane) ([Sollner et al., 1993](#)). However, it became clear that this classification cannot be applied to fusion events of two organelles of the same kind (homotypic fusion). The current, more precise, classification therefore takes structural features of the SNARE proteins into account. The structures of the neuronal ([Stein et al., 2009](#); [Sutton et al., 1998](#)), the late endosomal ([Antonin et al., 2002](#)), the early endosomal ([Zwilling et al., 2007](#)) and the yeast plasma membrane ([Strop et al., 2008](#)) SNARE complexes revealed a high degree of conservation and showed that each complex consists of a twisted bundle of four helices, each one contributed by a SNARE motif. Along the center of the SNARE complex, these four helices interact with each other in 16 positions, mainly via hydrophobic interactions. One special position in the center of the complex is the so-called “0”-layer, in which each SNARE motif contains either a glutamine (Q) or an arginine (R) residue. Accordingly, the contributing SNARE motifs are classified into Qa-, Qb-, Qc- and R-SNAREs ([Fasshauer et al., 1998](#); [Kloepper et al., 2007](#)).

SNARE-Mediated Fusion: The Zippering Hypothesis

One prerequisite for fusion is the existence of at least one transmembrane-domain-containing SNARE on each of the opposing membranes. Assembly of the SNARE complex starts at the N-terminus of the SNARE motifs and then proceeds in a

zipper-like fashion towards the C-terminus (Hanson et al., 1997). This part represents the formation of the so-called *trans*-SNARE complex, in which the SNAREs are still present on opposing membranes. The mechanical force that is exerted on the membranes by its formation is believed to provide the necessary energy for lipid mixing and fusion (Jahn and Scheller, 2006). After fusion, the assembled SNARE complexes are present on the newly united membrane, in the so-called *cis*-conformation. *Cis*-SNARE complexes are fusion incompetent, and their disassembly is crucial for the re-use of free, reactive SNARE molecules. The disassembly is mediated by the enzymatic activity of NSF, a hexameric AAA-ATPase (Block et al., 1988), together with its co-factor α -SNAP.

1.3.3 Early Endosome Docking and Fusion

In recent years, the sequential recruitment of protein complexes that mediate early endosomal docking and fusion has been thoroughly described. One crucial factor is the small GTPase Rab5 whose disruption has a great impact on the fusion rate of early endosomes. For example, the mutant variant Rab5 (Q79L) stimulates endosome fusion *in vitro* and leads to the formation of large endosomes (Barbieri et al., 1996), while Rab5 inactivation by the mutant S34N inhibits fusion (Stenmark et al., 1994). Furthermore, the inactivation of Rab proteins in general (and thus their removal from the membrane) via addition of recombinant Rab-GDI leads to a decreased fusion activity (Ullrich et al., 1994).

Rab5 is activated and recruited to the early endosomal membrane by Rabex-5, its GEF (Delprato et al., 2004; Horiuchi et al., 1997), where it activates a feedback-loop by recruiting one of its effectors, Rabaptin-5 (Stenmark et al., 1995). This factor in return assists Rabex-5, thereby leading to a further increased concentration of Rab-5 on the endosomal membrane (Lippe et al., 2001). Removal of Rabaptin-5 from the endosomal membrane thus leads to a decreased fusion rate, while overexpression leads to an activation (Stenmark et al., 1995). Apart from Rabaptin-5, the class III phosphatidylinositol-(3)-kinase (PI3K) Vps34 represents another prominent Rab5 effector, which is responsible for creating PI(3)-phosphate

(Christoforidis et al., 1999b). This increase in PI(3)P concentration leads to the recruitment of other downstream effectors such as the long coiled coil proteins Rabenosyn-5 (Nielsen et al., 2000), Rabankyrin-5 (Schnatwinkel et al., 2004) and EEA1 (Stenmark et al., 1996), which all bind to PI(3)P via their special FYVE domain (schematic representation in **Figure 1.2**).

Of these effectors, EEA1 has been the best studied one; it is a known endosomal docking factor (Christoforidis et al., 1999a) which has two binding sites for Rab5 and one for PI(3)P (Lawe et al., 2002). Yet, it is not entirely clear which of those domains are required for the docking function: the PI(3)P-binding FYVE domain alone is not sufficient to localize it correctly to the early endosomes, but it needs the Rab5-binding domain and a part of the coiled coil domain (Stenmark et al., 1996). On the other hand, EEA1 can also bind to the early endosomal membrane if the Rab5-binding site is mutated (Lawe et al., 2002).

Apart from Rab5 and its effectors, early endosomes contain a large variety of different SNAREs (Bethani et al., 2007), which is probably due to the fact that they receive material from many different endocytosis routes as well as from the TGN. However, using functional endosome fusion assays as well as reconstitution in liposomes (artificial vesicles), it has been established that only a distinct set of SNAREs, syntaxin 13, syntaxin 6, vti1a and VAMP4, mediates early endosome fusion (Brandhorst et al., 2006; Zwilling et al., 2007). These “cognate” SNAREs were shown to be enriched in the fusion site while the “non-cognate” ones are excluded (Bethani et al., 2007).

The endosomal docking machinery seems to be interconnected with the fusion machinery: microdomains have been identified which include EEA1, Rab5, NSF and also the early endosomal SNAREs syntaxin 13 (McBride et al., 1999) or syntaxin 6 (Mills et al., 2001; Simonsen et al., 1999). Further evidence came from the observation that a knock-down of the endosomal SNARE syntaxin 13 by more than 90% shows no effect on the endosomal fusion due to an increased recruitment of the docking factor EEA1 to the endosome membrane (Bethani et al., 2009).

Many assays have been used in the past to directly investigate endosomal fusion. Most of them are biochemical content mixing systems, in which two populations

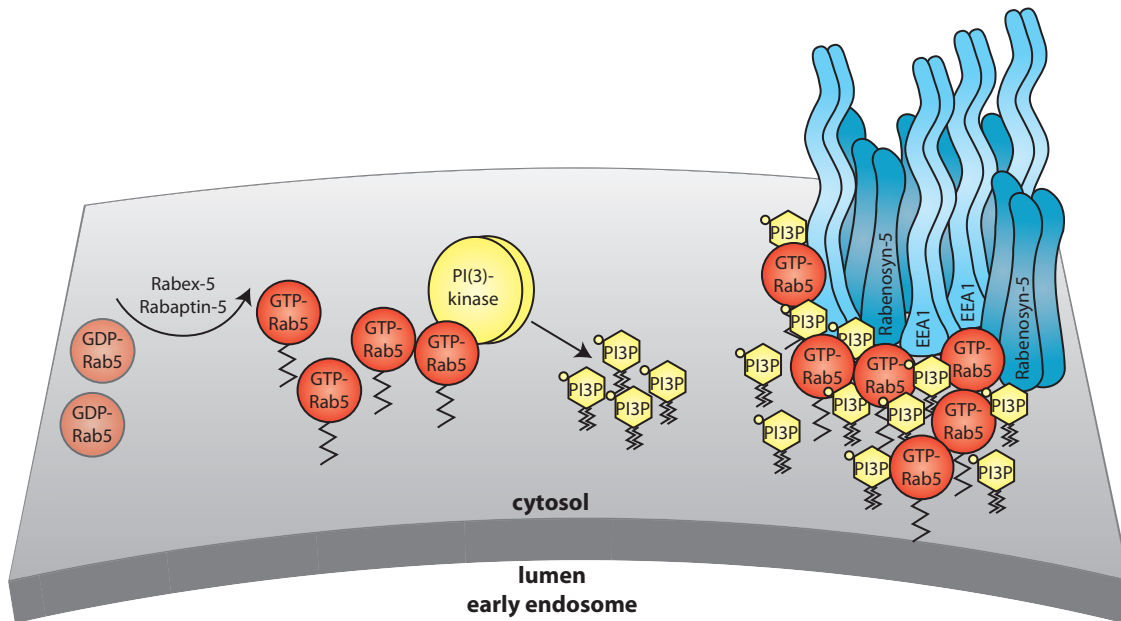


Figure 1.2: Rab5 is a hallmark of early endosomes and required for their docking. It is activated and recruited to the membrane by Rabex-5 and Rabaptin-5. This leads to a sequential activation and recruitment of downstream effectors: the PI(3)-kinase generates PI(3)P on the early endosome, which leads to the recruitment of the docking factors EEA1 and Rabenosyn-5 [modified from Zerial and McBride (2001)].

of endosomes are labeled with, for example, avidin (or streptavidin) and biotin, or antibodies and antigen, and the amount of fusion between them is inferred from the mixing of the markers (Gruenberg and Howell, 1989). Another assay was developed recently, using fluorescent dyes and microscopy as a readout (Brandhorst et al., 2006). Similar to the biochemical assays, two populations of endosomes are loaded separately with different fluorescent dyes (Figure 1.3). Upon fusion of two of those endosomes, the resulting organelles are double labeled, which can be visualized with fluorescence microscopy. This assay even has the ability to differentiate between docked and fused endosomes [see Results section and Geumann et al. (2008)]. The numerous *in vitro* fusion assays have defined our current knowledge of fusion dynamics, with cytosolic factors, ATP and calcium (Aballay et al., 1995; Geumann et al., 2008; Holroyd et al., 1999), as well as the above mentioned factors (such as the Rab-

EAA1 docking machinery, the correct SNAREs, NSF and α -SNAP) being required (Mills et al., 1999; Zerial and McBride, 2001).

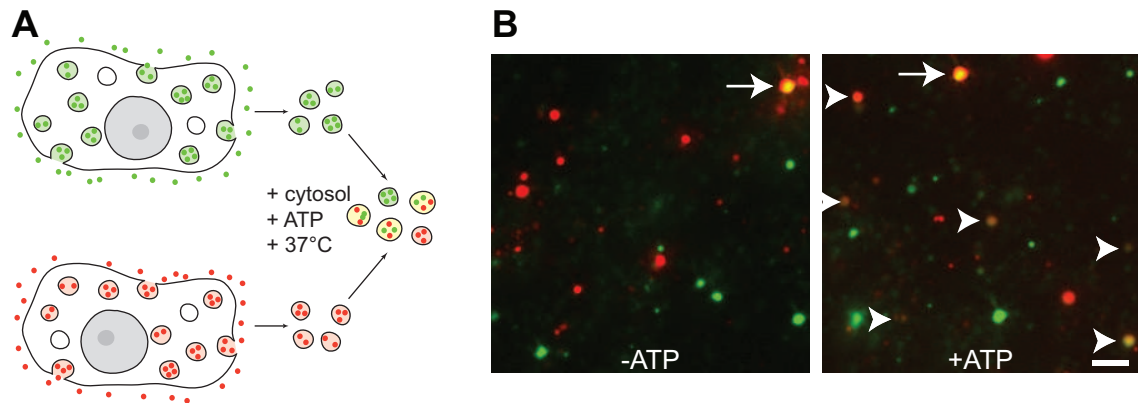


Figure 1.3: (A) Schematic overview of an *in vitro* homotypic early endosomal fusion assay. Two different sets of PC12 cells are labeled with differently colored fluorescent markers, and post-nuclear supernatants (PNS) are prepared. Mixing of the two PNS fractions in a reaction containing cytosol and an ATP-regenerating system results in the formation of double labeled endosomes via organelle fusion, which can be visualized by fluorescence microscopy. (B) Typical images of reactions with an ATP-depleting system (left) as negative control or an ATP-regenerating system (right) as positive control. Images taken in the different fluorescent channels are aligned by multi-colored fluorescent beads (arrows). Fused endosomes (arrow heads) are only present in the positive control. Size bar = 2 μm .

1.4 Sorting and Membrane Budding

Vesicle budding represents, together with membrane fusion, a key reaction in membrane trafficking. Even though it can be seen as the reverse reaction of fusion, the two processes of budding and fusion function via completely different mechanisms. For budding a complex protein and lipid machinery, involving coat proteins, is required, which induces local membrane curvature to form a new vesicle. Ultimately, budding ensures the separation and sorting of material that is present within a highly heterogeneous donor organelle by the selective incorporation of cargo proteins into the newly forming vesicle.

1.4.1 Vesicle Budding

Vesicle budding in eukaryotic cells can occur with or without coat proteins. However, the vesicles lacking coat proteins are difficult to distinguish from each other, and therefore, the transport steps they are involved in are largely unknown. As outlined before, coat proteins function (a) to deform the donor membrane for the budding of a vesicle and (b) in the selection of the vesicle cargo. There are three “classical” coat complexes that have been well characterized so far for budding steps in the secretory pathway: clathrin, coat protein-I (COPI) and COPII.

Clathrin coats are involved in two crucial transport steps, endocytosis from the plasma membrane to early endosome and transport from the TGN to endosomes. These two pathways are differently regulated: while endocytosis requires the adaptor proteins AP2 (and AP180), budding at the TGN uses AP1. In addition to AP1 and AP2, a large variety of other clathrin adaptors exist; among them are two other heterotetrameric ones, AP3 and AP4, GGA proteins and Hrs. AP-3 and Hrs are present on early endosomes and delivers proteins to late endosomes (and possibly to the TGN), even though the precise pathways are not known. AP4 and GGA proteins (see below) are localized to the TGN where they seem to be involved in the transport of lysosomal proteins (Boman, 2001; Newell-Litwa et al., 2007). Adaptor proteins act as scaffolds, bringing together membrane lipids, sorting motifs present in the cytosolic domains of membrane proteins, components of the vesicle fusion machinery and coat components of the budding machinery (Boehm and Bonifacino, 2001; Robinson, 2004; Sorkin, 2004). The classical adaptor complexes AP1, 2, 3 and 4 each comprise four subunits: one highly conserved large subunit (β -adaptin), one less-conserved large subunit (α -, γ - or δ -adaptin, depending on the complex), one medium subunit (μ -adaptin), and the small subunit σ . The large subunits each consist of three domains, the body, hinge and ear domain, which can interact with different proteins and lipids.

Other pathways use the coat proteins COPI and COPII, which share some homology to the clathrin machinery: while COPI and clathrin coats exhibit a high degree of structural and architectural similarity, COPII and clathrin resemble mechanis-

tic homology in their sequential assembly (Kirchhausen, 2000; McMahon and Mills, 2004; Pucadyil and Schmid, 2009; Stagg et al., 2007). COPI and COPII vesicles traffic between the ER and the Golgi complex - COPI primarily from the Golgi to the ER and between Golgi cisternae, and COPII from the ER to the Golgi. Both coats require the activation of small GTPases, such as Arf1 (for COPI) and Sar1 (for COPII), which represent the link between cargo and coat. In contrast to clathrin, which is necessary but not sufficient for budding, the COP coats together with their respective GTPases are both necessary and sufficient to mediate vesicle budding. The COPI coatomer is a complex of seven proteins, α , β , β' , γ , δ , ε , ϵ and ξ . The COPII machinery consists of the inner coat proteins Sec23 and Sec24, the outer coat proteins Sec13 and Sec31, as well as GTP-bound Sar1; these purified components are necessary and sufficient to generate coated vesicles from isolated ER membranes (Matsuoka et al., 1998). Biochemical and structural studies from William Balch's laboratory showed that the COPII coat can form in different conformations, depending on the size of the cargo molecules (Gurkan et al., 2006; Stagg et al., 2006, 2008).

The final pinching step for clathrin-coated vesicles, as well as for several other scission events in eukaryotic cells, is mediated by the GTPase dynamin or by other dynamin-like proteins (Hinshaw, 2000; Praefcke and McMahon, 2004).

Apart from the adaptor proteins, clathrin, COPI and COPII, another coat has been described recently: the retromer complex, which operates on endosomes and mediates the transport to the TGN (Bonifacino and Glick, 2004; Bonifacino and Hurley, 2008). Its core complex is built up by the subunits Vps26, Vps29 and Vps35, which transiently associate with dimeric complexes of sorting nexin proteins (Collins, 2008; Seaman, 2005). So far, 33 different mammalian sorting nexins have been identified (Cullen, 2008), their precise roles and relationship to the core Vps35-Vps26-Vps29 assembly being still under investigation.

Compared to fusion, there are fewer assays available for the investigation of budding. Most of them use the concept of separating the budded vesicles from purified donor organelles by centrifugation or density gradients. Instead of using native donor mem-

branes, some groups have even reconstituted different parts of the above mentioned budding machineries in artificial vesicles, such as proteoliposomes, giant unilamellar vesicles (GUVs), or supported bilayers with excess membrane reservoir (SUPER templates). The readout of budding in such systems is either based on biochemical density fractionation or microscopy [see for example [Matsuoka et al. \(1998\)](#), [Pucadyil and Schmid \(2008\)](#), [Sorre et al. \(2009\)](#) or [Manneville et al. \(2008\)](#)].

1.4.2 Cargo Selection and Sorting

One prerequisite for vesicle budding is protein sorting, which happens in almost every organelle in eukaryotic cells and is fundamental to proper cellular function. It can in principle occur by two different mechanisms: (a) by a signal that causes the protein to be retained within a certain organelle (by either a specific signal sequence on the protein, or by the induced formation of oligomers or aggregates that would be too large to enter into the budding vesicle) or (b) by a signal that specifies the protein as cargo for export, resulting in its selective packaging into a budding transport vesicle. One well characterized example for the first mechanism uses the retrograde transport route involving COPI coats, which fulfills several important functions such as the retrieval of escaped ER-resident proteins, retention of misfolded proteins or recycling of Golgi glycosyltransferases. This is achieved by a C-terminal KDEL-sequence present on the ER-resident proteins, which is both necessary and sufficient for ER-localization. This sequence is recognized by the KDEL receptor, which is localized to the ER and the Golgi. At the more acidic luminal pH of the Golgi, the binding affinity of KDEL motifs to the receptor is higher. Thus, escaped ER-proteins are captured at the Golgi and retrograde COPI vesicles are formed to return them back to the ER ([Harter and Wieland, 1996](#)). This pathway is also exploited by some bacterial toxins (e.g. cholera toxin or *Pseudomonas* exotoxin A), which also contain a C-terminal KDEL sequence that allows them to reach the ER by retrograde transport after their uptake by endocytosis. For the second mechanism, the presence of a transport signal results in selective packaging of a given protein into a budding transport vesicle. As for a retention signal, certain receptor or

binding proteins are required that specifically recognize the transport signal for a particular organelle. These signal sequences are mainly found in the cytoplasmic part of the transmembrane cargo receptors and are very diverse: for the COPII coats, for example, several ER export signal sequences can be recognized and bound by Sec24. Additionally, Sec24 binds active Sar1 (and thereby links the cargo to the coat) (Bonifacino and Glick, 2004).

The concepts of selective incorporation of material into the new vesicle and the retention of resident proteins into the donor organelle are not only valid for COPI and COPII vesicles, but are essential in any other organelle of eukaryotic cells. However, for some cellular organelles cargo selection and sorting additionally includes the separation of different cargoes into differently targeted vesicles. This is the case in the two main sorting stations in eukaryotic cells: (a) the *trans*-Golgi network (TGN), which sorts and distributes material from the biosynthetic pathway, and (b) the early endosomes, which mainly sort and distribute material that is taken up by the cells. In the TGN, different proteins destined to the plasma membrane have to be sorted at the level of the TGN, depending on their mode of secretion. For example proteins that are constitutively secreted (such as the heparan sulfate proteoglycane) are packed into different vesicles than proteins which undergo regulated exocytosis (such as the secretogranin II) (Tooze and Huttner, 1990). These two mechanisms have to be again distinguished from those targeting for example hydrolases or other enzymes to the early or late endosomes, indicating the high complexity of cargo sorting at the TGN. As key players for this sorting process, the GGA (Golgi-localized, γ -ear containing, ADP-ribosylation factor binding) proteins GGA1, GGA2 and GGA3 have been suggested. They are localized predominantly to the TGN (Boman et al., 2000; Dell'Angelica et al., 2000; Hirst et al., 2000; Poussu et al., 2000) and current evidence supports an exclusive role in the TGN-to-early endosome or TGN-to-late endosome pathway, respectively. GGA proteins represent another form of adaptor proteins and share homology with γ -adaptin, one large subunit of the AP1 complex (Dell'Angelica et al., 2000; Hirst et al., 2000). Their domain structure allows them to interact with (a) lysosomal cargo receptors such as mannose-6-phosphate receptor (MPR), (b) Arf proteins (e.g. Arf1 for GGA1), thereby competing with

other adaptor proteins, (c) coat proteins, leading for example to the recruitment of clathrin to the TNG, and (d) other regulatory proteins such as the Rabaptin-5/Rabex-5 complex (Boman, 2001; Kawasaki et al., 2005). Thereby, GGA-proteins appear to be important factors in cargo selection and sorting and represent a link between the correct cargo and coat proteins.

In the early endosome, the material that is destined to the TGN has to be distinguished from the one recycled back to the plasma membrane (via the fast, direct pathway and the slow, indirect one including the recycling endosome) and the material destined to the degradation route via the late endosome and lysosome. In specialized cells, even more sorting pathways need to be distinguished: the routes leading to the formation of synaptic vesicles in neuronal cells, transcytotic vesicles in epithelial cells, GLUT4 vesicles in adipocytes and MHCII-containing vesicles in B-lymphocytes requires. As indicated in the next section, sorting at the early endosome is less understood than sorting at the TGN.

1.4.3 Early Endosome Sorting and Budding

Due to the complexity of trafficking routes leading from the early endosome to different destinations, the endosomes represent highly heterogeneous sorting stations and it has been difficult to study these different sorting and budding modes. Compared to endosomal docking and fusion, limited information is available about some of the special sorting and budding events, and almost nothing is known about the connection and regulation of the different pathways.

An endosomal budding event investigated since many years is the biogenesis of SLMVs in PC12 cells. There is strong evidence that this budding process differs from the one occurring at the plasma membrane: Kelly and coworkers found that synaptic vesicle formation from the endosome is Arf1-dependent (Faundez et al., 1997) and requires neuronal AP3 (Blumstein et al., 2001; Faundez et al., 1998), while clathrin, AP2 and dynamin seem to not be involved (Faundez et al., 1997). In contrast, the formation of synaptic vesicles at the plasma membrane is dependent on clathrin,

AP2 and dynamin ([Schmidt et al., 1997](#); [Shi et al., 1998](#)).

Budding of transferrin-containing vesicles has also been studied using different approaches, suggesting the requirement of Rab4 ([de Wit et al., 2001](#)), syntaxin 13 ([Prekeris et al., 1998](#)), AP1, Arf1, clathrin and Rabex-5/Rabaptin-5 ([Pagano et al., 2004](#)).

The best studied pathway of endosome sorting is the targeting of ubiquitinated membrane proteins into multivesicular bodies. This process requires the ESCRT machinery which has been described by Emr and coworkers [for reviews see [Saksena et al. \(2007\)](#) and [Raiborg and Stenmark \(2009\)](#)]. The ubiquitinated receptor together with the endosomal lipid PI(3)P act as the two signals that lead to the sequential recruitment of four complexes, ESCRT-0, ESCRT-I, ESCRT-II and ESCRT-III. This mediates the inward budding of luminal vesicles (and thus the formation of MVBs from the early endosome) containing the ubiquitinated receptors that can then be degraded.

Furthermore, it has been shown that the retromer complex (see above) mediates the endosome-to-TGN transport of the mannose-6-phosphate receptor and bacterial toxins ([Bonifacino and Hurley, 2008](#); [Collins, 2008](#); [Seaman, 2005](#)) and requires the sorting nexins SNX1 and SNX2 ([Carlton et al., 2004](#); [Rojas et al., 2007](#)). Sorting nexins (SNXs) are a large family of proteins and they are classified by the presence of a particular type of phox-homology (PX) domain, which mainly binds PI(3)P, thus leading to the enrichment of SNXs on early endosomes. They have been proposed to function in endocytosis, endosomal sorting and endosomal signalling. Sorting and endosome tubule formation is most likely achieved by the 12 members of the SNX-BAR subfamily, which contain a C-terminal BAR-domain that can induce membrane curvature and stabilize tubules. Another subclass contains only a SNX-PX domain and a third class exhibits other special binding domains which might be involved in endosomal signalling. While SNX1 and SNX2 have been implicated in the retrograde endosome-to-TGN trafficking, SNX9 seems to be involved in many plasma membrane remodeling events such as clathrin-dependent and -independent endocytosis, and SNX4 can interact with the transferrin receptor, suggesting a role

in receptor recycling. However, many other SNXs are not yet characterized and may thus function in the regulation of distinct sorting and budding events at the endosome (Carlton et al., 2005; Cullen, 2008).

Apart from cargo sorting it is unclear how the budding of the cargo-enriched endosomal tubule proceeds. Recent data have suggested that it might function by recruiting dynamin-like EHD (Eps15 homology (EH)-domain) proteins (Grant and Caplan, 2008; Sharma et al., 2008). Mammals express four different isoforms, EHD1, EHD2, EHD3 and EHD4, all of which consist of a C-terminal EH-domain. They have been suggested to be part of different trafficking pathways from the early endosome (Grant and Caplan, 2008), a model which remains to be confirmed.

In summary, of all the different sorting and budding pathways that occur at the early endosome, only the transport of membrane-bound cargo destined to MVBs and the TGN has been studied some detail, leading to an emerging picture on how these processes may work. In contrast, sorting and separation of most soluble cargoes, as well as molecules targeted to the plasma membrane, is largely unknown. Even though the identification of some of the involved molecules (see above) is promising, many of them appear to be only single components in a complex series of required factors. Thus, many other molecules need to be identified in order to obtain a global view on one or the other endosomal sorting and budding process. Once several pathway have been dissected, it will be additionally challenging to understand how they are regulated.

1.5 Aims of this Work

Given that the endosome acts as a sorting station with many different outgoing trafficking routes, it is intriguing to understand the molecular and regulatory mechanisms underlying these processes. Due to the fact that endosomal sorting and budding assays are scarce and mainly based on rather complicated or indirect methods, the aim of this study was to develop convenient *in vitro* assays, based on fluorescence microscopy and biochemical methods, which allow the investigator to study

cargo sorting and budding in endosomes. The choice of an *in vitro* system was based on the fact that this allows to apply drugs and reagents that would not enter the cell through the plasma membrane. Unlike genetic knock-down or overexpression approaches in cells, *in vitro* assays lead to acute effects when inhibitory reagents are added and thus expand the flexibility in the type of such inhibitory tools. Further requirements for such an assay were ease of operation and the ability to investigate several conditions at one time.

Based on this assay, I wanted to identify molecular players that are required for the differential cargo sorting within early endosomes. Does budding for differently targeted vesicles differ in the mechanisms and pathways involved - e.g. do recycling vesicles and other types of vesicles, such as those targeted to the *trans*-golgi network, differ in their formation? Which molecules are involved? How are the different budding events regulated? Are molecular “budding domains” involved and how are they organized? Are fusion and budding events mechanistically coupled? Answering (part of) these questions required a large variety of tools for potentially inhibiting different known pathways. A significant part of this study was dedicated to the generation of such tools.

Furthermore, I wanted to validate some of the candidates required in sorting and budding in living cells. This required the further development of convenient tools cell-based tools, allowing to study membrane trafficking in living cells.

“The true method of knowledge is
experiment.”

(William Blake)

2

Materials and Methods

2.1 Materials

2.1.1 Antibodies

Antibodies used in this study are listed in **Table 2.1**. All antibodies were generated in our laboratory or were obtained from Abcam (Cambridge, UK), BD Biosciences (Erembodegem, Belgium), BioRad (Hercules, CA, USA), Calbiochem (San Diego, CA, USA), Dianova (Hamburg, Germany), Invitrogen (Carlsbad, CA, USA), Jackson ImmunoResearch Europe (Newmarket, UK) or Synaptic Systems (Göttingen, Germany).

For fusion or budding reactions (F/B), antibodies were added at a dilution of 1:17 of the total reaction volume. Primary and secondary antibodies for immunofluorescence (IF) were used at a 1:100-dilution. For western blotting (WB) or dot blotting (DB), primary antibodies were used at 1:1000 and secondary antibodies at 1:2000-1:5000. For the biochemical fusion assay, antibodies were used at 1:10 for coupling to protein A beads.

The *r*-anti-EEA1 antibody (serum) was generated by C. Holroyd against the N-terminal peptide of EEA1 (CLRRILQRTPGRV). The *r*-anti-*beta*-COP antibody (affinity purified) by Abcam was raised against the peptide EAGELKPEEEITVG-PVQK (Duden et al., 1991).

Table 2.1: Antibodies used in this study: IF (Immunofluorescence), WB (Western Blot), DB (Dot Blot), F/B (Fusion or Budding assay), F (biochemical fusion assay), *r*: rabbit (affinity purified or serum), *m*: mouse (monoclonal), *g*: goat (affinity purified).

Antibody	Applica- tion	Reference
<i>r</i> -anti-Alexa 488 (affinity purified)	DB, WB	Invitrogen
<i>r</i> -anti- <i>beta</i> -COP (affinity purified)	F/B	Abcam
<i>r</i> -anti-Clathrin light chain (serum)	F/B	Takamori et al. (2006)
<i>r</i> -anti-EEA1 (serum)	F/B	Takamori et al. (2006)
<i>r</i> -anti-SNAP-25 (serum)	F/B, IF	Synaptic Systems
<i>r</i> -anti-sorting nexin 1 (serum)	F/B	Haft et al. (2000)
<i>r</i> -anti-sorting nexin 2 (serum)	F/B	Haft et al. (2000)
<i>r</i> -anti-Synaptobrevin 2 (serum)	F/B	Synaptic Systems
<i>r</i> -anti-Synaptophysin 1 (serum)	F/B	Synaptic Systems
<i>r</i> -anti-Syntaxin 1A (serum)	F/B	Synaptic Systems
<i>r</i> -anti-Syntaxin 6 (serum)	F/B, IF	Synaptic Systems
<i>r</i> -anti-Syntaxin 13 (serum)	F/B, IF	Synaptic Systems
<i>r</i> -anti-VAMP3 (affinity purified)	IF	Abcam
<i>r</i> -anti-VAMP4 (serum)	F/B, IF	Synaptic Systems
<i>r</i> -anti-Vps26 (serum)	F/B	Haft et al. (2000)
<i>r</i> -anti-Vps29 (serum)	F/B	Haft et al. (2000)
<i>r</i> -anti-Vps35 (serum)	F/B	Haft et al. (2000)
<i>r</i> -anti-Vt1a (serum)	F/B	Synaptic Systems
<i>m</i> -anti-Clathrin heavy chain	F/B	Dianova
<i>m</i> -anti-Clathrin light chain (Cl 57.1)	F/B	Synaptic Systems
<i>m</i> -anti-Synaptobrevin 2 (Cl 69.1)	IF	Synaptic Systems
<i>m</i> -anti-Vt1a	IF	BD Biosciences
<i>g</i> -anti-avidin	F	Calbiochem
<i>g</i> -anti-mouse (Cy2, Cy3 or Cy5 labeled)	IF	Jackson Immunoresearch
<i>g</i> -anti-mouse (HRP labeled)	WB	BioRad
<i>g</i> -anti-rabbit (Cy2, Cy3 or Cy5 labeled)	IF	Jackson Immunoresearch
<i>g</i> -anti-rabbit (HRP labeled)	DB, WB	BioRad

Polyclonal rabbit antibodies (serum) against human sorting nexin 1 and 2 (SNX1, SNX2) as well as the human retromer subunits Vps26, Vps29 and Vps35 were generously provided by Carol R. Haft, Raul Rojas and Juan S. Bonifacino (NIH, Bethesda, MD, USA).

2.1.2 Chemicals, Enzymes and Kits

Chemicals

The chemicals listed below were used in this study and obtained from the indicated sources. Other standard chemicals were obtained from either Sigma-Aldrich (Steinheim, Germany), Roth (Karlsruhe, Germany), Merck (Darmstadt, Germany) Boehringer (Ingelheim, Germany), Fluka (Buchs, Germany), Serva (Heidelberg, Germany) or Applichem (Darmstadt, Germany), unless otherwise stated. All chemicals were of at least analytical purity.

N-Ethylmaleimide (NEM), GTP γ S, GMP-P(NH)P, latrunculin, phalloidin, nocodazole, brefeldin A (BFA), wortmannin, LY 294,002, ionomycin, FCCP, horseradish peroxidase (HRP), insulin and 2,2'-Azino-bis(3-ethylbenzothiazoline-6-sulfonic acid) (ABTS) were all purchased from Sigma-Aldrich. W-7 and avidin were bought from Calbiochem. BAPTA, EGTA, LDL-DiI, transferrin-Alexa 488, transferrin-Alexa 594, transferrin-Alexa 647, dextran-Alexa 488, dextran-Alexa 594, acetylated LDL-Alexa 594, cholera toxin subunit B-Alexa 647, TetraspeckTM beads (0.2 μ m) and Fluospheres[®] carboxylate-modified yellow-green or red fluorescent (0.2 μ m) were obtained from Invitrogen. Hexokinase, creatine phosphokinase and creatine phosphate were purchased from Roche, Basel, Switzerland. The chemical (E)-*N'*-(3,4-dihydroxybenzylidene)-3-hydroxy-2-naphthohydrazide, previously described as dynasore (Macia et al., 2006), was bought from ChemBridge Corporation, San Diego, CA, USA. Cell culture solutions (DMEM medium, L-glutamine, fetal calf serum, horse serum, PenStep) were obtained from Cambrex (Verviers), Lonza GmbH (Wuppertal, Germany) and PAA (Clöbe, Germany).

Enzymes

The enzymes that were used in this study are listed in **Table 2.2** and were obtained from Applichem (Darmstadt, Germany), Fermentas (St. Leon-Rot, Germany), New England Biolabs (NEB; Ipswich, MA, USA), Promega (Madison, WI, USA) or Roth (Karlsruhe, Germany). All restriction enzymes, ligases and polymerases were used according to manufacturer's instructions (including the supplied buffers).

Table 2.2: Enzymes used in this study

Enzyme	Application	Reference
DNase	protein purification	Applichem
lysozyme	protein purification	Roth
restriction enzymes	DNA digest	NEB or Fermentas
ligase	ligation of DNA fragments	NEB
Pfu polymerase	polymerase chain reaction	Promega
thrombin	protein purification	Merck

Kits

The commercially available kits that were used in this study are listed in **Table 2.3** and were used for the stated application according to manufacturer's instructions (including the supplied buffers).

2.1.3 Mammalian Cell Lines and Bacterial Strains

The mammalian cell lines and bacterial strains listed in **Table 2.4** were used in this study. PC12 cells were used for *in vitro* and *in vivo* studies, BHK-21 cells for *in vitro* experiments and COS-7L cells were used for *in vivo* studies. *E.coli* XL-1 blue bacteria were used for molecular cloning and *E.coli* BL21 (DE3) bacteria for protein expression.

Table 2.3: Commercial kits used in this study

Kit	Application	Reference
NucleoBond TM PC	preparative scale plasmid purification ('maxi prep')	Macherey-Nagel
NucleoSpin TM Plasmid PC	analytical scale plasmid purification ('mini prep')	Macherey-Nagel
Lipofectamine TM 2000	transient transfection	Invitrogen
Pierce [®] BCA Protein Assay WESTERN	protein quantification	ThermoFisher
LIGHTENING TM <i>Plus</i> -ECL	detection of chemoluminescence	PerkinElmer

Table 2.4: Mammalian cell lines and bacterial strains used in this study

Cell Line	Description	Reference
PC12	Pheochromocytoma cells, clone 251	Heumann et al. (1983)
BHK-21	Baby hamster kidney-21 cells	European Collection
COS-7L	Green monkey kidney cells	Invitrogen
XL-1 blue	recA1 endA1 gyrA96 thi-1 hsdR17 (rk-, mk+) supE44 relA1 lac [F' traD36 proAB lacIqZΔM15 Tn10 (Tet ^R)]	Stratagene
BL21 (DE3)	F- dcm ompT hsdS(rB- mB-) gal λ (DE3)	Novagen

2.1.4 Recombinant Proteins and Peptides

The following peptides (single-letter amino acid code) were purchased from GenScript Corporation (Piscataway, NJ, USA):

QVPSRPNRAP (dynamamin-amphiphysin)

PAVPPARPG (dynamamin-endophilin)

INFFEDNFVPEI (amphiphysin-AP2)

INFFEDPFVPEI (control)

CLRRILQRTPGRV (EEA1-N-terminal peptide).

Purified recombinant GDP dissociation inhibitor (GDI) and purified Rabex-5 (nucleotide exchange domain Vps9) were a generous gifts from Aymelt Itzen and Roger S. Goody (MPI of Molecular Physiology, Dortmund, Germany). The recombinant proteins for syntaxin 13 (cytosolic fragment 1-250), syntaxin 6 (cytosolic core fragment 169-234) and vti1a (cytosolic fragment 1-217) were generously provided by D. Zwilling (San Francisco) or S.O. Rizzoli (MPI for Biophysical Chemistry, Göttingen, Germany).

2.1.5 DNA Constructs

The DNA constructs listed in **Table 2.5** were used in this study.

2.2 Methods

2.2.1 Molecular Biology and Biochemical Standard methods

Molecular Cloning

For molecular cloning, standard methods for ligation, heat-shock transformation in competent *E.coli* XL-1 blue cells, plasmid 'mini prep', plasmid 'maxi prep', analytical restriction digest, quantification of DNA and DNA sequencing were used

Table 2.5: DNA constructs used in this study

Construct	Application	Reference
α -SNAP wildtype	protein purification	U. Winter
α -SNAP L294A	protein purification	U. Winter
Rab4A (h. sapiens)	protein purification	R.S. Goody
Rab5A (h. sapiens)	protein purification	R.S. Goody
Rab7 (c. familiaris)	protein purification	R.S. Goody
Rab9 (h. sapiens)	protein purification	R.S. Goody
Rab11A (r. norvegicus)	protein purification	R.S. Goody
Rab18A (m. musculus)	protein purification	R.S. Goody
Rab22A (h. sapiens)	protein purification	R.S. Goody
Rab35 (r. norvegicus)	protein purification	R.S. Goody
Rab5A wildtype	transfection	Bethani et al. (2007)
Rab5A S34N	transfection	Bethani et al. (2007)
Rab5A Q79L	transfection	Bethani et al. (2007)

([Sambrook and Russell, 2001](#)). DNA primers were ordered from Sigma-Genosys and DNA sequencing was carried out using Eurofins MWG Operon (Ebersberg, Germany)

Protein Determination

Protein concentration was determined according to Bradford ([Bradford, 1976](#)). A set of standards containing 1, 2, 3, 4, 5 μ g bovine serum albumin and the proteins were diluted in 200 μ l H₂O and then mixed with 800 μ l Bradford solution. After incubation for 5 min at RT the absorbance at 595 nm wavelength was measured using a photometer. The protein concentrations of interest were obtained from interpolation onto the linear trace obtained from the standards.

BCA assays ([Smith et al., 1984](#)) were used to quantify the total protein contents

of cell lysates. BCA assays were performed using Pierce[®] BCA Protein Assay Kits (ThermoFischer) according to the manufacturer's manual.

SDS-PAGE and Western Blotting

Samples were separated in a 10% denaturing Tris/Tricine SDS polyacrylamide gel electrophoresis system, as described by [Schagger and von Jagow \(1987\)](#) and [Schagger \(2006\)](#). The resolving gel contained 10% bis-acrylamide (Rotiphorese Gel 30, Roth GmbH, Karlsruhe, Germany), 1 M Tris (pH 8.45), 0.1% SDS, 10% glycerol; the stacking gel contained 4% bis-acrylamide 1 M Tris (pH 8.45), 0.1% SDS. Ammonium persulfate and TEMED (N, N, N', N'-Tetramethylethylenen-diamine) were added for polymerization. Before loading, all samples were boiled for 5 min. 5 μ l PageRuler prestained protein ladder solution (Fermentas) were used for each gel, for approximate sizing of the proteins. Separation was performed in a discontinuous buffer system, with a 0.2 M Tris (pH 8.9) solution in the tank and a 0.3 M Tris (pH 8.45), 0.03% SDS solution as the gel buffer.

Western blotting was described in [Towbin et al. \(1989\)](#): proteins were transferred to Protran nitrocellulose membrane (PerkinElmer Life Sciences, Boston, MA USA), via a semi-dry procedure in buffer containing 200 mM Glycine, 25 mM Tris (pH 7.4), 0.04% SDS, 20% methanol. For the transfer, 45 mA were applied per blot for 1 hour in a Biorad PowerPac 300 blotting apparatus. The membranes were blocked for 30 min at room temperature in blocking solution (PBS pH 7.4, 5% non-fat milk powder, 0.1% Tween 20) and then incubated overnight with the appropriate dilutions of the primary antibody in blocking solution, at 4°C. After 3 washes with blocking solution (10 min each), the blots were incubated with horseradish peroxidase-conjugated secondary antibodies (diluted 1:2000-1:5000), for 1 hour at room temperature. Protein bands were detected using the enhanced chemiluminescence (ECL) system (PerkinElmer LAS, Inc., Boston) on a FujiFilm LAS-1000 imaging station.

Alternatively, mainly for analyzing the results of the protein purifications, gels were directly stained with Coomassie-blue ([Schagger, 2006](#)), instead of processing for

Western Blotting. For staining, the stacking gel was discarded and the separation gel was incubated for 15-30 min in 50% (v/v) methanol, 10% (v/v) acetic acid and 0.2% (w/v) Coomassie Brilliant Blue R-250 under agitation. The gel was de-stained in 50% (v/v) ethanol and 10% (v/v) acetic acid for 15-30 min and then in 10% (v/v) ethanol and 5% (v/v) acetic acid until no background staining was visible. After scanning, the gel was hydrated in ddH₂O, dried in a gel dryer by wrapping it in cellophane foil, and preserved for further analysis.

Quantification of HPR Using the ABTS-Assay

For the quantification of horseradish-peroxidase (HRP) with a colorimetric ABTS reaction (Matsuda et al., 1984), the samples were mixed with homogenization buffer containing 1% Triton X-100 to a final volume of 100 μ l and incubated for 10 min at room temperature (with mixing once every minute). 100 μ l homogenization buffer were used as a reference. Meanwhile, ABTS buffer was prepared by freshly adding ABTS (0.4-1 mg/ml) to a buffer containing 60 mM Na Citrate, 80 mM Na₂HPO₄, 0,3% triton-X-100, pH 5.0. After addition of 900 μ l ABTS buffer, the colorimetric reaction was started by adding 10 μ l 3% H₂O₂ in ddH₂O. After incubating the samples for 20 min at 37°C, the absorption was measured at 414 nm.

2.2.2 Protein Expression and Purification

DNA constructs of the respective proteins were transformed into electrocompetent *E.coli* BL21 (DE3) cells (Sambrook and Russell, 2001). All recombinant proteins were expressed in shaking cultures, in LB medium (10 g tryptone, 5 g yeast extract and 10 g NaCl per 1 l) for α -SNAP, and in TB medium (13.3 g tryptone, 27.8 g yeast extract and 4.4 g glycerol) including 1:10 TB-salt (720 mM K₂HPO₄ and 170 mM KH₂PO₄) for the adaptor ear domains and the Rab proteins. Protein expression was induced with 0.5 mM IPTG (FORMEDIUM™) for various lengths of time. The bacteria were harvested by a 10 min centrifugation step at 1000 \times g at 4°C, the pellets were resuspended in the appropriate buffers and stored at -20°C until the

purification. After purification, all proteins were snap-frozen in liquid nitrogen and stored at -80°C .

α -SNAP

The constructs for α -SNAP wildtype and the mutant L294A were kindly provided by Dr. Ulrike Winter and Dr. Dirk Fasshauer. Both variants were expressed as His-tagged fusion proteins in *E.coli* BL21 (DE3) cells in LB medium and the bacterial pellets were resuspended in Ni^{2+} -wash buffer (20 mM Tris/HCl, 500 mM NaCl, 15 mM Imidazole, pH 7.4). For disruption of the bacterial cells, 1 mM MgCl_2 , 1 mM PMSF, 1 mM DTT, one spatula tip lysozyme, one spatula tip DNase I and 1% Triton X-100 (v/v) were added and the extracts were incubated for 20 min at RT. All following steps were performed at 4°C or on ice. For more efficient bacterial disruption, additional ultrasound pulses of $3 \times 40\text{s}$ were performed. The extracts were then centrifuged for 45 min at $12,000 \times g$ (Beckman SS-34 rotor). The resulting pellets were discarded and the supernatants incubated with Ni-NTA beads (Qiagen) for 2 hours. This mix was then poured into a column (15 cm length, 3 cm width) and the beads were allowed to settle. The beads were then washed three times with 100 ml wash buffer. The protein was then eluted with 3 bed volumes of elution buffer (20 mM Tris/HCl, 500 mM NaCl, 400 mM imidazole, pH 7.4). The proteins were dialyzed over night at 4°C against dialysis buffer (20 mM Tris/HCl, 50 mM NaCl, 1 mM DTT, 1 mM EDTA) using Spectra Por molecularporous membranes (Spectrum) with the presence of the protease thrombin ($20 \mu\text{l}$ of a $4 \text{U}/\mu\text{l}$ stock on 30 ml eluate) in the dialysis tube. The proteins were further purified using Mono-Q or Mono-S columns on a FPLC system (Amersham Pharmacia Biotech, Uppsala, Sweden). After dialysis the protein was loaded on an ion-exchange column, washed with several column volumes and then eluted with a linear gradient, increasing salt concentration from 0 mM to 1000 mM NaCl in 20 mM Tris/HCl buffer, pH 7.4 containing 1 mM EDTA and 1 mM DTT. The protein was collected in fractions and each peak fraction was analyzed via SDS-PAGE.

Rab Proteins

The constructs for the full-length Rab proteins Rab4, Rab5, Rab7, Rab9, Rab11, Rab18, Rab22 and Rab35 were kindly provided by Dr. Aymelt Itzen and Dr. Roger S. Goody (Max-Planck-Institute of Molecular Physiology). The proteins were expressed as soluble His-tagged, His-GST-tagged or His-MBP-tagged fusion proteins in *E. coli* BL21(DE3) cells at 20°C over night. The bacterial pellets were resuspended in buffer A (500 mM NaCl, 50 mM HEPES-NaOH, 1 mM MgCl₂, 0.5 mM DTT, 10 μM GDP, pH 7.4). For disruption of the bacterial cells, 1% Triton X-100 (v/v), 1 mM PMSF, one spatula tip lysozyme and one spatula tip DNase I were added and the extracts were incubated for 20 min at RT. All following steps were performed at 4°C or on ice. For more efficient bacterial disruption, additional ultrasound pulses of 3×40s were performed. The extracts were then centrifuged for 45 min at 12,000×g (Beckman SS-34 rotor). The pellets were discarded and the supernatants loaded onto 2×1ml HisTrap FF Ni-columns (GE Healthcare) using an Äkta-purifier FPLC system (GE Healthcare). The columns were washed with 35 ml 25 mM imidazole in buffer A and eluted with a linear gradient from 25 mM to 500 mM imidazole buffer. The eluted Rab-proteins were dialyzed to a buffer containing 150 mM NaCl, 10 mM HEPES-NaOH, 1 mM MgCl₂, 2 mM DTT, 10 μM GDP, pH 7.4 using Spectra Por molecularporous membranes (Spectrum) with 14-16kD cut off and concentrated to final concentrations of 20 mg/ml by using Vivaspin 500 centrifugal concentrators (Sartorius Stedim Biotech GmbH, Göttingen, Germany). For loading the proteins with the nucleotide GMP-P(NH)P, 2-5 mg of each Rab protein were incubated with a 25-fold excess of the nucleotide (which corresponds to 10 mM) and 5 mM EDTA for 4 hours at room temperature in a total volume of 200-500 μl. The EDTA and the free nucleotide were then removed by a Sephadex G-25 column (NAP TM-5, GE Healthcare). The efficient nucleotide exchange was analyzed by reverse phase chromatography [using a protocol modified from [Tucker et al. \(1986\)](#)], where isocratic elution (50 mM potassium phosphate, pH 6.6, 10 mM tetra-N-butylammonium bromide, 8% (v/v) acetonitrile) was used to separate different nucleotides (GDP, GTP and GMP-P(NH)P) on a ProntoSil C18 120-5-C18-AQ column (Bischoff chromatog-

raphy). The column was calibrated with solutions of appropriate nucleotides at known concentrations, which allowed to quantify the amount of each nucleotide bound to the Rab proteins. If the loading efficiency with GMP-P(NH)P was found to be less than 95%, the loading procedure was repeated. The proteins were again concentrated to a final concentration of 10-20 mg/ml (400 μ M).

2.2.3 Preparation of Rat Brain Cytosol

The preparation of rat brain cytosol was carried out as described in [Huttner et al. \(1983\)](#) with some modifications. All solutions and glassware were detergent-free and all the steps were carried out on ice or at 4°C. 20 to 40 rats were killed, decapitated and the brains were removed into a beaker of ice cold sucrose buffer (320 mM sucrose, 5 mM HEPES, pH 7.4). They were washed 2-3 times with sucrose buffer, to remove most of the blood remaining in solution, and were then homogenized. For this purpose, sucrose buffer containing protease inhibitors (1 μ g/ml Pepstatin A and 200 μ M PMSF) and 10 brains were filled into a 50 ml homogenizer and homogenized by 10 strokes (where one stroke is one up and down movement) at 900 rpm. This homogenate was centrifuged for 10 minutes at 5000 rpm in a SS-34 rotor (Sorvall centrifuge), resulting in a pellet containing nuclei and cell fragments (pink color), as well as fractions of synaptosomes/myelin/mitochondria (cream-yellow). The supernatant and the very soft part of the cream-yellow pellet (which also contains some cytosol) were collected and centrifuged again for 15 minutes at 16,500 rpm in a SS-34 rotor. In order to obtain pure cytosol, the resulting supernatant (crude cytosol) was centrifuged for 30 minutes at 90,000 rpm in a 100.3 rotor, in thick-walled plastic tubes. The cytosol was carefully collected, aliquoted, snap-frozen and stored at -80°C. The concentration determined with the Bradford method was usually between 6 and 9 mg/ml.

2.2.4 Cell Culture

PC12 Cells

PC12 cells were cultured in Dulbecco's modified Eagle's medium (DMEM with 4.5 g/l glucose) with the following additions: 5% fetal calf serum (FCS), 10% horse serum, 4 mM glutamine and 100 units/ml each of penicillin and streptomycin. Cells were grown to 70% confluence on culture dishes, at 37°C with 10% CO₂ and 90% humidity. PC12 cells were usually passaged 1:2 - 1:6 by detaching them from the plates using trypsin/EDTA (Lonza GmbH, Wuppertal, Germany).

COS-7 Cells

COS-7 cells were cultured in Dulbecco's modified Eagle's medium (DMEM with 4.5 g/l glucose) with the following additions: 10% fetal calf serum (FCS), 4 mM glutamine and 100 units/ml each of penicillin and streptomycin. Cells were grown to 90% confluence on culture dishes, at 37°C with 10% CO₂ and 90% humidity. COS-7 cells were usually passaged 1:5 - 1:20 by detaching them from the plates by using a cell scraper (Sarstedt, Nümbrecht, Germany).

BHK Cells

BHK cells were cultured in Dulbecco's modified Eagle's medium (DMEM with 4.5 g/l glucose): 5% fetal calf serum (FCS), 10% tryptose phosphate, 4 mM glutamine and 100 units/ml each of penicillin and streptomycin. Cells were grown to 90% confluence on culture dishes, at 37°C with 5% CO₂ and 90% humidity. BHK cells were usually passaged 1:20 - 1:50 by detaching them from the plates by using a cell scraper (Sarstedt, Nümbrecht, Germany).

Primary Neurons

Primary neurons were prepared from brains from newborn E1 rats using a standard protocol (Kaeche and Banker, 2006). The cultures were kindly provided by Ina Herfort (Max-Planck-Institute for biophysical Chemistry, Göttingen, Germany) and used in a stage between 14 and 24 days *in vitro*.

2.2.5 Transient Transfection

Prior to transient transfection, 12 mm or 18 mm diameter coverslips were coated with poly-L-lysine: Coverslips in pure ethanol were sterilized by singeing and placed into 12-well or 24-well plates (Sarstedt, Nümbrecht, Germany). Poly-L-lysine was diluted to a final concentration of 0.1 mg/ml in sterile ddH₂O, placed onto the coverslips (150 μ l per 12 mm and 300 μ l per 18 mm coverslip) and incubated for 30 min at room temperature. The poly-L-lysine was removed, the plates washed twice with sterile ddH₂O and dried over night. They could be kept in the refrigerator for up to several weeks before use.

Cells were passaged in their normal growth medium without antibiotics into 12-well or 24-well plates containing the coated coverslips. For transient transfection on the next day, the kit LipofectamineTM 2000 was used. For each coverslip in 24-well plates, 0.8 μ g of purified plasmid DNA was mixed with 50 μ l OptiMEM (Invitrogen, Carlsbad, CA, USA), and 2 μ l LipofectamineTM 2000 reagent were mixed with another 50 μ l OptiMEM and left for 5 min at room temperature. Afterwards, the lipofectamine-solution was carefully added to the DNA-solution and left for 20-40 min at room temperature (without mixing or strong movement of the solution during that time). In the meantime, the medium was changed on the cells and one well received 500 μ l growth medium without antibiotics. Finally, the total volume of 100 μ l lipofectamine-DNA-mixture was added to the coverslip and left for 4-6 hours on the cells. Afterwards, the medium was changed again and the (transfected) cells were analyzed 12-36 hours later. For 12-well plates, the volume was doubled.

2.2.6 Preparation of Postnuclear Supernatants

For the preparation of postnuclear supernatants (PNS), the protocol was adapted from [Holroyd et al. \(1999\)](#). Briefly, PC12 cells were grown in 15-cm dishes (Greiner Bio-One, Frickenhausen, Germany), the culture medium was removed from each plate and every plate was washed with 5 ml saline PBS (150 mM NaCl, 20 mM Na₂HPO₄, pH 7.4). The cells were harvested by trypsin/EDTA treatment (2 ml per plate; Lonza GmbH, Wuppertal, Germany). This reaction was terminated by addition of 5 ml cold culture medium and the cells collected by a centrifugation step at 4°C. The cells were resuspended in cold PBS, the centrifugation step was repeated and the resulting pellet was washed with cold internalization medium (OptiMEM, containing 10 mM glucose). After centrifugation, the cells were prewarmed at 37°C for several minutes and incubated for 5 min at 37°C with the markers dextran-Alexa 488 or Alexa 594 (500 µg/ml), transferrin-Alexa 488 or Alexa 594 (50 µg/ml), LDL-DiI (1-10 µg/ml), acetylated LDL-Alexa 595 (10 µg/ml), cholera toxin subunit B-Alexa 647 (3-10 µg/ml), biotin-HRP (2.5 mg/ml), avidin (3.3 mg/ml) or horseradish peroxidase (2 mg/ml) dissolved in internalization medium. For this step, the fluorescent markers had to be concentrated twice as high as indicated above, they were added 1:1 to the cellular pellet. Internalization was stopped by chilling on ice; the cells were then washed three times with ice-cold PBS containing 5 mg/ml BSA and once with homogenization buffer (250 mM sucrose, 3 mM imidazole-HCl, pH 7.4). The cellular pellet was resuspended 1:3 in homogenization buffer with protease inhibitors (0.2 mM PMSF and 1 µg/ml pepstatin A, leupeptin and aprotinin) and homogenized by 10-20 passages through a stainless steel ball homogenizer ([Balch and Rothman, 1985](#)) with a clearance of 0.02 mm (Industrial Tectonics Inc, Dexter, Michigan). The homogenate was centrifuged at 1,200×g for 15 min and PNS was collected, divided into aliquots, snap-frozen and stored at -80°C. The protein concentration of the PNS was determined by the Bradford assay.

2.2.7 *In vitro* Endosomal Docking/Fusion and Sorting/Budding Assays

Sorting/Budding and Docking/Fusion Reactions

Reaction mixtures contained, as final concentrations, 2 mg/ml rat brain cytosol, 11.25 mM HEPES at pH 7.0, 1.35 mM magnesium acetate, 0.18 mM DTT, 45 mM potassium acetate and PNS. For sorting/budding reactions, 4 mg/ml PNS (labeled with transferrin-Alexa 488, transferrin-Alexa 594, LDL-DiI, cholera toxin subunit B-Alexa 647, dextran-Alexa 488, dextran-Alexa 594, acetylated LDL-Alexa 594, or HRP) was added. For docking/fusion reactions, 2 mg/ml of two differently labeled PNS (labels as above, or biotin-HRP and avidin) were used. As ATP-regenerating system, 3.2 mM ATP, 26 mM creatine phosphate and 0.132 mg creatine kinase (800 units/mg) or as ATP-depleting system, 5 μ l hexokinase (1,500 units/ml dissolved in 250 mM glucose) were added. The reaction mixtures were incubated for 45 min (unless otherwise stated) at 37°C with slow agitation, control reactions were kept on ice.

Colocalization Assay

Sorting/budding or docking/fusion reactions were carried out in a 50 μ l final volume. 5-8 μ l of each reaction were transferred into 1 ml of PBS on coverslips (18 mm diameter) in 12-well plates. After centrifugation for 45 min at 5,868 \times g at 4°C, coverslips were analyzed by using a Zeiss Axiovert 200M fluorescence microscope. Images were acquired in the blue channel and two or three of the following channels: green (Alexa 488), orange (DiI), red (Alexa 594) or dark red (Alexa 647). Before use of coverslips, Tetraspeck beads (200 nm diameter, dilution 1:50,000 in 1 ml PBS) were bound to the surface by centrifugation for 45 min at 5868 \times g. The Zeiss Axiovert 200M fluorescence microscope was equipped with a 1.4 numerical aperture 100 \times objective and a CCD camera with a 1317 \times 1035 Kodak chip (pixel size 68 \times 68 nm, Princeton Instruments Inc., Trenton, NJ, USA). Alexa 488 fluorescence was detected with the excitation filter 480/40 HQ, the beamsplitter 505 LP Q and

the emission filter 527/30 HQ. Alexa 594 fluorescence was detected using the excitation filter 560/55 HQ, the beamsplitter 595 LP Q and the emission filter 645/75 HQ. DiI fluorescence was detected using the excitation filter 545/30 HQ, the beamsplitter 570 LP Q and the emission filter 610/75 HQ. Alexa 647 fluorescence was detected using the excitation filter 620/60 HQ, the beamsplitter 660 LP Q and the emission filter 700/75 HQ. Blue fluorescence (dapi) was detected using the excitation filter 350/50 D, the beamsplitter 400 DCLP and the emission filter 460/50 D. All filters were purchased from Chroma, Rockingham, VT, USA. Image acquisition was performed using METAMORPH (Universal Imaging Corporation, West Chester, PA, USA).

Data analysis was done using a custom-written routine in Matlab (The Mathworks Inc., Natick, MA, USA) and is attached in the Appendix. First, images were filtered using a high-pass or an *unsharp* filter and appropriate thresholds above background were applied to the images; all objects persisting above the thresholds (excluding single pixels) were then used in the analysis. The x and y coordinates of the intensity centers of the objects were determined and the shift between the images was corrected by use of the coordinates of a Tetraspeck bead (identified in the blue channel). Distances between the objects were determined, and the percentage of green objects that were within 100 nm of red objects was calculated. Accidental colocalization (between the objects in the green image and the objects in a mirror image of the red channel) was always subtracted. Typically, 6000-7000 transferrin-labeled organelles were analyzed per coverslip, with a similar number for cholera toxin and dextran. LDL is taken up less efficiently, which results in about 600-800 organelles being analyzed per coverslip. Two coverslips are always analyzed per condition, in every experiment. For the analysis of docked endosomes, the amount of organelles having their green and red intensity centers within 150-500 nm distance were calculated and the distances within 500-850 nm were subtracted as random colocalization. For experiments shown in **Figure 3.5**, **Figure 3.6** and **Figure 3.7 B**(distance measurements of endosomes and multi-colored fluorescent beads), distances to the closest object in the other channel were determined and binned in 25 nm classes. The single color beads were strongly fluorescent in green or red, re-

spectively. They also were fluorescent in blue, which allowed us to correct for the shift between the green and red images by aligning each of them to the blue image.

Time-lapse Budding Assay

For time-lapse imaging of labeled endosomes in **Figure 3.15**, 10 μg PNS (labeled with transferrin-Alexa 488 and LDL-DiI) were attached to the surface of a coverslip (12 mm diameter) by centrifugation for 45 min at $5868\times g$ (before the use of the coverslips, Tetraspeck beads were attached, as described above). The microscope stage was preheated to 37°C and imaging was started immediately after adding the cytosol-ATP-mixture (see above) to the endosomes. Two images were recorded in the green, red and blue channel for each time point (0, 10 and 30 minutes, respectively).

For data analysis, images were imported into Matlab and aligned by a least root-mean-square-deviation routine in order to compensate for a possible shift in x and y direction between the images. For selection of spots, an inner circle (diameter of 21 pixels) for the spot itself and an outer circle (diameter of 61 pixels) for background fluorescence around the spots were created. Labeled organelles were selected in both green (transferrin) and red (LDL) channels (beads were selected in the dapi-image and not used for analysis). The program then calculated the average fluorescence for each spot and subtracted its corresponding background in every image.

Biochemical Budding Assay

Sorting reactions with PNS containing HRP or transferrin-Alexa 488 labeled endosomes were carried out in a $300\ \mu\text{l}$ volume. The reactions were then diluted in 3 ml ice cold PBS and centrifuged for 35 min at $10,000\times g$ in a table top centrifuge at 4°C (similar centrifugation speeds were used to pellet PC12 organelle membranes in the past ([Lichtenstein et al., 1998](#)), with $27,000\times g$ thought to pellet all endosomal/vesicular membranes). Equal volumes of the supernatants (3 ml) were then centrifuged for 30 min at $300,000\times g$ (Beckman TLA100.3 rotor). The pellets were resuspended

in 50-100 μ l extraction buffer (20 mM Na_2HPO_4 , 150 mM NaCl, 5 mM EDTA, 5 mM EGTA, 1% (v/v) Triton-X-100) and analyzed for the amount of HRP (using ABTS, see above) or transferrin-Alexa 488 (using anti-Alexa 488 dot-immunoblots), respectively.

Dot-immunoblot experiments in **Figure 3.14 C** were performed as described in [Jahn et al. \(1984\)](#) with some modifications. In brief, the pellets were adjusted to a final SDS concentration of 2% (w/v). Samples were boiled for 5 min and 5 μ l (1/10 of the total volume) were spotted on nitrocellulose membranes. After drying the membranes they were fixed for 15 min in a solution containing 10% (v/v) acetic acid and 25% (v/v) isopropanol, rinsed with water and blocked in 5% (w/v) fat free milk. Membranes were incubated with rabbit antibodies against Alexa 488 and goat anti-rabbit antibodies coupled to HRP. Blots were then analyzed by using the Western Lightning Chemoluminescence System from PerkinElmer Life Science and a FujiFilm LAS-1000 reading device. For quantification of the signal, the intensities of the dots were measured and the background signal subtracted (using self-written routines in Matlab).

Biochemical Fusion Assay

The biochemical fusion assay uses PNS-fractions containing biotin-HRP and avidin, respectively. Only when endosomes fuse and undergo content mixing, the biotin-HRP and the avidin meet and thereby form stable complexes. The amount of formed complexes is therefore the readout of fusion efficiency, it can be measured by immunoprecipitation of avidin and quantification of HRP ([Gorvel et al., 1991](#); [Gruenberg et al., 1989](#); [Holroyd et al., 1999](#)).

Preparation of this assay required the biotinylation of HRP or insulin and the production of anti-avidin-beads. For biotinylation of HRP, 40 mg HRP or insulin were dissolved in 19 ml buffer (0.1 M $\text{NaHCO}_3/\text{Na}_2\text{CO}_3$, pH 9.0) and 22.8 mg biotin-X-NHS (biotinyl- ϵ -aminocaproic acid N-hydroxysuccinimide ester, Calbiochem) were dissolved in 1 ml dimethylformamide in a glass tube. Both components were mixed and incubated with gentle stirring for 2 hours at room temperature (50:1 molar

excess of biotin). The unreacted active groups were quenched with 2 ml of 0.2 M glycine pH 8.0 and mixed for an additional 30 min. The mixture was then dialyzed against 3x 0.5 l internalization medium (OPTIMEM and glucose) and stored at -20°C until use. For preparation of anti-avidin-beads, 1 ml Protein A sepharose beads were 3x washed in PBS, 100 μ l anti-avidin antibody were added and the tube was filled up to 2 ml with PBS. The beads were rotated over night at 4°C and, 3x washed in PBS and stored at 4°C 1:1 in PBS.

Biochemical fusion reactions (**Figure 3.7 E**) PNS containing biotin-HRP and avidin, respectively, were carried out in 200 μ reactions as normal fusion reactions with the following changes. 10 μ l biotin-insulin (1 mg/ml, Sigma) was added to the cytosol mixture to quench all the free avidin. After sequential addition and mixing of the two PNS-fractions (avidin-containing PNS first, then biotin-HRP-containing PNS) the reactions were incubated at 37°C. They were then chilled on ice and 10 μ l biotin-insulin were added again. For extraction of the avidin-biotin-HRP complexes (that could only be formed from the content mixing of two endosomes containing biotin-HRP and avidin, respectively), 10 μ l 20% triton-X-100 were added and the samples were incubated with agitation for 1 hour at 4°C. The samples were then cleared by centrifugation 2 min at 4°C in a table-top centrifuge at maximum speed and incubated with 75 μ l avidin bead solution (50%) for 1 hour at room temperature. The beads were 3x washed in PBS and bound HRP was quantified by an ABTS colorimetric reaction.

Size Determination of Endosomes using STED Microscopy

Transferrin-Alexa 488 was labeled with the dye Atto647N (ATTO-TEC, Siegen, Germany), via its succinimidyl ester, using a conventional protocol recommended by Invitrogen. Sorting/budding reactions were carried out in 50 μ l volumes and 15 μ l were centrifuged on coverslips (18 mm diameter) as described above. The PNS was then fixed with 4% paraformaldehyde (PFA) in PBS for 30 min and the unreacted PFA was quenched with PBS containing 100 mM ammoniumchloride. After washing them again with PBS, coverslips were mounted in Mowiol ([Willig et al.](#),

2006) medium. Samples were imaged using a TCS STED (Stimulated Emission Depletion) superresolution fluorescence microscope from Leica Microsystems GmbH (Mannheim, Germany), with a 1.4 NA 100 \times objective (Leica). Excitation was performed with a 635 nm diode laser, and depletion was achieved via a Spectra-Physics MaiTai tunable laser at 750 nm. Signal was detected by use of an avalanche photodiode. The system resolution limit was approximately 70-90 nm, measured by analysis of crimson-fluorescent beads (20 nm diameter, Invitrogen).

For image analysis, line scans (11 pixels width, 41 pixels length) through the endosomes were made and lorentzian curves were fitted

$$y = y_0 + \frac{a}{1 + \left(\frac{x-x_0}{b}\right)^2}$$

where $2b$ is the full width at half maximum. The full width at half maximum was measured for at least 600 spots in each condition, for each independent experiment. The values were binned into 10 nm or 20 nm classes and histograms were plotted.

Size Determination of Endosomes using Electron Microscopy

In vitro reactions using HRP-labeled PNS were carried out and subjected to a centrifugation step at 100,000 $\times g$ in a Beckmann TLA 100.0 rotor. The resulting pellets were washed with homogenization buffer and incubated in homogenization buffer containing 1.5 mg/ml di-amino-benzidine (DAB) and 0.02% H₂O₂ for 15 minutes at room temperature (Stoorvogel et al., 1991). Samples were washed with homogenization buffer, fixed with 2.5% glutaraldehyde for 40 minutes, and quenched with PBS containing 100 mM NH₄Cl for 20 minutes. The samples were then postfixed for 50 min with osmium (1% in PBS), dehydrated using a series of ethanol and propylene oxide dilutions, and embedded in Epon resin. This was done as described in Rizzoli and Betz (2004) and Denker et al. (2009), using a dehydration series of 30%, 50%, 70% ethanol for 5 min each, 90% and 95% ethanol for 10 min each, 100% ethanol for 3 \times 10 min, 50% propylene oxide in ethanol for 10 min, 100% propylene oxide for 3 \times 10 min, 50% epon resin in propylene oxide over night with rotation and 100% epon resin for 8 hours. Samples were cured for 48 hours at 60 $^{\circ}$ C and cut into

90 nm-thick sections (silver-gold). Sections were placed on formvar-coated grids and imaged using a Philips CM-12 electron microscope. Data analysis was performed semi-manually, using a line-scan routine in Matlab.

Immunostainings

Budding reactions were carried out in a 50 μ l volume using PNS labeled with transferrin-Alexa 488. To ensure distinct spots in the staining, 1.25 - 3.75 μ l were centrifuged on BSA-coated coverslips (overnight incubation in 10 mg/ml BSA at 37°C) after Tetraspeck beads were attached. Antibodies (see above) were added 1:100 in PBS complemented with 1.5% (w/v) BSA for 1 hour at room temperature (RT). The coverslips were washed with PBS and Cy5-labeled secondary antibodies were added 1:100 in PBS+BSA for 45 min RT. After washing the coverslips again with high-salt PBS (500 mM NaCl, 20 mM Na₂HPO₄, pH 7.4) and normal PBS, coverslips were mounted in Dako Fluorescent Mounting Medium (DakoCytomation). Images were acquired in the green (Alexa 488) and dark red (Cy5) channel. For the analysis of correlation between transferrin-Alexa 488 fluorescence and SNARE stainings, line scans (3 pixels widths, 15 pixels length) were made through endosomes in the green and red channels (using Matlab). Correlation coefficients between the curves were calculated as previously described (Rizzoli et al., 2006), and the fraction of objects with a high degree of colocalization (correlation coefficient ≥ 0.8) was measured. Values were corrected for accidental colocalization.

2.2.8 Endosomal Sorting/Budding Assays in Intact Cells

Spot-by-Spot Assay in PC12 Cells

PC12 cells grown on poly-L-lysine-coated coverslips were labeled with fluorescent markers as for the *in vitro* assays (see above). They were then either fixed immediately in 4% paraformaldehyde (PFA) in PBS, or washed with PC12 medium and chased for another 30 min before fixation. Unreacted PFA was quenched with PBS containing 100 mM ammoniumchloride. After washing the fixed cells again with

PBS, coverslips were mounted in Dako Fluorescent Mounting Medium (DakoCytomation). Samples were imaged using a TCS SP5 STED fluorescence microscope from Leica Microsystems GmbH (Mannheim, Germany), with a 1.4 NA 100x objective (Leica). Fluorescence was excited at 488 nm (Argon laser) and 547 nm (HeNe laser), and was collected via appropriately positioned AOTF filters. For the analysis of correlation between transferrin-Alexa 488 and LDL-DiI, we made line scans (3 pixels widths, 21 pixels length) through endosomes in the red channel using Matlab. Correlation coefficients between the curves were calculated as previously described (Rizzoli et al., 2006), and the fraction of objects with a high degree of colocalization (correlation coefficient ≥ 0.9) was measured. Values were corrected for accidental colocalization.

Correlation Assay in PC12 Cells

PC12 cells were grown on poly-L-lysine coated coverslips over night, labeled with the fluorescent markers transferrin-Alexa 488, LDL-DiI and cholera toxin subunit B-Alexa 647 for 5 minutes, chased the cells for various length of time and fixed, as above. Imaging was performed by use of an epifluorescence microscope Olympus IX71 microscope, equipped with a F-View II camera, via a 100 \times , 1.4 NA, UplansApo objective (Olympus). An optovar lens of 1.6 \times was used to enlarge the image zoom. The same filtercubes were used as described above for the Zeiss Axiovert 200M fluorescence microscope. The overlap between the differently labeled endosomes was calculated by a custom-written Matlab routine and normalized to the initial (before starting the chase) levels.

Size Determination of Endosomes using STED Microscopy

For the size determination of early endosomes in intact cells, PC12 cells were grown on poly-L-lysine coated coverslips over night. The next day, the cells were washed and incubated (15 minutes, on ice) with transferrin-Atto647N (see above) dissolved at 50 $\mu\text{g}/\text{ml}$ in internalization medium (OptiMEM; Invitrogen, Carlsbad, CA, USA,

containing 10 mM glucose). Cells were then washed with Ringer buffer (130 mM NaCl, 4 mM KCl, 5 mM CaCl₂, 1 mM MgCl₂, 48 mM glucose, 10 mM HEPES/NaOH pH 7.4) and incubated for different lengths of time at 37°C. The cells were fixed as described above and imaging and data analysis was performed using the TCS SP5 STED fluorescence microscope (Leica) and the Matlab routine as described for the *in vitro* STED experiments (see above).

Colocalization Assay in COS-7 Cells

COS-7 cells were grown over night in the presence of Tetraspeck beads (200 nm diameter, dilution 1:100). The next day, the cells were starved with Dulbecco's modified Eagle's medium (DMEM with 4.5 g/l glucose) and 4 mM glutamine for 30 minutes. They were then washed with Ringer buffer (130 mM NaCl, 4 mM KCl, 5 mM CaCl₂, 1 mM MgCl₂, 48 mM glucose, 10 mM HEPES/NaOH pH 7.4), incubated with the fluorescent markers transferrin-Alexa 488 and LDL-DiI for 5 minutes and chased in COS-7 medium for different lengths of time at 37°C.

For experiments shown in **Figure 3.28**, cells were grown over night, the next day transfected with the respective GFP-constructs and only then incubated over night with the Tetraspeck beads (1:70). The cells were then also starved, washed with Ringer buffer and incubated with the fluorescent markers transferrin-Alexa 647 and LDL-DiI for 5 minutes and chased in COS-7 medium for 45 minutes at 37°C.

The cells were fixed and embedded, as described above. Imaging and data analysis was performed exactly as described for the *in vitro* colocalization assay with one difference. Fluorescent Tetraspeck beads that were lying within the cells were excluded for aligning the images. This was achieved by excluding those beads for which another intensity center in any of the channels was found within 25 pixel radius.

“The important thing in science is not so much to obtain new facts as to discover new ways of thinking about them.”

(Sir William Bragg)

3

Results

3.1 Establishing a Microscopy-Based Assay for Early Endosomal Sorting

To investigate cargo sorting in early endosomes, I took advantage of the fact that transferrin (as a recycling marker) and LDL (as a marker for the degradative pathway) are separated within these organelles. Transferrin remains bound to its receptor and is sorted into vesicles that bud off from early endosome precursors. The majority of transferrin is therefore directly recycled back to the plasma membrane by means of small carrier vesicles whereas another fraction is first transported to recycling endosomes before returning to the plasma membrane. In contrast, LDL is destined for lysosomal degradation. Thus, it remains in early endosomes during their maturation to late endosomes ([Maxfield and McGraw, 2004](#)). PC12 cells, a neuroendocrine cell line, have been used extensively to study early endosomal trafficking. Like many other mammalian cells, PC12 cells rapidly recycle transferrin, while they target LDL for degradation. I incubated PC12 cells in culture for 5 minutes with transferrin (linked to the fluorescent dye Alexa 488) and LDL (linked to the fluorescent dye DiI). As expected, they endocytose large amounts of both LDL and transferrin (**Figure 3.1 A**), with a substantial fraction of the organelles being double labeled. After a chase period the amount of double labeled organelles is drastically reduced, but not eliminated (see **Figure 3.1 B** for quantification), mainly through transferrin recycling (note the strong decrease in transferrin signal

after the chase, **Figure 3.1 A**).

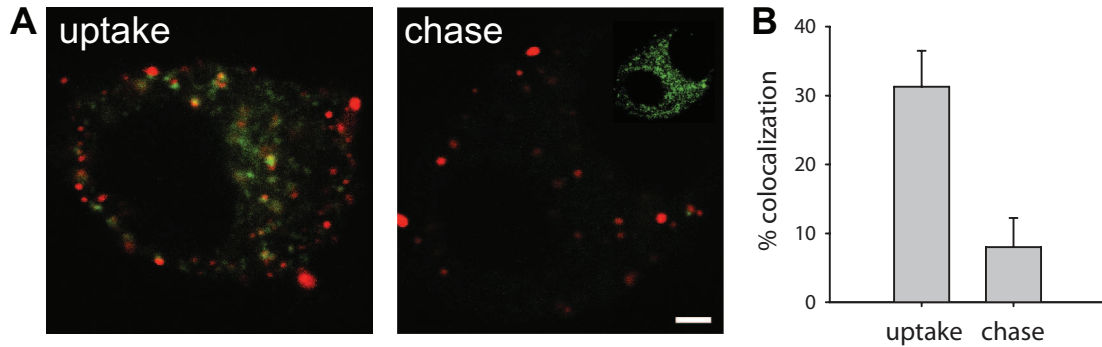


Figure 3.1: (A) Segregation of labeled cargo in intact cells analyzed by confocal microscopy. PC12 cells were loaded simultaneously with transferrin (green) and LDL (red) for 5 minutes (left panel). During a chase period of 30 minutes (right panel), a substantial amount of the transferrin is released from the cells, thus clearly segregating from the LDL label, which remains trapped. However, some transferrin still persists within intracellular organelles (see inset; the chased cell is depicted with increased contrast). (B) Quantification of colocalization. Approximately 30% of the organelles were initially double labeled, decreasing to about 8% after the chase. Bars represent means from three independent experiments (+/- SEM).

To allow easier manipulations of the sorting process, I next proceeded to reproduce this in an *in vitro* assay. I prepared post-nuclear supernatants (PNS) from cells labeled with both endocytotic tracers (see schematic in **Figure 3.2 A**). I then incubated the PNS at 37°C (or kept it on ice as a negative control) in a reaction mixture containing rat brain cytosol and an ATP-regenerating system, centrifuged the samples onto glass coverslips and imaged them using an epi-fluorescence microscope. In the negative control (the “ice” or “initial” condition), many endosomes appeared double labeled (**Figure 3.2 B**, yellow, arrowheads). After incubation at 37°C, fewer colocalized (i.e. double labeled) spots were visible, suggesting that endosomal sorting and cargo separation do occur *in vitro*.

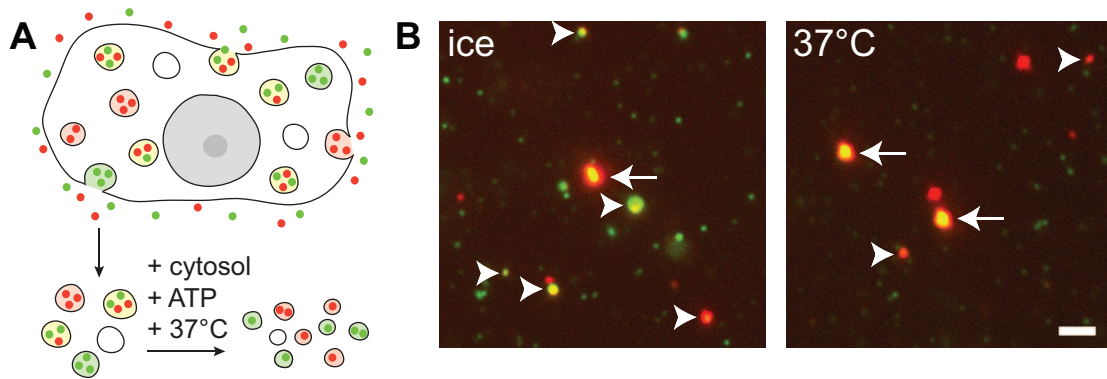


Figure 3.2: (A) Schematic overview of the *in vitro* sorting assay. PC12 cells are loaded simultaneously with labeled transferrin (green) and LDL (red), and post-nuclear supernatant (PNS) is prepared. Incubation of the PNS in the presence of ATP and cytosol results in cargo sorting and separation of the two labels. (B) Fluorescence images from samples incubated on ice (negative control) and samples incubated at 37°C (positive control). Images acquired in the green (transferrin) and red (LDL) channels were aligned by using fluorescent beads (arrows) as reference. Many endosomes appear initially double labeled (yellow, arrowheads). After sorting, fewer colocalized (i.e. double labeled) spots are visible. Scale bar = 2 μm .

3.2 Verification of the Assay

3.2.1 The Assay is not Affected by De-Aggregation, Cargo Degradation or Organelle Leakage

The decrease in colocalization hints to the fact that the assay represents endosomal sorting and cargo separation. However, does this visible decrease in the amount of double labeled endosomes indeed represent cargo sorting from one endosome? One possibility would be that this decrease represents the break-up of aggregates containing red and green endosomes. However, **Figure 3.3** clearly shows that upon incubation the number of aggregates (i.e. clustering) increases. This confirms that the colocalization in the assay is likely independent of clustering - as colocalization decreases upon incubation, while clustering increases.

Another possibility for the decrease in colocalization could be cargo degradation

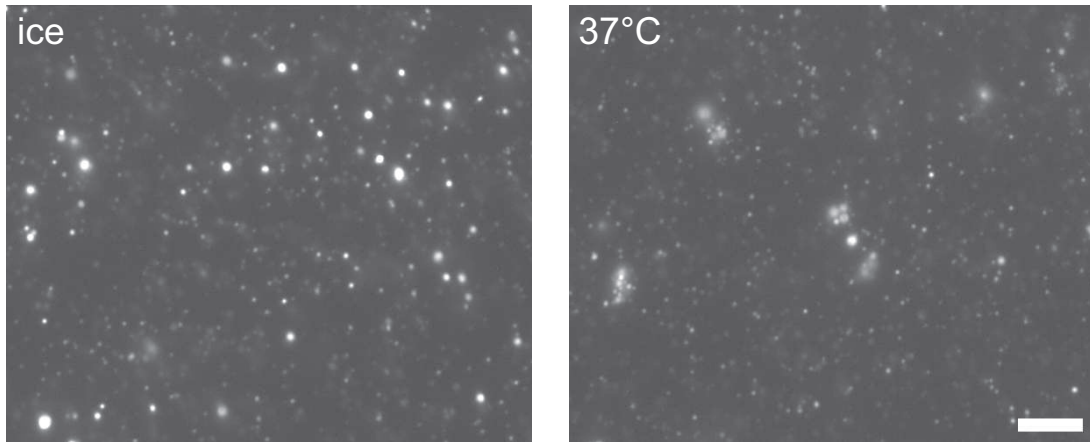


Figure 3.3: Typical images from PNS fractions labeled with transferrin-Alexa 488 before and after the sorting reaction. Upon incubation, the number of aggregates increases, while colocalization, as measured in the assay presented above, decreases. Scale bar = 5 μm .

or leakage of the endosomes (note that the transferrin-spots in the green channel do seem to become dimmer, **Figure 3.2 B**, right panel). In order to test this, I subjected the two reaction mixtures (incubated on ice or at 37°C) to a high-speed centrifugation, leading to the separation of all membrane-bound or -enclosed proteins from soluble ones. Quantification of the amount of the cargo transferrin-Alexa 488 by western blotting served then as a measure for cargo degradation and organelle leakage. Since the amount of fluorescent transferrin did not change in the pellet fraction (**Figure 3.4**), the possibility of unwanted leakage and degradation can be excluded.

3.2.2 Determination of Double Labeled Early Endosomes

As the assay is not affected by unspecific effects such as cargo degradation or leakage, I could continue to measure and quantify the amount of endosomes double labeled with transferrin and LDL (which were visually detected, **Figure 3.2 B**). As a first step, I calculated centers of intensity for all spots in both channels and measured the minimal distance of every green transferrin-containing organelle to its closest

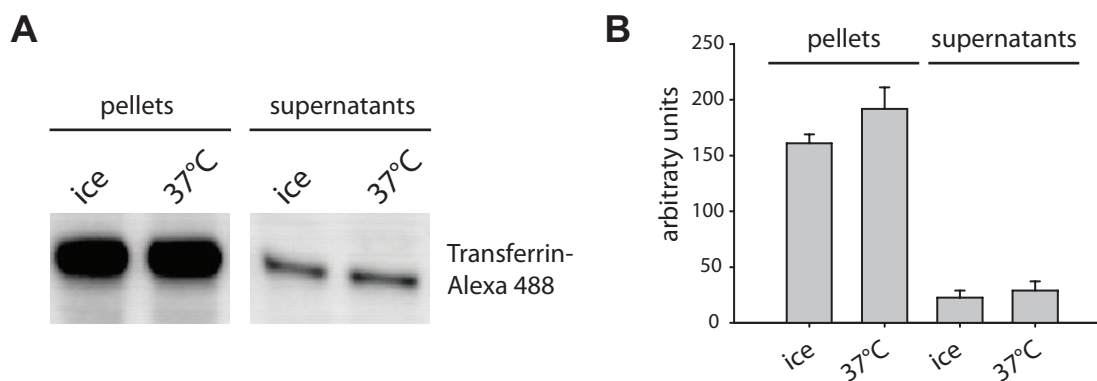


Figure 3.4: (A) Reaction mixtures (incubated on ice or at 37°C) were centrifuged at 250,000×g for 30 minutes to pellet all membranes. Equal amounts of pellet fraction and supernatant were subjected to western blotting and stained with anti-Alexa 488 antibodies. (B) Quantification shows that the levels of transferrin-Alexa488 are the same in both conditions, excluding the possibility of marker degradation and/or leakage from early endosomes upon 37°C incubation. Bars represent means from five independent experiments (+/- SEM).

LDL-containing neighbor in the red color. The histograms in **Figure 3.5** show that upon incubation at 37°C the amount of organelles lying within 1000 nm from each other decreases. This reverses only at distances above 1500 nm, which most likely represent a random positioning of organelles on the coverslip, rather than truly double labeled or docked endosomes. At low distances, a shoulder fraction up to about 100 nm and a clear peak with the maximum of about 200 nm are visible.

From this measurement the question arises what a faithfully double labeled endosome and a closely apposed (or docked) one is. To get more insight into this and to determine whether it is generally possible to discriminate between docked and genuinely double labeled organelles, I turned to fluorescent beads of sizes similar to those of endosomes (200 nm in diameter). As expected, multi-color beads gave green and red images which were scored as virtually 100% colocalized (**Figure 3.6 A**). In contrast, no significant colocalization was seen by visual inspection of the image when green and red fluorescent beads were mixed (**Figure 3.6 B**) (compare the amount of yellow spots in the overlays). As in **Figure 3.5**, I measured the distances between the intensity centers of the green and red spots, and recorded for

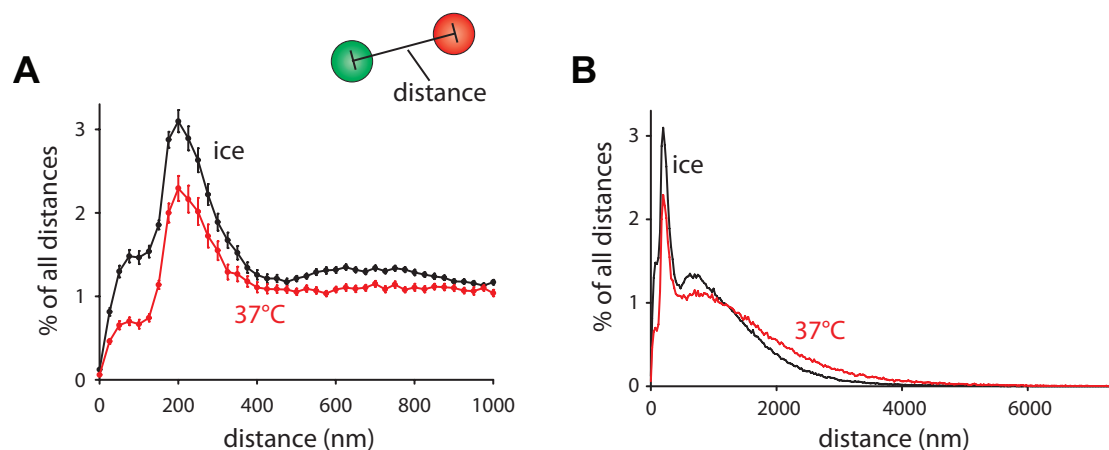


Figure 3.5: Images in taken in the green and red channel were aligned by using multi-colored fluorescent beads (see methods). Intensity centers from all the endosomes in both the green and red channel were calculated, and the distance from each transferrin spot to the closest LDL one was measured and plotted in a histogram before (ice) and after (37°C) the sorting reaction. (A) For clarity, the plot only shows distances up to 1000 nm. (B) The same plot showing distances up to 7000 nm. The graphs represent means from 43 independent experiments (+/- SEM).

each green spot the distance to its closest red neighbor. As shown in the histograms in **Figure 3.6 C**, for every green spot generated by a multi-colored bead, a red one could be found within at most about 75-100 nm, which is thus what one would also expect for a double labeled endosome. Note that the resulting peak in the histogram exhibits its maximum at 50 nm (and not at 0 nm), which is to be expected since (a) the localization along each axis is (as an approximation) following a Gaussian distribution with the maximum at 0 nm, and (b) the normal distributions along these axes are independent of each other [see [Geumann et al. \(2008\)](#) for details]. In contrast, single-colored beads could not get closer to each other than ~ 150 -200 nm, allowing to conclude that the intensity centers of single labeled endosomes cannot get much closer to each other without fusion taking place. Determining the position of intensity centers in the two channels thus allowed me to obtain a spatial resolution of objects at distances substantially below the resolution limit for the set-up (around 250 nm for the green channel, and higher for the red channel).

To get further insight into distinguishing closely apposed (i.e. docked) from double

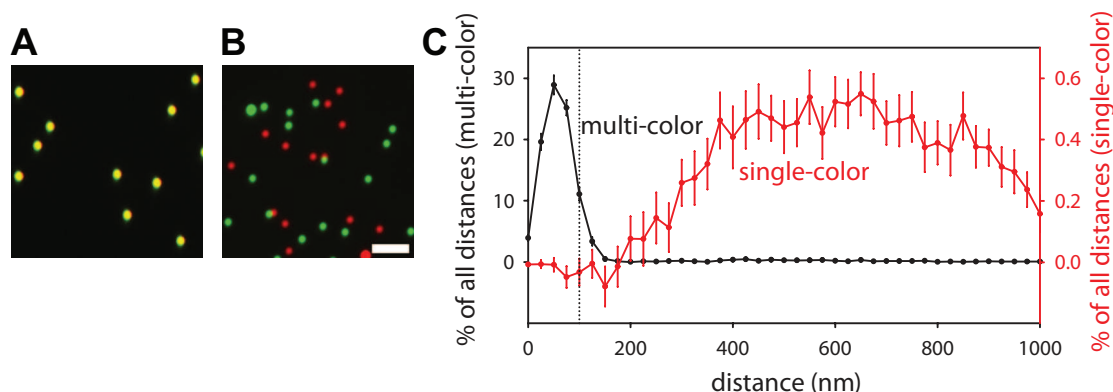


Figure 3.6: (A, B) Typical images from multi-colored (A) or single-colored (B) fluorescent beads. (C) Images acquired in the green and red channels were aligned (see methods), intensity centers from all the spots (beads) in both the green and red channel were calculated, and the distance from each spot to the closest one in the other channel was measured and plotted in a histogram. While the distance between single colored objects never falls below about 200 nm, virtually all double labeled beads have their green and red intensity centers within a 100 nm distance (vertical dotted line). The graph shows means from three independent experiments (+/- SEM).

labeled (i.e. fused) endosomes, I used the fusion assay described in **Figure 1.3** and [Brandhorst et al. \(2006\)](#). Endosomes were labeled by fluid-phase uptake of either Alexa 488- or Alexa 594-conjugated dextran, isolated from the cells and used in *in vitro* reactions containing rat brain cytosol and an ATP-regenerating system, as before. Upon incubation, many endosomes appeared fused or docked (yellow spots in **Figure 3.7 A**). Next, I applied the distance measurement to those endosomes (**Figure 3.7 B**). While samples incubated on ice or those with an ATP-depleting system exhibited only one peak at around 200 nm, the samples incubated at 37°C revealed two peaks. The first one showed a maximum at around 75 nm (which corresponds precisely to the peak of the controls with the multi-colored beads), thus confirming that this peak represents fused (or double labeled) organelle populations. The second peak exhibited a span between 150-500 nm, thus representing a population of endosomes that are not double labeled but closely associated with each other. Quantification of the first peak (0-100 nm) revealed that incubation on ice and without an energy source leads to virtually 0% colocalization. Incubation with

the fusion inhibitors NEM and α -SNAP (L294A) also blocked the formation of this peak (**Figure 3.7 C**). In contrast, this treatment had much weaker effects on the second peak (**Figure 3.7 D**). Comparing these results with a biochemical fusion (i.e. content-mixing) assay, which uses endosome populations labeled with avidin and biotin-HRP (horseradish peroxidase) and quantifies the binding of the two upon fusion as a readout ([Holroyd et al., 1999](#)), clearly showed that colocalization within 100 nm represents true fusion (**Figure 3.7 E**).

3.2.3 Quantification of the Sorting Reaction

After having identified the exact conditions under which endosomes can be counted as double labeled ones, I could quantify the results from the sorting assay. The number of double labeled organelles was in line with the observations from living cells, with about 15-30% of all LDL-containing organelles being co-labeled with transferrin (which, as more organelles were labeled with transferrin, translated into 2-6% of all transferrin-containing organelles being co-labeled in independent PNS preparations). Also, just as in the cellular context, the amount of double labeled organelles dropped substantially (but did not disappear) after incubation, allowing me to conclude that the *in vitro* sorting reaction faithfully follows the *in vivo*¹ situation. The colocalization of transferrin and LDL decreased exponentially with incubation time at 37°C with a half-time of 11.5 minutes by approximately 60% (**Figure 3.8 A**). Since the reaction seems to have reached its maximal decrease in colocalization after 30 minutes, I incubated the samples for 45 minutes in all the following experiments. Furthermore, the depletion of ATP and omission of cytosol led to a complete block of the reaction (**Figure 3.8 B**). This clearly demonstrates the dependence of endosomal sorting on an energy source and cytosolic factors, as one would expect.

¹Throughout this thesis, “*in vivo*” is used to describe experiments performed in intact cultured cells.

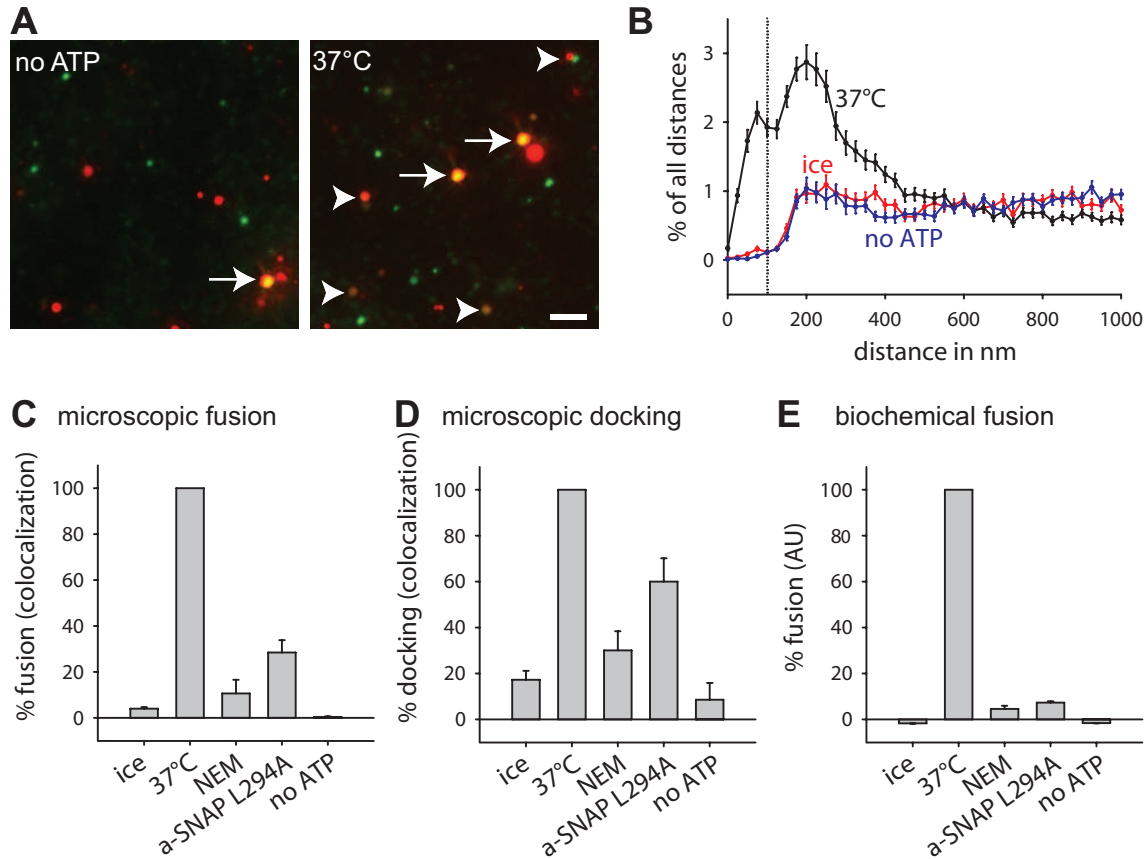


Figure 3.7: (A) Typical images from endosomes labeled with green and red dextran in an ATP-depleting system (left panel, negative control) or an ATP-regenerating system (right panel, positive control). Images taken in the different fluorescent channels are aligned by multi-colored fluorescent beads (arrows). Fused endosomes (arrow heads) are only present in the positive control. (B) Distance measurement between the intensity centers of green and red spots as in **Figure 3.5** and **Figure 3.6** shows two distinct peaks, representing fusion and docking. (B, C, D) Reactions were incubated on ice, without ATP (both negative controls), at 37°C (positive control) and with two inhibitors of the fusion factor NSF, 2 mM NEM and 50 μM of the dominant-negative α-SNAP mutant L294A. Comparing the first (C) and the second (D) peak with a biochemical content mixing fusion assay (E) confirms that the first peak represents fusion and the second one docking. The graph shows means from three to four independent experiments (+/- SEM).

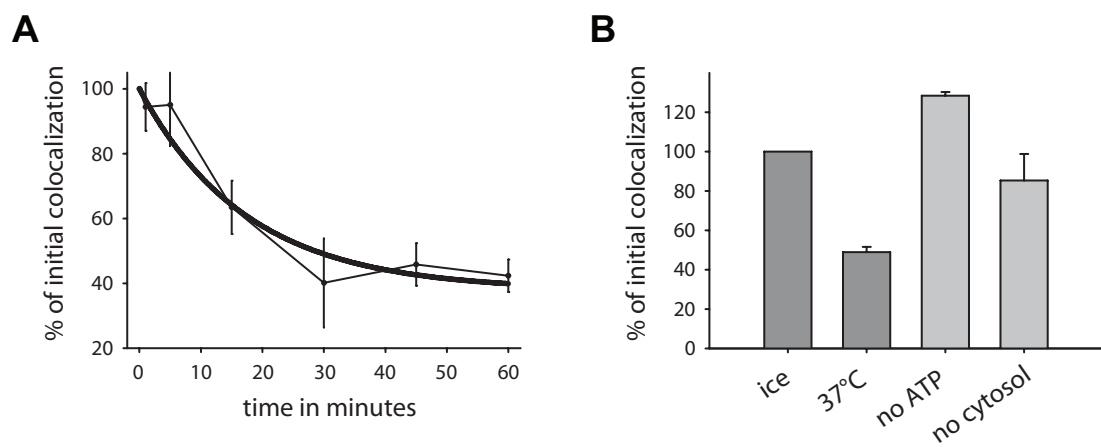


Figure 3.8: Quantification of colocalization by measuring the percentage of organelles that have their green and red intensity centers within 100 nm. (A) Samples were incubated at 37°C for various time periods. Cargo separation follows an exponential curve with a half time of 11.5 minutes. Graph represents means from two to three experiments (+/- range of values). The solid line represents an exponential decay fit. (B) Colocalization decreases by 50% after the sorting reaction. Removal of ATP or omission of cytosol completely blocks this reaction. Bars represent means from four independent experiments (+/- SEM).

3.2.4 Endosomal Sorting of Different Cargoes

I next tested whether fluorescent markers other than transferrin and LDL can be used in the assay. First, as expected, acetylated LDL acted in a very similar fashion to LDL, being segregated from transferrin in a temperature and ATP-dependent fashion (**Figure 3.9 A**).

Second, upon co-incubation with fluorescently labeled LDL and the cholera toxin subunit B (a molecule known to traffic through endosomes to the Golgi apparatus), a number of early endosomes were double labeled. *In vitro* incubation resulted in a strong reduction, as for transferrin and LDL (**Figure 3.9 B**).

Third, the inert label dextran (10 kDa molecular mass) was endocytosed in abundant amounts, and colocalized with transferrin to a substantial extent. A significant reduction was observed after incubation. However, as dextran (an inert label) also is expected to diffuse to some extent into transferrin-containing recycling vesicles, the change in colocalization is smaller than for transferrin and LDL (**Figure 3.9 C**). Finally, no significant separation could be observed when using a mixture of green- and red-labeled transferrin (**Figure 3.9 D**).

One possible complication of the *in vitro* sorting assay is that newly budded vesicles could in principle also fuse with each other. To test this, I modified the *in vitro* fusion assay [**Figure 1.3**, **Figure 3.7** and [Brandhorst et al. \(2006\)](#)] by using different cargos. Therefore, I incubated different sets of cells with each of the differently labeled markers (transferrin, dextran, cholera toxin and LDL), prepared PNS fractions, and incubated them *in vitro*. The number of fused organelles was then quantified (**Figure 3.10**). As expected, fusion was lowest between transferrin or cholera toxin and LDL, and quite high between transferrin and dextran or cholera toxin (which resulted in relatively poor cargo separation in the budding assay). Thus, while label segregation seems to follow a similar pattern for many different labels, the segregation of LDL and transferrin was least affected by post-segregation vesicle fusion, and was therefore the assay of choice for investigating the requirements of the sorting process.

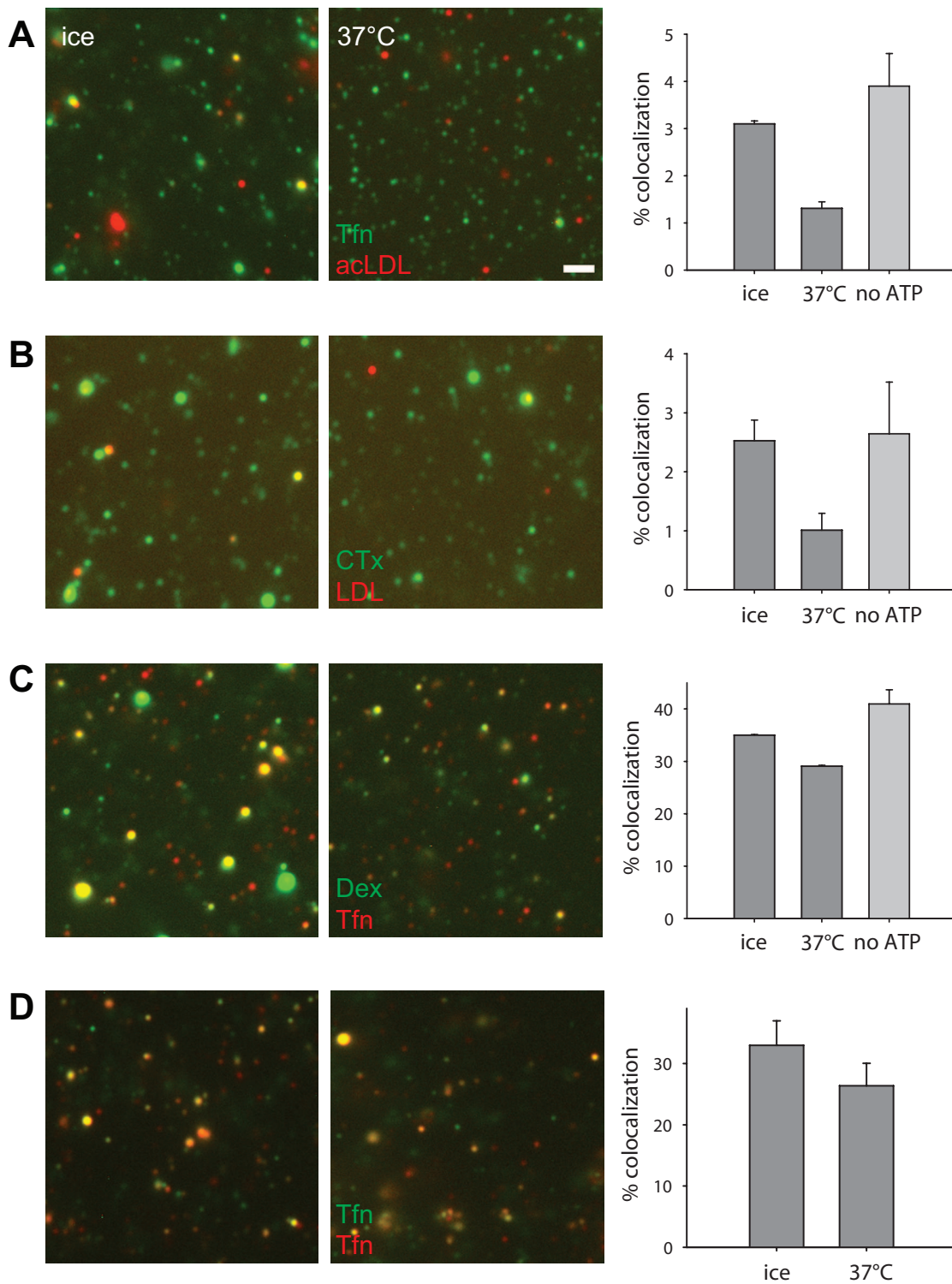


Figure 3.9 (facing page): (A) Typical images from endosomes labeled with transferrin-Alexa 488 (green) and acetylated LDL-Alexa 594 (red). Initial colocalization is about 3% and decreases by approximately 60% through an ATP-dependent process. Bars represent means from three independent experiments (\pm SEM). Scale bar = $2\ \mu\text{m}$. (B) Typical images from endosomes labeled with cholera toxin subunit B-Alexa 647 (green) and LDL-DiI (red). Initial colocalization is about 2.5% and decreases by approximately 60%. The process is ATP-dependent. Bars represent means from two independent experiments (\pm range of values). (C) Typical images from endosomes labeled with dextran-Alexa 488 (green) and transferrin-Alexa 594 (red). Initial colocalization is approximately 35% and decreases only by about 25%. Bars represent means from two independent experiments (\pm range of values). (D) Typical images from endosomes labeled with transferrin-Alexa 488 (green) and transferrin-Alexa 594 (red). Initial colocalization is about 33% and does not change significantly. Bars represent means from four independent experiments (\pm SEM).

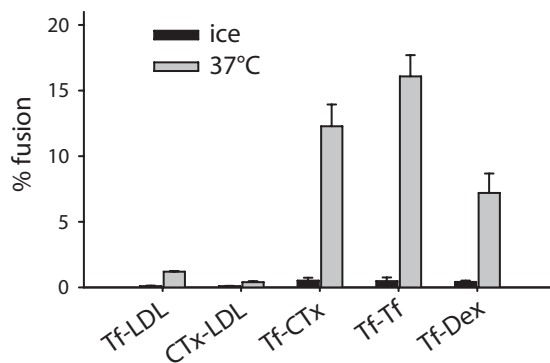


Figure 3.10: Quantification of *in vitro* fusion assays. Different pairs of labeled PNS fractions (containing transferrin, LDL, cholera toxin or dextran) were incubated as described, and results from three independent experiments are shown for each pair (\pm SEM). Transferrin and cholera toxin-labeled early endosomes fuse only to a low percentage with LDL-containing ones, while transferrin-labeled endosomes fuse strongly with cholera toxin, dextran- and transferrin-labeled ones.

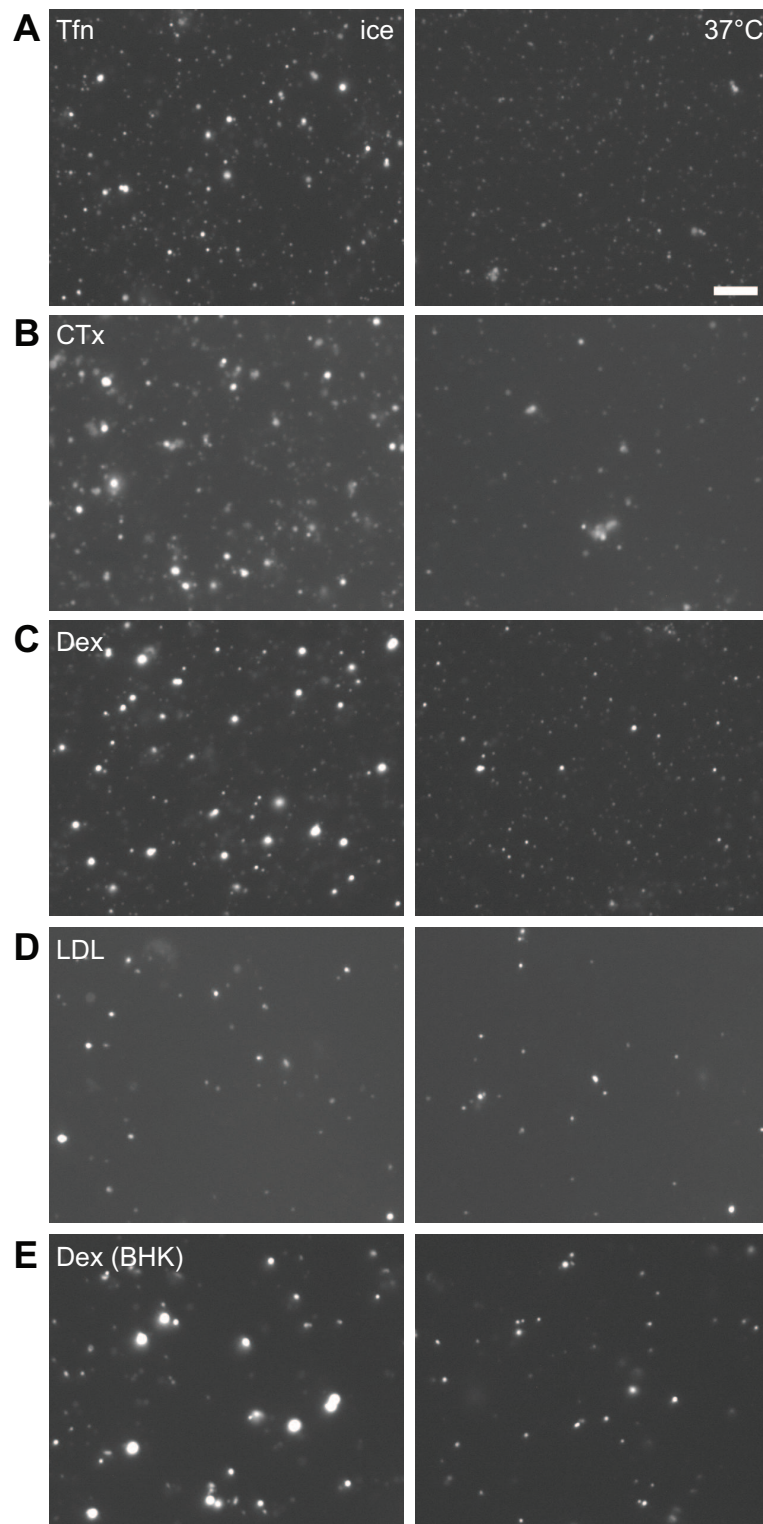
3.2.5 *In vitro* Sorting Results in the Formation of Small Transferrin-Containing Vesicles

While the presented sorting assay clearly results in the separation of transferrin and LDL from endosomes, it is still an open question whether it does so by physiological mechanisms, i.e. by the budding of small transferrin-containing vesicles. I used a number of different methods to test this.

First, I observed that, in addition to the decrease in colocalization, transferrin-, cholera toxin- and dextran-containing organelles seemed to become less bright upon incubation (which is also true for endosomes from Baby Hamster Kidney fibroblast cells, BHK). Interestingly, no such change could be observed for LDL-containing organelles (**Figure 3.11**). This is in agreement with endocytosed transferrin being sorted away from endocytosed LDL by budding of small vesicles from the endosomal precursor.

Second, to directly determine the size of the budded vesicles, I turned to a diffraction-unlimited fluorescence microscopy technique, Stimulated Emission Depletion [STED; [Donnert et al. \(2006\)](#); [Willig et al. \(2006\)](#)]. I first analyzed whole cells incubated with transferrin labeled with a STED-efficient dye, Atto647N. The cells were allowed to bind and internalize transferrin, and then were chased for various lengths of time. While the transferrin-containing organelle size was relatively high initially, an abundant fraction of smaller vesicles was observed after 5 minutes (**Figure 3.12 A, B**) of chase, indicative of budding of recycling vesicles from the endosomes. To

Figure 3.11 (facing page): (A-D) Typical images from PC12-endosomes that were either labeled with transferrin-Alexa488 (A), cholera toxin subunit B-Alexa647 (B), dextran-Alexa488 (C) or LDL-DiI (D) before (ice) and after (37°C) the *in vitro* sorting reaction. It appears that transferrin-, cholera toxin- and dextran-containing organelles get significantly dimmer while LDL-containing endosomes do not change in fluorescence intensity. (E) Typical images from BHK-endosomes that were labeled with dextran-Alexa488 before and after the reaction. Also BHK endosomes lose a substantial amount of the dextran fluorescence with incubation, indicative of the formation of small vesicles. Scale bar = 2 μm .



test whether the *in vitro* assay functions in a similar fashion, I next imaged PNS fractions using STED. As for the *in vivo* situation, a significant shift towards smaller sizes could be observed after budding (**Figure 3.12 C, D**). Additionally, a shoulder appeared around 60-80 nm, which was not present at substantial levels in the original endosome pool, in agreement with the formation of small carrier vesicles during the reaction. Together with the results from [Lim et al. \(2001\)](#) who found GLUT4 and transferrin-containing vesicles derived from early endosomes to have a similar size, this correlation of the endosome sizes observed *in vivo* and *in vitro* suggest that the *in vitro* assay faithfully reproduces the *in vivo* situation.

Third, I employed electron microscopy as an independent measure of endosome sizes and budding. I used endosomes preloaded with the fluid phase marker horseradish-peroxidase (HRP) for the *in vitro* reaction, pelleted all membranes with a high speed centrifugation and visualized the labeled endosomes by HRP-mediated di-amino-benzidine (DAB) precipitation before imaging. As for the *in vitro* STED experiments, a significant shift towards smaller sizes could be observed after incubation at 37°C (**Figure 3.13**) with a new peak appearing at around 75-100 nm. This size reduction after incubation observed by electron microscopy was very similar to the one observed with STED microscopy, further confirming the the ability of endosomes to bud small vesicles *in vitro*.

Fourth, I used differential centrifugation to examine whether endosomes can be separated from small transferrin-containing transport vesicles. Endosomes were labeled with HRP or transferrin-Alexa 488. In an initial step, slow speed centrifugation was carried out to sediment larger (not budded) endosomes. The small vesicles remaining in the supernatant were then collected by high speed centrifugation (**Figure 3.14 A**). The HRP content in the high-speed pellet was measured by a colorimetric reaction, while transferrin was quantified by immunoblotting with anti-Alexa 488 antibodies. In the presence of ATP, a major increase of the two markers could be observed (**Figure 3.14 B, C**).

Thus, the assays employed here concur in suggesting that small vesicles containing transferrin form from the double labeled endosome precursors. Finally, do LDL vesi-

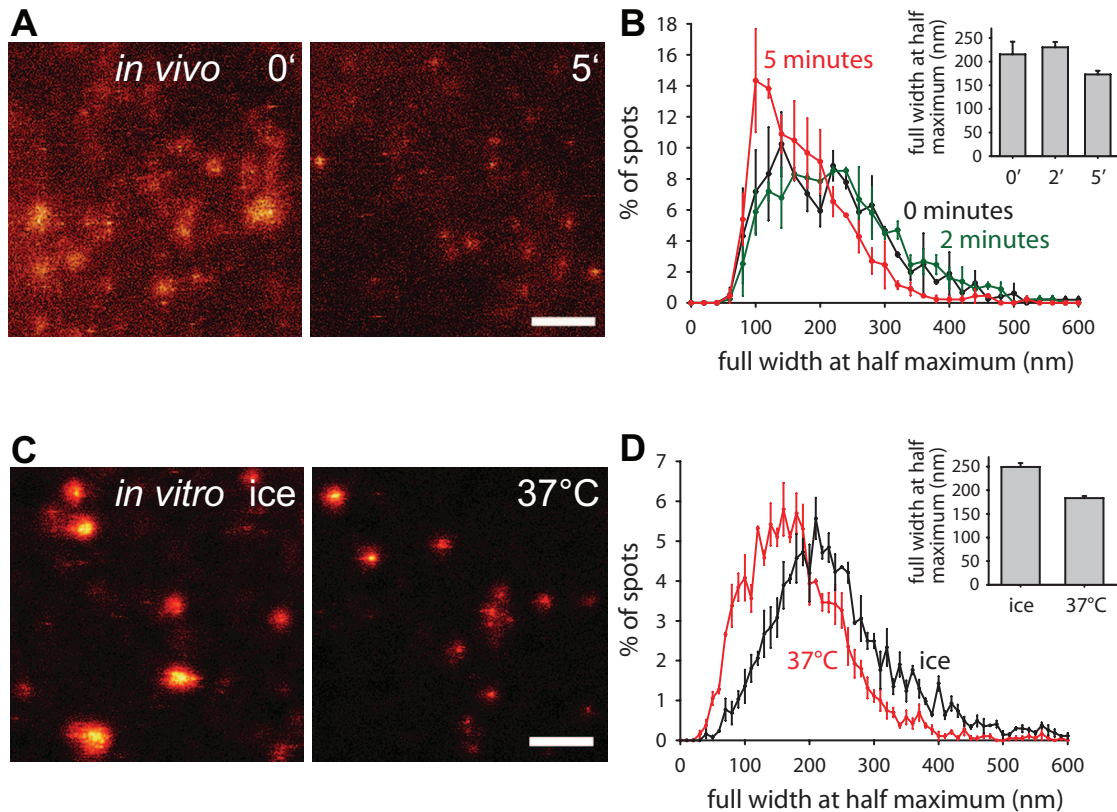


Figure 3.12: (A) STED microscopy images of PC12 cells labeled with transferrin-Atto647N. Cells were allowed to bind and internalize transferrin for 15 minutes on ice. After washing the unbound transferrin, cells were chased for different lengths of time (0, 2 and 5 minutes) at 37°C. After 5 minutes of chase, organelles appear smaller compared to the initial situation. Scale bar = 1 μ m. (B) Size distribution of transferrin-containing endosomes in intact cells as determined by STED microscopy. The sizes from 600-1000 organelles per condition per experiment were measured by taking line scans, fitting lorentzian curves and calculating the full width at half maximum (see methods). A bar graph with the average sizes for each condition (inset) and a histogram with 20 nm bins show a decrease in the size of organelles after 5 minutes. Bars represent means from two independent experiments (+/- range of values). (C) STED microscopy images of endosomes labeled with transferrin-Atto647N before (ice) and after the *in vitro* sorting reaction (37°C). Endosomes appear initially much larger than after the reaction. Scale bar = 1 μ m. (D) Size distribution of transferrin-containing endosomes *in vitro* as determined by STED microscopy. The sizes from 600-1000 organelles per condition per experiment was measured as in B. A bar graph with the average sizes for each condition (inset) and a histogram with 10 nm bins show a decrease in the size of transferrin-containing organelles after the reaction. Bars represent means from three independent experiments (+/- SEM).

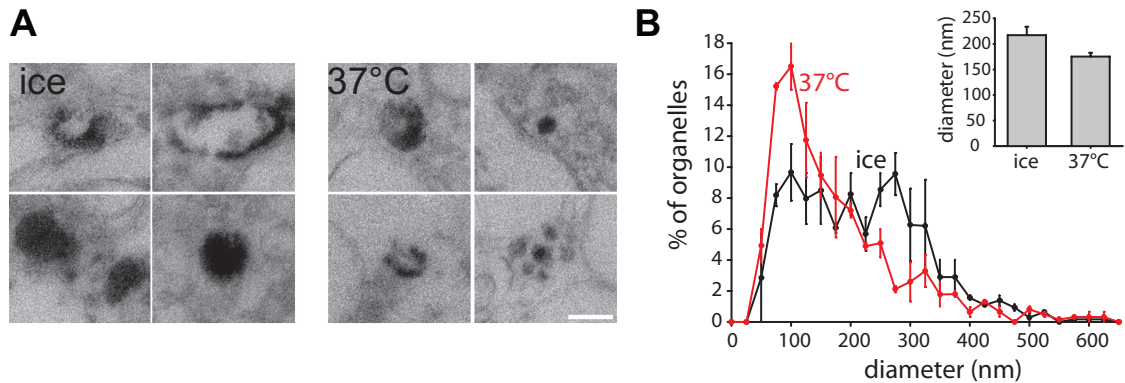


Figure 3.13: (A) Typical images of endosomes labeled with HRP/DAB precipitation product before (ice) and after the *in vitro* sorting reaction (37°C). Scale bar = 100 nm. (B) Size distribution of HRP-containing endosomes *in vitro* as determined by EM. I measured the diameters from 170-320 organelles per condition, per experiment. A decrease in the size of labeled endosomes after the reaction is shown in the histograms (25 nm bins). Graphs show means of two independent experiments (+/- range of values)

cles also bud from the double labeled endosomes? From the hypothesized model that early endosomes mature into late endosomes (Stoorvogel et al., 1991), one would expect the LDL-containing early endosome to maintain their size. This can only be addressed if one monitors individual endosomes over time. For this purpose, I adsorbed labeled organelles containing transferrin and LDL to coverslips before adding the cytosol-ATP mixture in a temperature-controlled microscopy incubation chamber. The transferrin-containing endosomes lost a substantial fraction (but not all) of their initial fluorescence, again indicative of budding of small transferrin-containing vesicles. LDL-containing organelles, however, did not get dimmer compared to the bleaching control (Figure 3.15). The efficiency of budding (i.e. the loss of fluorescence) in this assay is somewhat lower than for freely diffusing endosomes (Figure 3.11), which, however, is to be expected from glass-adsorbed organelles.

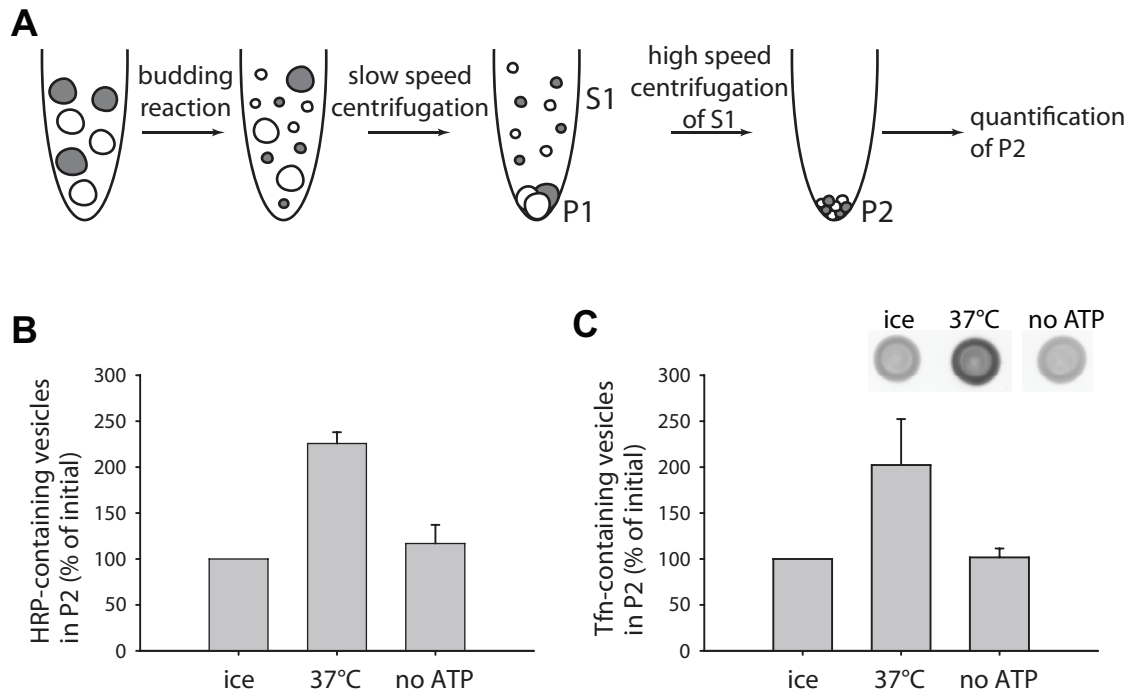


Figure 3.14: (A) To investigate whether the *in vitro* sorting reaction results in budding of small vesicles, I used a biochemical budding assay (see schematic overview). A typical reaction was performed with HRP- or transferrin-Alexa488 containing endosomes. To separate small vesicles from larger organelles, a slow speed centrifugation step was performed. The supernatant containing the small vesicles was then subjected to a high speed centrifugation, which ensured that all remaining membranes were pelleted (P2). The amount of newly formed small vesicles in P2 was then analyzed by an HRP-colorimetry reaction, or by blotting for transferrin-Alexa 488 (see below). (B) Quantification of HRP-containing vesicles from P2 by a colorimetric ABTS reaction. Bars represent means from six independent experiments (+/- SEM). (C) Quantification of small, transferrin-Alexa 488-containing vesicles from P2 by dotblots stained with antibodies against Alexa 488 (inset). Bars represent means from four to five independent experiments (+/- SEM). Note that in both of the biochemical assays, the amount of small vesicles increases with budding, in an ATP-dependent manner.

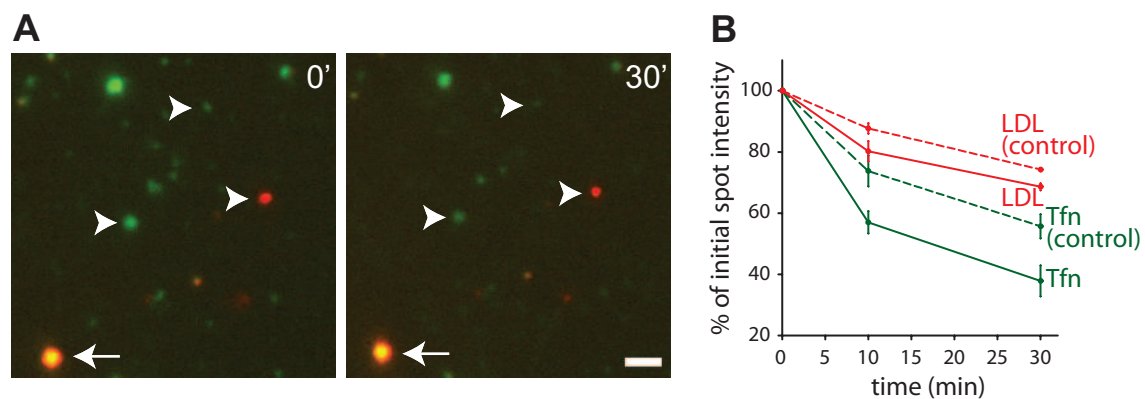


Figure 3.15: (A) To study the fate of single organelles over time (i.e. during sorting), labeled endosomes were adsorbed to coverslips before exposing them to the cytosol mix and investigating the dimming of single organelles by time-lapse imaging. The images show a field of endosomes labeled with transferrin (green) and LDL (red) immediately after the start of the reaction (0') and 30 minutes afterwards (30'). Green transferrin-containing organelles appear to lose a substantial amount of fluorescence intensity while LDL spots seem to stay bright (see arrowheads). Scale bar = $2\ \mu\text{m}$. (B) Quantification of the fluorescence of single organelles over time. Images were aligned using the fluorescent beads (arrows in A), the average fluorescence for each spot was calculated, and the corresponding background fluorescence was subtracted. While LDL-containing organelles do not get substantially dimmer (compared to a bleaching control), transferrin-containing endosomes lose much of their initial fluorescence. Graph represents means \pm SEM from three independent experiments, with each individual experiment performed at least in triplicate.

3.3 Characterization of Early Endosomal Sorting and Budding

3.3.1 Basic Requirements of Endosomal Sorting and Budding

As shown in the previous sections, it is possible to reconstitute the differential sorting of the endocytic markers transferrin and LDL in endosomes *in vitro.*, which occurs through budding of small transferrin-containing recycling vesicles. After setting-up the assay and verifying its proper functioning, I next proceeded to obtain further insight into the sorting process using the assay described in **Figure 3.2**. Therefore, several chemicals were used to block different potential effector molecules (**Figure 3.16**).

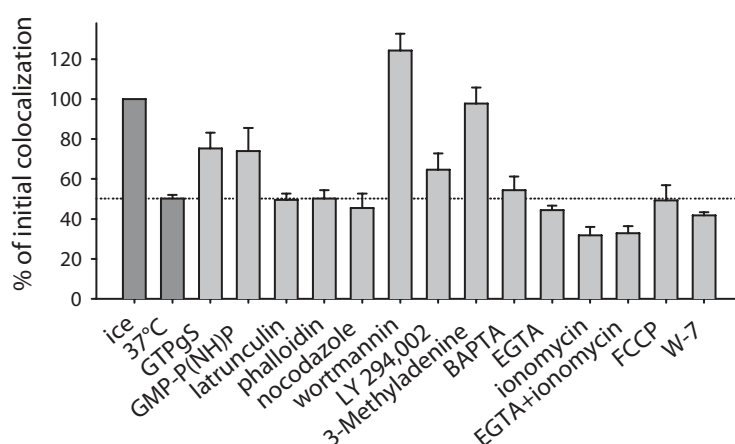


Figure 3.16: Effects of different reagents on early endosomal sorting of cargo: GTP γ S (200 μ M), GMP-P(NH)P (1 mM), latrunculin (15 μ M), phalloidin (10 μ M), nocodazole (20 μ M), wortmannin (50 nM), LY 294,002 (100 μ M), 3-Methyladenine (5 mM), BAPTA (10 mM), EGTA (10 mM), ionomycin (10 μ M), FCCP (50 μ M), and W-7 (100 μ M) were added. Inhibition of GTPases by either GTP γ S or GMP-P(NH)P blocks sorting by about 50%. The PI3K inhibitors block the reaction significantly. Bars represent means from three to ten independent experiments (+/- SEM).

Inhibition of GTPases by the non-hydrolyzable GTP-analogues GTP γ S or GMP-P(NH)P reduced the sorting efficiency by about 50%. Since endocytic sorting has been linked to the requirement of cytoskeletal elements (Murray and Wolkoff, 2003; Starnes, 2002), I also tested actin- and microtubule-inhibitory drugs (latrunculin, phalloidin, nocodazole), but found these substances not to inhibit the reaction. Interestingly, however, transferrin/LDL segregation was strongly inhibited by the phosphatidylinositol-3-kinase (PI3K) inhibitors wortmannin and 3-Methyladenine in a dose-dependent manner. As shown in **Figure 3.17**, the inhibitory concentrations (IC₅₀; 15.6 nM for wortmannin and 3.2 mM for 3-Methyladenine) are clearly lying in a range at which these substances are known to act specifically on PI3Ks (Egami and Araki, 2008; Hirosako et al., 2004; Martys et al., 1996; Spiro et al., 1996). LY 294,002, another PI3K-inhibitor, however, was less potent in blocking the sorting reaction.

Finally, I tested the effects of chelating calcium ions, or of disturbing the endosomal proton gradient on the reaction, as such treatments have been proposed in the past to interfere with endosome function (Brandhorst et al., 2006). No significant effects were seen (**Figure 3.16**), suggesting that neither calcium nor a pH gradient is required for cargo sorting, which is in line with previous findings (Wessling-Resnick and Braell, 1990).

3.3.2 EEA1 and Rab Proteins Are Required for Early Endosomal Sorting

The finding that PI3K-inhibitors block sorting suggested that phosphatidyl-inositol-(3)-phosphate (PI(3)P) is involved in the reaction. PI(3)P plays a key role in demarcating membrane domains within sorting endosomes (Di Paolo and De Camilli, 2006). As outlined in the introduction, PI(3)P is part of the Rab5 docking machinery and serves as coincidence detector in recruiting Rab5-effectors such as the early endosome antigen 1 (EEA1). PI3K inhibition also releases EEA1 from the endosome membrane in our assay (data not shown). Thus, I tested whether sorting

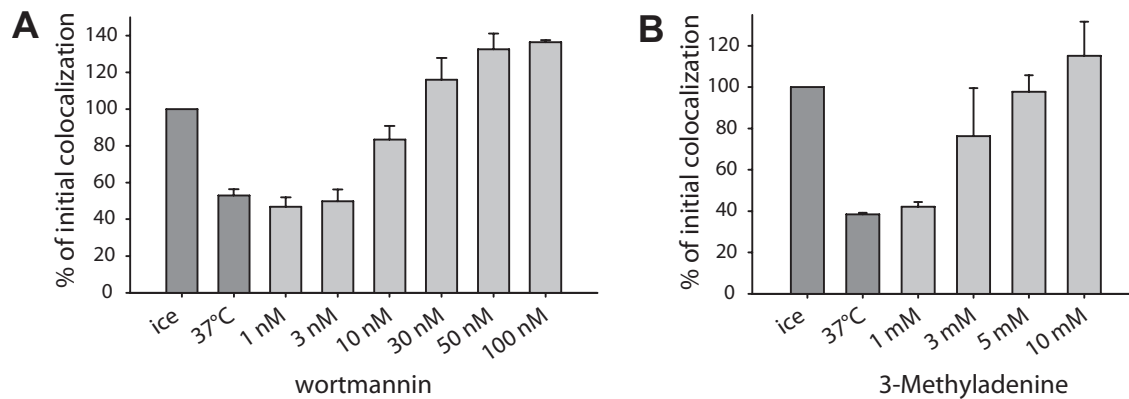


Figure 3.17: (A) Wortmannin inhibits cargo separation in a dose-dependent manner, with an IC₅₀ of 15.6 nM. Bars represent means from three to six independent experiments (+/- SEM). (B) 3-Methyladenine inhibits cargo separation in a concentration-dependent manner, with an IC₅₀ of 3.2 mM. Bars represent means from three independent experiments (+/- SEM).

also requires Rab GTPases and whether EEA1 is not only involved in membrane docking and fusion, but also in sorting and budding. For this purpose, purified GDP dissociation inhibitor (GDI), which strips Rab proteins from the organelle membrane, was added to the reaction, resulting in a strong inhibition (**Figure 3.18 A**). Additionally, a polyclonal antibody against the N-terminal peptide of EEA1 fully blocked segregation of transferrin and LDL. This inhibition was specific, as the reaction could be rescued by incubating the antibody with the antigenic peptide. Interestingly, the effects of wortmannin, GDI and of the EEA1 antibody on sorting and budding were much stronger than on fusion, which was only inhibited by 15-30% under our experimental conditions (**Figure 3.18 B**).

3.3.3 SNARE Disassembly but not SNARE Function is Required for Early Endosomal Sorting

The data shown so far indicate that segregation is sensitive to interference with proteins that are known to act in docking and fusion. Thus, the question arises whether these proteins function in sorting and budding independent of fusion, or

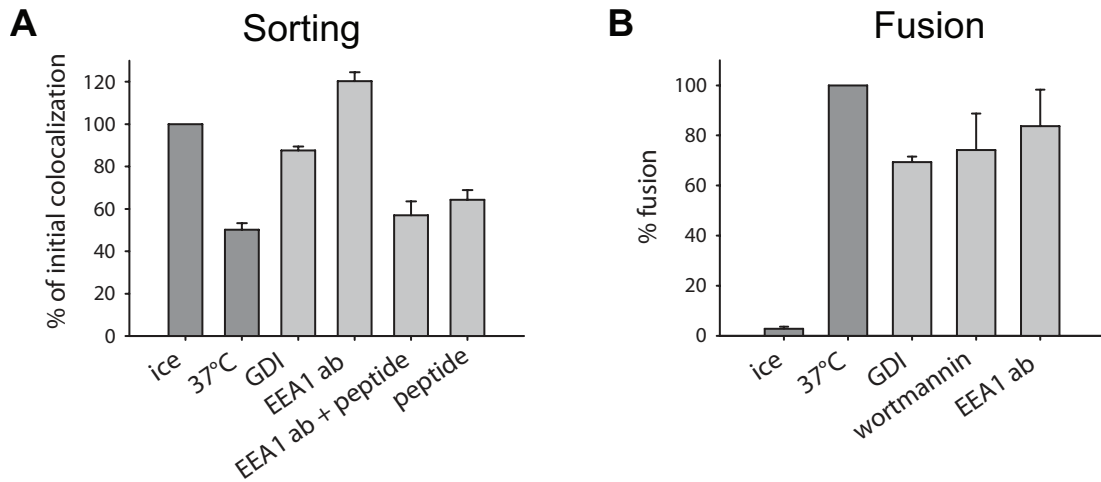


Figure 3.18: (A, B) The indicated reagents were added to *in vitro* sorting reactions (A) or *in vitro* fusion reactions (B): 10 μ M recombinant GDI, polyclonal antibodies against the N-terminal peptide of EEA1 (1:17), 200 μ M of antigenic peptides, 50 nM wortmannin). While GDI and the antibodies block cargo separation completely, they only have a minor effect on fusion. Bars represent means from three to six independent experiments (+/- SEM).

whether fusion is a prerequisite for budding. In order to differentiate between these possibilities, I tested whether budding is also dependent on the function of SNARE proteins that catalyze the final step in fusion. For this purpose, I used soluble recombinant SNARE fragments (as competitive inhibitors) and anti-SNARE antibodies to interfere with SNARE function. In agreement with previous observations (Brandhorst et al., 2006), all of these reagents inhibited fusion (albeit to a different extent, ranging from 15% to 60%). However, none inhibited sorting/budding (**Figure 3.19 A**). I then analyzed whether the sorting reaction is dependent on the activity of the *N*-ethylmaleimide (NEM)-sensitive factor (NSF). NSF, together with its cofactor α -SNAP, is required for all fusion steps in the secretory pathway. NSF functions by dissociating SNARE complexes, keeping the SNAREs in a “ready for fusion” state. When NSF is inhibited, fusion stops rapidly, as most available SNAREs on the endosome membrane spontaneously form stable four-helical SNARE complexes (Bethani et al., 2007). NEM, a potent, but non-specific, NSF inhibitor (Glick and Rothman, 1987), blocked the sorting reaction

(**Figure 3.19 B**, upper panel), in agreement with previous findings (Prekeris et al., 1998; Wessling-Resnick and Braell, 1990). To test whether this was due to a specific block of NSF, I used a dominant negative variant of the cofactor α -SNAP [α -SNAP L294A, Barnard et al. (1996)], which also blocked sorting; wild-type α -SNAP was, as expected, ineffective (**Figure 3.19 B**, upper panel). These tools potentially blocked fusion as well (**Figure 3.19 B**, lower panel), consistent with previous findings (Brandhorst et al., 2006).

Why is NSF activity, but not SNARE function, required for cargo sorting and budding? As indicated above, without NSF, the SNAREs form stable complexes on the endosomal membrane, which are entirely non-selective - any four compatible SNAREs will form a complex, irrespective of their function in different pathways (Bethani et al., 2007). However, the SNAREs need to be separated during recycling, as newly derived vesicles contain only the subset of SNAREs necessary for their function and exclude other SNAREs present in the compartments they were generated in [which has for example been demonstrated for trafficking organelles such as synaptic vesicles (Takamori et al., 2006) or COPII coated vesicles derived from the ER (Barlowe et al., 1994)]. This would explain the need for NSF activity. Are indeed newly formed vesicles different in their contents of SNAREs, when compared with the original endosomes? To test this, I immunostained the transferrin-positive organelles with antibodies against different SNAREs, and found that although the presence of some SNAREs (such as syntaxin 6, syntaxin13, VAMP4 and synaptobrevin) did not change after incubation, the levels of vti1a, VAMP3 and SNAP-25 were indeed changed (**Figure 3.20**). These observations suggest that SNAREs must be dissociated in order to be sorted into transport vesicles, and also indicate that sorting of SNAREs may be needed for carrier vesicle budding.

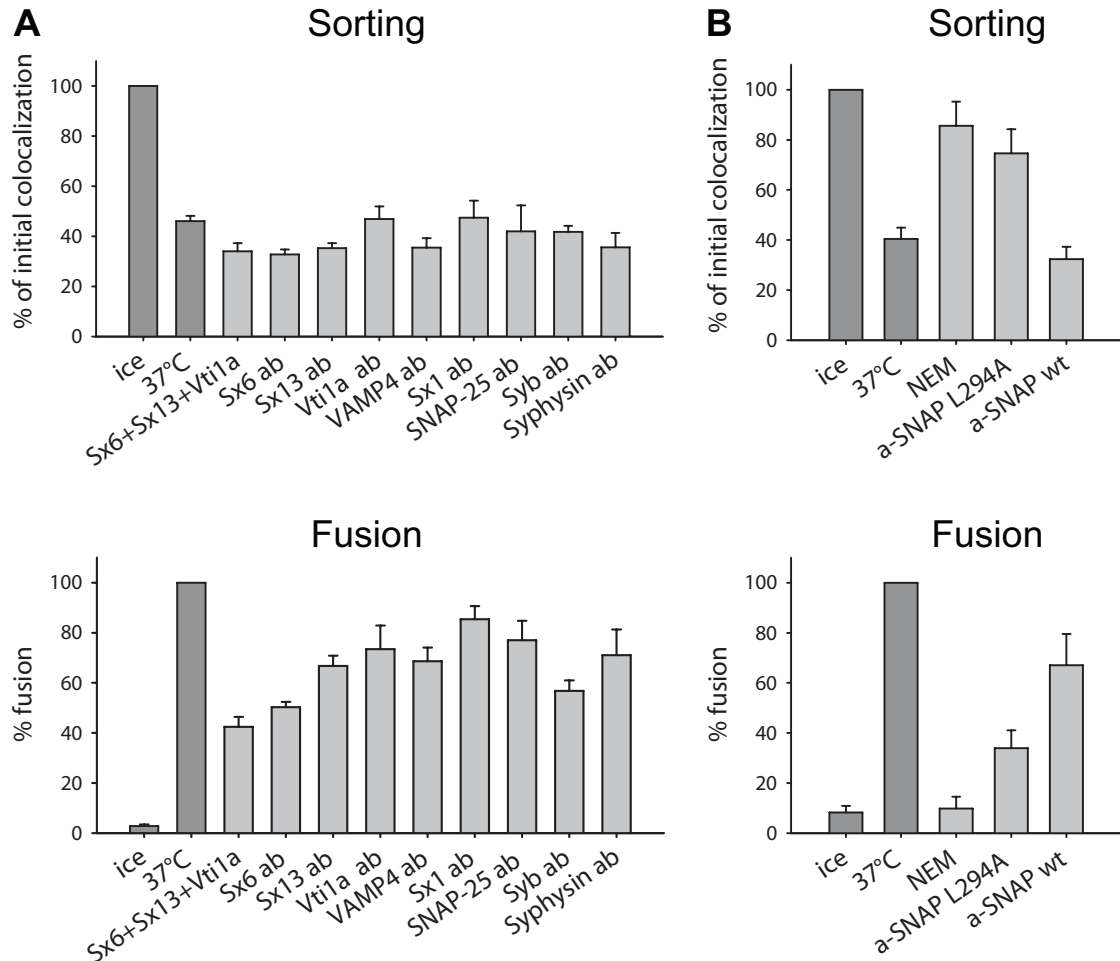


Figure 3.19: (A) Addition of the recombinant cytosolic SNARE fragments syntaxin 6, syntaxin 13 and vit1a ($30 \mu\text{M}$ each) or several polyclonal sera against SNAREs inhibit fusion efficiently (lower panel) although they have no effect on cargo separation (upper panel). Bars represent means from three to five independent experimentes (\pm SEM). (B) Inhibition of the fusion factor NSF by *N*-Ethylmaleimide (NEM, 2 mM) or the dominant-negative mutant of the NSF-cofactor α -SNAP (L294A, $50 \mu\text{M}$) block budding and fusion while the wildtype α -SNAP has no effect. Bars represent means from four to ten independent experiments (\pm SEM).

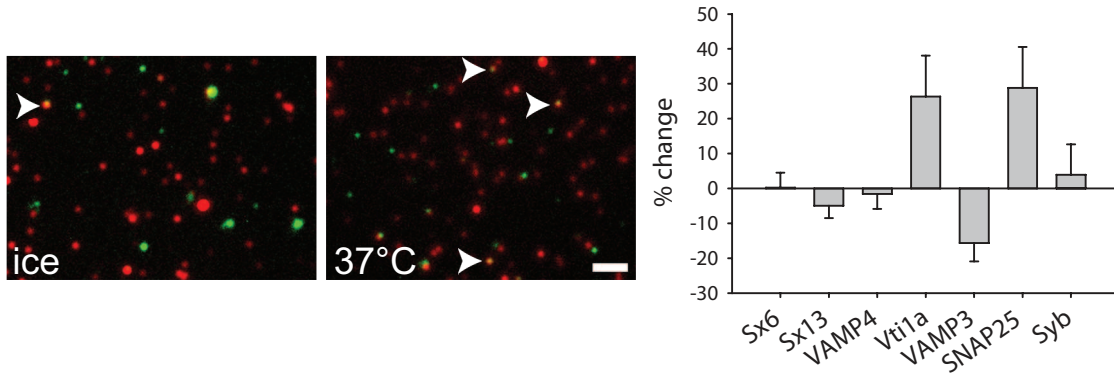


Figure 3.20: (A, B) Immunostainings of transferrin-Alexa 488-containing organelles (green) before and after sorting. The endosomes were centrifuged onto coverslips and immunostained with antibodies against vti1a (A) or syntaxin 6 (Sx6), syntaxin 13 (Sx13), VAMP4, VAMP3, synaptobrevin (Syb) and SNAP-25. Arrowheads show colocalized organelles. Bars show the change in colocalization after budding for the respective SNAREs (B), from three to six independent experiments (means \pm SEM). Scale bar = 2 μ m.

3.3.4 Cholera Toxin Subunit B Sorting also Depends on EEA1 and NSF

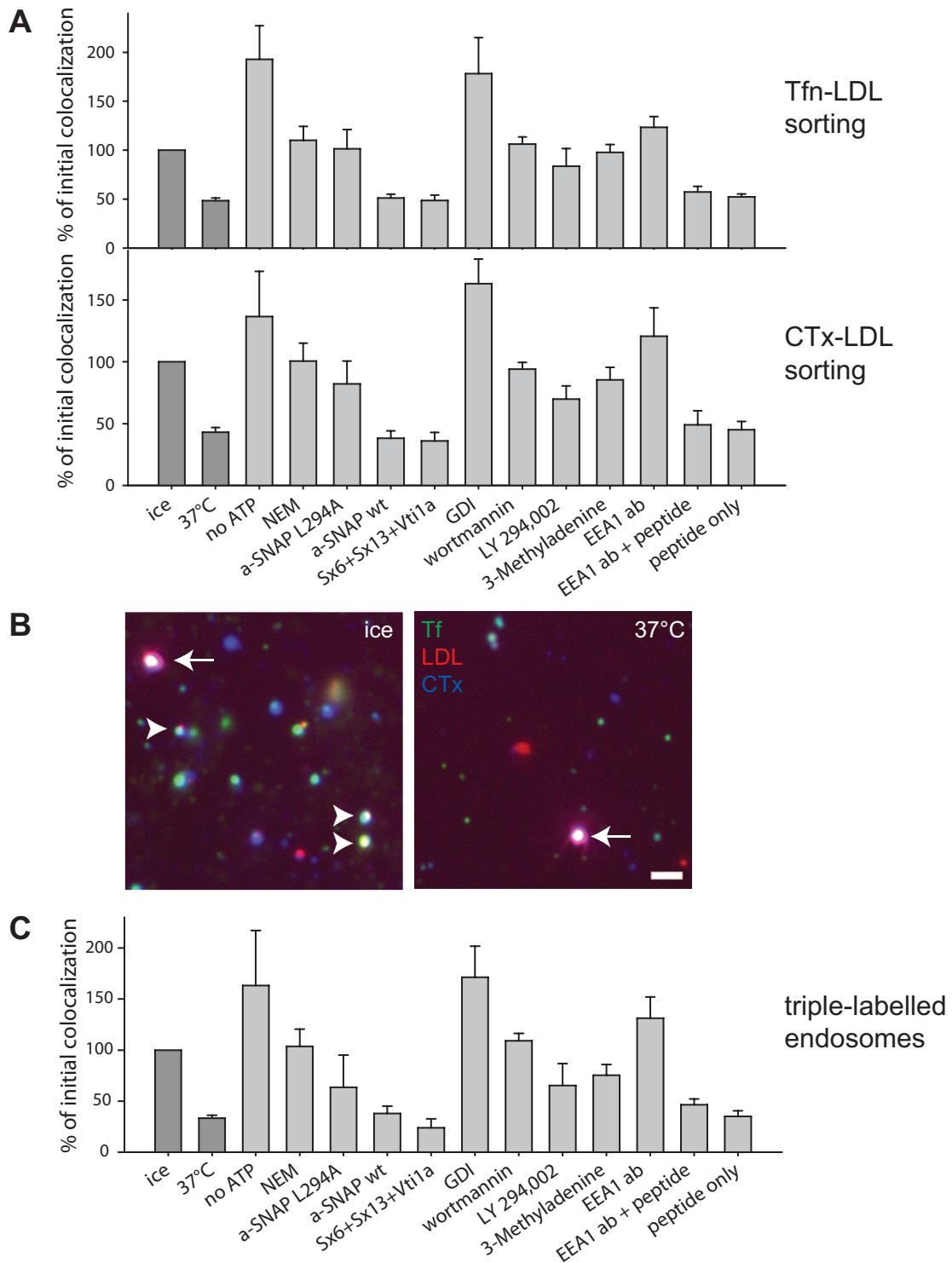
To test whether the previous findings are restricted to the sorting of transferrin from LDL, I analyzed the main conditions in triple labeled preparations, containing fluorescently labeled transferrin, LDL and cholera toxin subunit B. A substantial fraction of the organelles were multiply labeled: approximately 20% of the LDL-labeled endosomes were positive for transferrin, 15% for cholera toxin, and 6% were triple labeled. This paradigm thus allowed me to investigate in parallel not only the sorting of transferrin from LDL, but also the sorting of cholera toxin from LDL. As indicated in **Figure 3.21 A**, for both reactions sorting was dependent on ATP and temperature, as expected. The sorting was drastically reduced by the NSF inhibitors NEM and α -SNAP L294A, but not by wild-type α -SNAP, and was unaffected by addition of soluble recombinant SNARE fragments. Rab molecules were essential, as indicated by the inhibition obtained by GDI addition; the same was true for PI(3)P,

as shown by the inhibition induced by wortmannin. Finally, the polyclonal antibody against the N-terminal peptide of EEA1 fully blocked sorting, with inhibition eliminated by addition of the antigenic peptide. Thus, cholera toxin/LDL sorting exhibits all of the characteristics of the transferrin/LDL sorting process.

Moreover, I also investigated the behavior of the triple labeled endosomes (**Figure 3.21 B**) in presence of different inhibitors. While the triple labeled endosomes made up only a small proportion of all endosomes (see above), their behavior followed the same pattern as the segregation of doubly labeled organelles (**Figure 3.21 C**). While this result is entirely expected, it is important in the sense that it confirms the homogeneity of the endosome populations investigated: the triple labeled population of endosomes, constituting only about a third of any of the two double labeled populations, nevertheless reacts identically to various conditions.

Figure 3.21 (facing page): (A) Sorting of cholera toxin subunit B from LDL. PC12 cells were incubated in presence of cholera toxin subunit B-Alexa 647, LDL-DiI and transferrin-Alexa 488. PNS fractions were then prepared, and sorting reactions (top: transferrin sorting from LDL; bottom: cholera toxin sorting from LDL) were performed as described above, in presence of the following reagents: ATP depletion system, NEM, α -SNAP L294A, α -SNAP wildtype, a mixture of the endosomal Q-SNAREs Sx6, Sx13 and Vti1a, Rab GDI, wortmannin, LY 294,002, 3-Methyladenine and the anti-EEA1 antibody, in presence or absence of the antigenic peptide. All reagents were used at the concentrations mentioned above. Bars represent means from three independent experiments (+/- SEM). (B) Triple labeled PNS (cholera toxin B subunit labeling shown in blue, transferrin in green, and LDL in red). The number of triple labeled endosomes (arrowheads) decreases with *in vitro* incubation; arrows indicate multi-fluorescent beads used for image alignment. Scale bar = 1 μ m. (C) The influence of different reagents on the amount of triple labeled endosomes. The experiments were performed exactly as in (A).

3.3 CHARACTERIZATION OF EARLY ENDOSOMAL SORTING AND BUDDING



3.4 Both Carrier Formation and Endosome Maturation are Required for Cargo Sorting

After identifying several important factors that are required for cargo sorting in general, I next proceeded to investigate which factors are involved in vesicle formation (budding) from the sorting endosome. Therefore, I performed reactions in the presence of inhibitory reagents for molecules proposed to function in several budding reactions. As outlined in the introduction, there is a large variety of proteins known to be directly or indirectly involved in vesicle budding in different systems. I started to investigate a possible function of some of the “classical” and well-studied budding factors, such as clathrin, dynamin and COPI, since all of them have been proposed to be involved in budding from the early endosome (Aniento et al., 1996; Pagano et al., 2004; Praefcke and McMahon, 2004). I also tested the dependence on the retromer complex, which has been shown to be required for the early endosome to TGN transport (Bonifacino and Hurley, 2008; Bonifacino and Rojas, 2006). Due to this known function of the retromer complex, I have used the triple labeled endosomes described above, since they involve the investigation of the retrograde transport of cholera toxin from the endosome to the TGN, and could thus serve as a positive control.

To investigate the role of dynamin in early endosomal budding, I used a variety of reagents, among them a dynamin-specific inhibitor previously described as “dynasore” (Macia et al., 2006). Since dynasore was not available as such and therefore bought as the chemical (E)-*N'*-(3,4-dihydroxybenzylidene)-3-hydroxy-2-naphthohydrazide, I tested its proper functionality in cultured neurons. The concentration used was sufficient to drastically perturb synaptic vesicle recycling, a process known to require dynamin activity (Figure 3.22). Incubation with dynasore or peptides known to disrupt the interaction of dynamin with amphiphysin or endophilin (Anggono and Robinson, 2007; Jockusch et al., 2005) did not block the budding reaction (Figure 3.23 B). Furthermore, no inhibition of budding was observed in the presence of a peptide that perturbs the interaction of amphiphysin

with AP2 (Praefcke et al., 2004) or in the presence of antibodies directed against the clathrin light chain and heavy chain (Figure 3.23 B). Next I investigated whether COPI coats are involved in budding. However, no inhibition was observed in the presence of brefeldin A or of antibodies against the EAGE-peptide of COP (Duden et al., 1991), both reagents known to block coatomer formation (Orci et al., 1991; Pepperkok et al., 1993) (Figure 3.23 B). I also tested antibodies against the retromer subunits Vps26, Vps29 and Vps35, as well as against the sorting nexins 1 and 2 (Haft et al., 2000). Only a combination of the three anti-Vps antibodies resulted in mild inhibition.

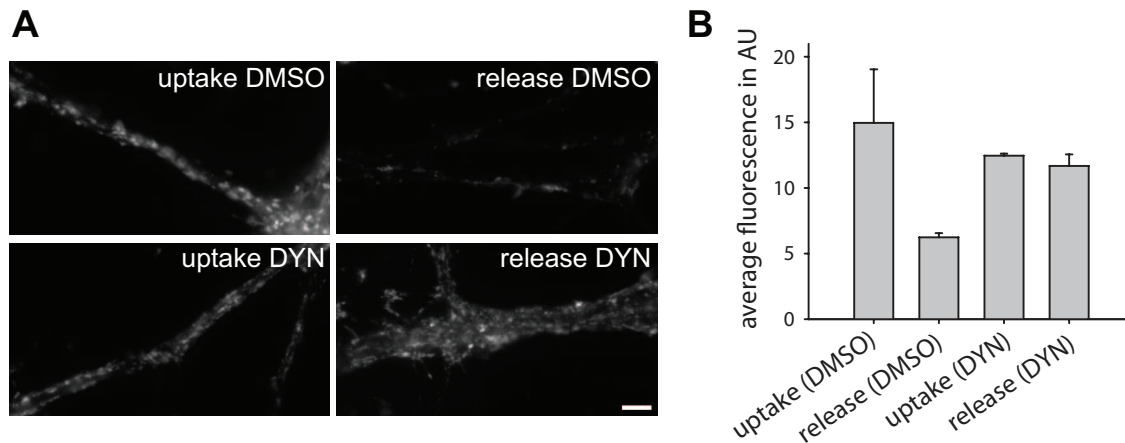


Figure 3.22: (A) Cultured hippocampal neurons were stimulated (via addition of 70 mM KCl) in presence of the styryl dye FM 2-10, which results in vesicle fusion to the plasma membrane, and subsequent endocytosis and recycling. During endocytosis, the vesicles are labeled with the dye (top left panel). Stimulating the neurons again in absence of the dye causes it to be released from the vesicles, which results in a dimming of the synaptic puncta (top right panel). Dynasore incubation ($80\mu\text{M}$) appears to inhibit somewhat the dye uptake, and to completely eradicate dye release (bottom panels). Scale bar = $5\mu\text{m}$. (B) Quantification of synaptic fluorescence. The fluorescence of the images (above background) was measured with a self-written routine in Matlab, from two independent experiments. The bars show means from two independent experiments (+/- range of values). Note that formation of new fusion competent vesicles (i.e. recycling) is, as expected, completely blocked by dynasore.

One explanation for the limited inhibition we observed is that separation of cargoes

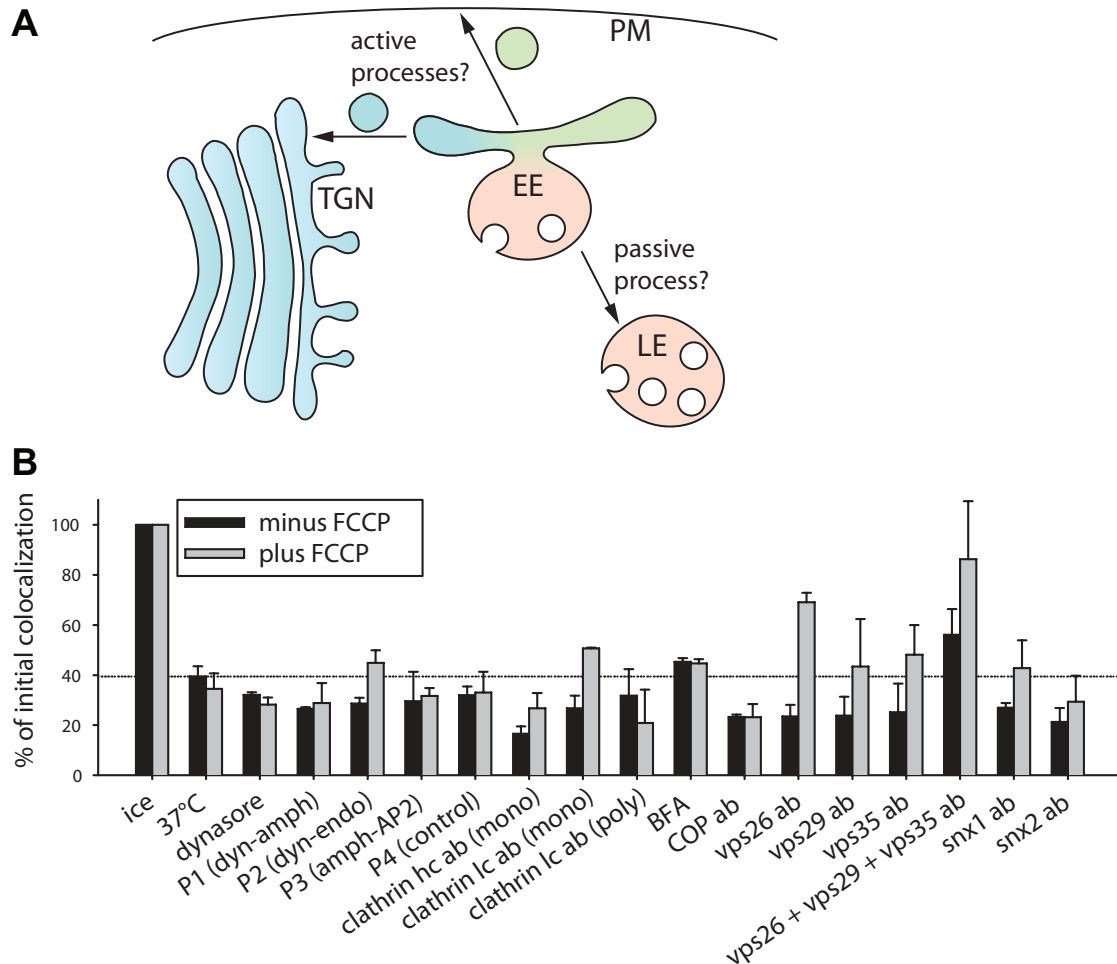


Figure 3.23: (A) Hypothetic model of cargo separation. Early to late endosome maturation may be either a passive or an active process, while cargo vesicle formation can only be seen as active. (B) Effects of different reagents on early endosomal cargo sorting, both in absence (black bars) and in presence (gray bars) of 50 μM FCCP, using triple-labeled endosomes as in **Figure 3.21**. The following reagents were used: dynasore (80 μM), peptides (1 mM for P1 and P2 and 100 μM for P3 and P4), brefeldin A (360 μM) and antibodies (1:17) were added. Bars represent means from two to three independent experiments (+/- SEM; when only two experiments were performed, the range of values is shown instead).

requires not only the budding of transferrin or cholera toxin carrier vesicles, but also active maturation of the LDL-containing organelle (**Figure 3.23 A**). To block maturation, I inhibited the acidification of the triple-labeled organelles using the proton gradient perturber FCCP; this treatment alone was not sufficient to block cargo separation (**Figure 3.16**). I next combined FCCP with the tools mentioned above (**Figure 3.23 B**, gray bars). Addition of FCCP to anti-retromer tools resulted in a strong inhibition of the reaction, while anti-clathrin/dynamin, or COP I tools were still ineffective. Similar results were obtained when quantifying the separation of transferrin from LDL, or cholera toxin from LDL (data not shown), as was also the case for the conditions indicated in **Figure 3.21**. I therefore conclude that endosome sorting requires both active maturation, as well as carrier vesicle formation. Also, these data suggest that the clathrin/dynamin pathway is not involved in sorting and budding of transferrin or cholera toxin vesicles, while they confirm the involvement of the retromer complex (Bonifacino and Hurley, 2008; Bonifacino and Rojas, 2006).

3.5 Analysis of Early Endosomal Sorting in Intact Cells

Using the new *in vitro* sorting assay, I was able to show that PI(3)-kinase, Rab proteins, EEA1, NSF, but not SNARE proteins, and two active processes (carrier vesicle formation and maturation) are required for efficient cargo sorting in early endosomes. In order to investigate the relevance of some of these findings in living cells, I next aimed at setting up a specific cellular sorting assay, which would allow to easily monitor several different conditions at one time.

First, using PC12 cells, the system that was used for the *in vitro* assay, I internalized transferrin-Alexa 488, LDL-DiI and cholera toxin subunit B-Alexa 647 for 5 minutes, and chased the cells for various length of time (**Figure 3.24**). This approach was based on the experiment described in **Figure 3.1** with the difference being the image acquisition and data analysis. While **Figure 3.1** was based on confocal microscopy and semi-manual spot-by-spot-analysis (which is relatively

slow and thus limits the amount of conditions per each experiment), data shown in **Figure 3.24** were obtained with an epi-fluorescence microscope and an automatic cross-correlation analysis. This allowed me to obtain larger data-sets for each condition and also to monitor many conditions at one time. With a half time of 9.7 minutes, the separation of transferrin and LDL *in vivo* followed a similar time course (**Figure 3.24 B**) compared to the one *in vitro* (11.5 minutes), supporting the view that the *in vitro* assay successfully reproduces sorting in intact cells.

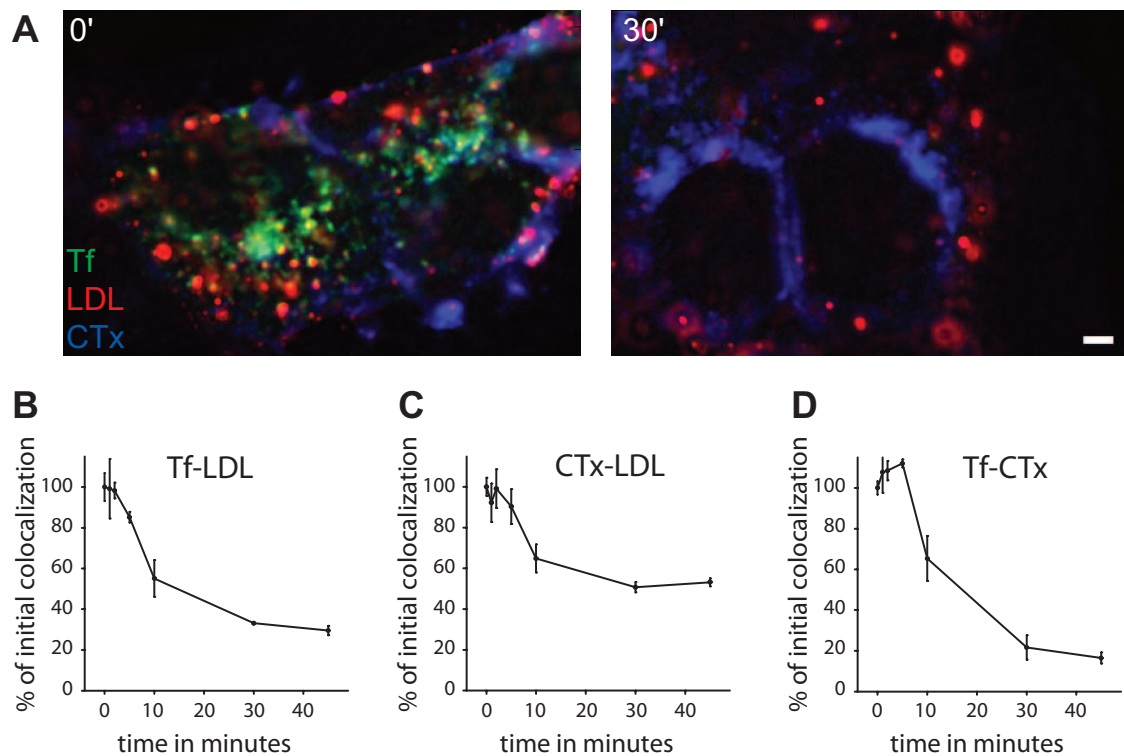


Figure 3.24: (A) PC12 cells were loaded simultaneously with transferrin (green), LDL (red) and cholera toxin B subunit (blue) for 5 minutes (left panel). A chase period of 30 minutes (right panel) releases most of the transferrin from the cells; cholera toxin now appears to localize mainly to the perinuclear (Golgi) area. Scale bar = $2\mu\text{m}$. (B-D) Quantification of colocalization *in vivo*. The overlap between the differently labeled endosomes was calculated in three independent experiments (+/- SEM). The colocalization between the three different sets of labeled endosomes is shown, normalized to the initial (before starting the chase) levels. The three kinetics can be fitted by single exponentials, with half times of approximately 9.7 (Tfn-LDL), 8.2 (CTx-LDL) and 13.9 (Tfn-CTx) minutes.

One difficulty in the analysis of PC12 cells is, however, that they are relatively round and form clusters of cells. Therefore, one can only investigate sorting on the basis of single endosomes using confocal microscopy (as shown in **Figure 3.1**), which results in a relatively poor axial resolution in such compact cells and the definition of labeled endosomes is biased by the manual analysis. In order to take advantage of the analysis I used to study the *in vitro* reactions, I turned to different cells, COS-7, which are larger and also have a flat morphology. This allowed me to identify single organelles even with an epi-fluorescence microscope, just as in the *in vitro* assay (**Figure 3.25**).

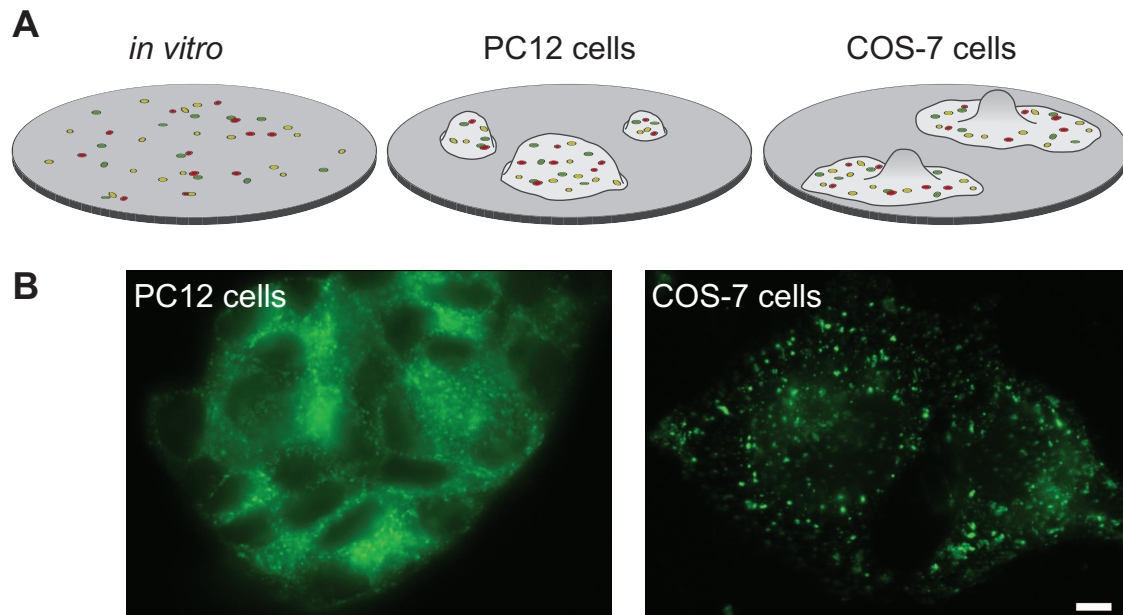


Figure 3.25: (A) Schematic overview comparing the *in vitro* sorting assay (left panel) with the *in vivo* one when using PC12 cells (middle panel) and COS-7 cells (right panel). (B) PC12 cells (left panel) and COS-7 cells (right panel) were incubated for 5 minutes with transferrin-Alexa 488. Compared to the round PC12 cells, COS-7 cells have a flat morphology, which enables to identify single endosomes using an epi-fluorescence microscope. Scale bar = 5 μm .

Since COS-7 cells are much larger than PC12 cells they might also contain larger endosomes. However, the size of the organelles might affect the distance threshold for truly double labeled endosomes (which was determined as 100 nm for the *in vitro*

assay). In order to test which threshold is appropriate for analyzing COS-7 cells, I double labeled them with transferrin-Alexa 488 and transferrin-Alexa 647, leading to virtually 100% co-staining (**Figure 3.26**, yellow spots). Images taken in the green and red channel were, again, aligned by multi-colored fluorescent beads, which were added when the cells were split and plated. **Figure 3.26** shows one broad peak of 0-250 nm for the uptake condition (right panel, black graph). However, for the chased cells one peak was visible within 125 nm (right panel, red graph) and a second, very small one at 175-200 nm. Similar observations were made when I double labeled the cells with transferrin and LDL (**Figure 3.27**). The degree of colocalization appears initially (after uptake) relatively high and drops after chase. Also, the histogram of the chase condition shows a very distinct peak ending at 125 nm until a very small second peaks arises. Since the nature of this second peak was not entirely clear and might not represent truly double labeled endosomes, I used a 125 nm threshold for this assay. An experiment with different lengths of time for the chase revealed a 9.1 minutes half-time for the sorting reaction in COS-7 cells, very similar to the values obtained for the PC12 cells *in vitro* (11.5 minutes) and *in vivo* (9.7 minutes).

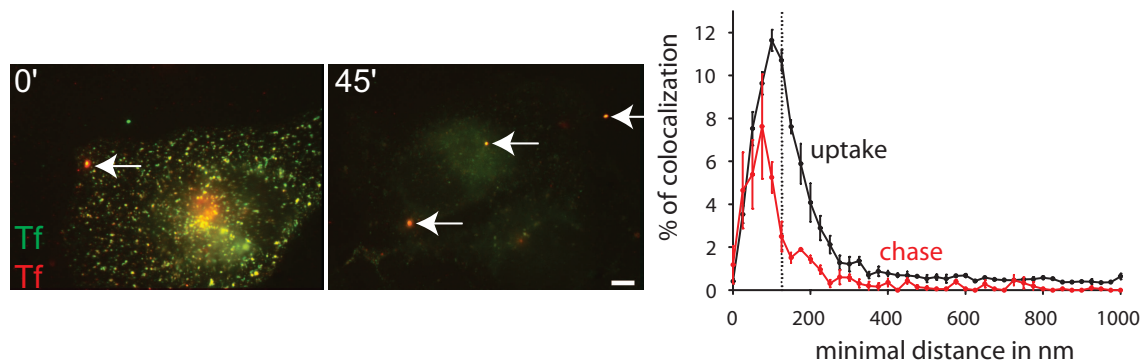


Figure 3.26: In order to identify a distance threshold for faithfully double labeled endosomes in COS-7 cells, two colored transferrins (Alexa 488 and Alexa 647) were simultaneously internalized for 5 minutes and chased for 45 minutes. Images were aligned by multi-colored fluorescent beads (arrows), centers of intensity for every spot were calculated and the distance between the closest spots in different channels was measured. The histogram (right panel) shows the distributions with a clear peak at 75-100 nm (the dotted line represents 125 nm). Scale bar = 5 μ m.

3.6 Further Investigation of the Role of Rab Proteins in Early Endosomal Sorting and Budding

3.6.1 Function of Rab GTPases Studied *in vivo*

As shown in **Figure 3.18**, the *in vitro* sorting could be blocked by the addition of recombinant GDI, suggesting the requirement for Rab GTPases in endosomal sorting and budding. It was, however, not easy to determine which Rab proteins are exactly required since there are not many specific tools available that would block the endogenous proteins. Therefore, I turned to the cellular system described above, which allows to perturb the function of Rab proteins by transiently expressing different Rab-mutants: using dominant-negative and dominant-active Rab-variants (which are very common and readily available as GFP-tagged constructs), I could label the cells with LDL-DiI and transferrin-Alexa 647 (**Figure 3.28**). In such experiments, the modified cells could be analyzed for their sorting ability. As shown in **Figure 3.28**, cells transfected with the Rab5 wildtype construct were able to separate transferrin and LDL. However, cells transfected with the dominant-negative Rab5 (S34N) were defective in sorting. Additionally, the uptake of transferrin and LDL was inhibited in those cells (data not shown), in line with observations from ([Sharma et al., 2004](#)), further suggesting that the transferrin receptor was unable to recycle back to the plasma membrane. The dominant-active variant of Rab5 led to the formation of large endosomes due to its increased fusion activity ([Barbieri et al., 1996](#)). Since the intensity centers could not be determined with a high precision in those large endosomes, the colocalization within 125 nm was measured to be initially lower.

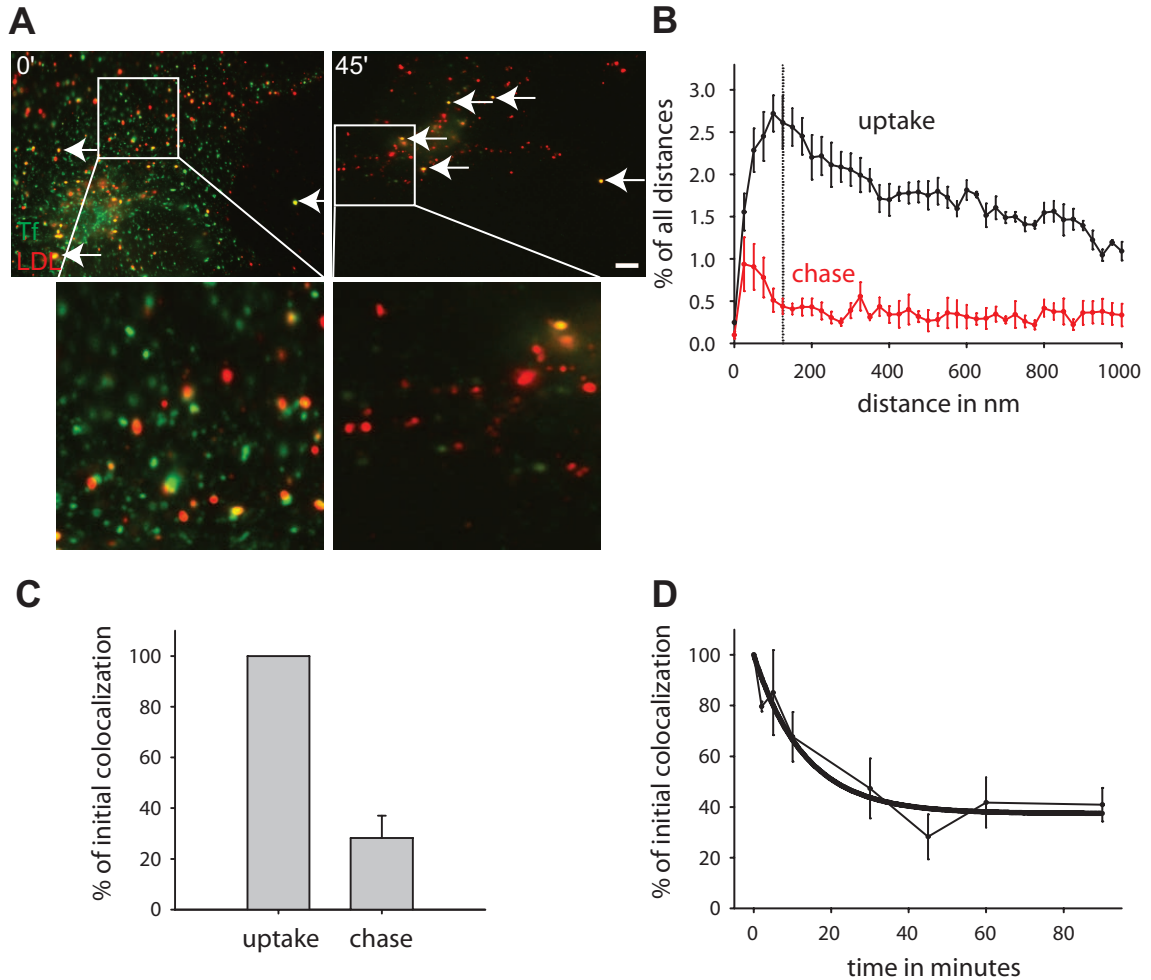


Figure 3.27: (A) Transferrin and LDL were simultaneously internalized for 5 minutes, leading to the presence of double labeled endosomes, and chased for 45 minutes. Images were aligned by multi-colored fluorescent beads (arrows). Scale bar = 5 μm . (B) Distance measurement between the closest transferrin and LDL endosomes, where the dotted line represents 125 nm. (C) Quantification of colocalization, within 125 nm (D) Time course of the *in vivo* sorting reaction in COS-7 cells with a half time of 9.1 minutes. Graphs represent means from three to four independent experiments (+/- SEM).

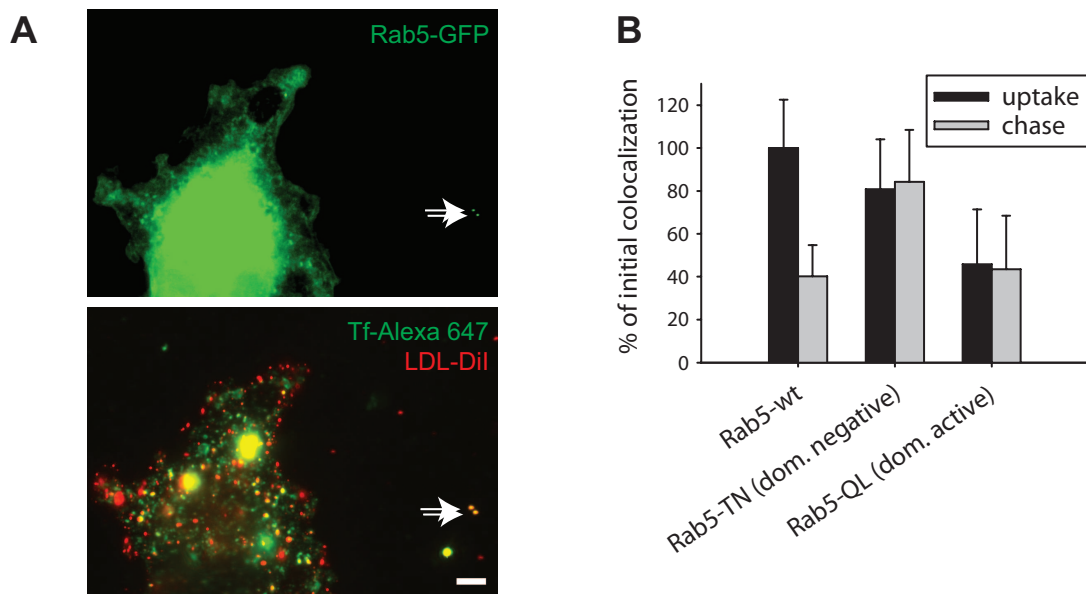


Figure 3.28: (A) COS-7 cells were transfected with different variants of GFP-tagged Rab5 (wild-type, dominant-negative [S34N] and dominant-active [Q79L]). 24 hours later, an *in vivo* sorting assay as in **Figure 3.27** was performed using LDL-DiI and transferrin-Alexa647. Scale bar = 5 μm . (B) Quantification of the sorting efficiency. Cells transfected with the wildtype Rab5 can separate transferrin and LDL normally, the dominant-negative variant fails to separate them.

3.6.2 Function of Rab GTPases Studied *in vitro*

In an independent set of experiments, I used the above mentioned *in vitro* assay to investigate the function of Rab proteins. First, I used the purified nucleotide exchange domain of Rabex-5. In the presence of high amounts of GDP, the nucleotide exchange factor will load specifically Rab5 with GDP, leading to its constant inactivation. Under this condition, sorting was completely blocked, while Rabex-5 or GDP alone caused only a mild inhibition (**Figure 3.29 A**). Second, I expressed and purified different Rab proteins in their soluble form (i.e. without prenyl-anchor) and loaded them with the non-hydrolyzable GTP analogue GMP-P(NH)P. Thus, these soluble Rab proteins are constitutively active and can bind and extract possible effector molecules from the endosomal membranes. Only the addition of Rab5 led to a strong block in the sorting reaction, while Rab4, Rab7, Rab9, Rab11, Rab22 and Rab35 had no effect (**Figure 3.29 B**). Furthermore, no increased effect could be detected upon addition of FCCP, suggesting that these Rab proteins, or their specific effectors, are not directly required for budding.

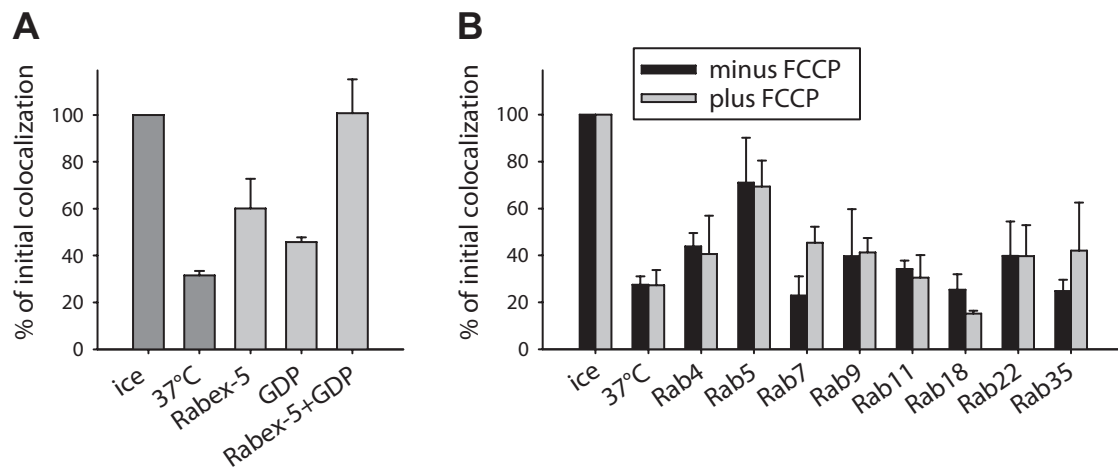


Figure 3.29: (A) *In vitro* sorting reactions were performed in the presence of 15 μ M nucleotide-exchange-domain of Rabex-5, 5 mM GDP, or the combination of both, using the triple labeled endosomes from **Figure 3.21**. Rabex-5 together with GDP block cargo separation completely. Bars represent means from two independent experiments (+/- range of values). (B) Sorting reactions were performed using 50 μ M of each Rab, in the presence or absence of FCCP. For this experiment, the prenylation inhibitor BMS-3 (8 μ M) was added to avoid unspecific *in vitro* prenylation of the Rab proteins. Only the addition of Rab5 blocks the reaction. Bars represent means from two to four independent experiments (+/- range of values).

“Science may set limits to
knowledge, but should not set limits
to imagination.”

(Bertrand Russell)

4

Discussion

4.1 A Novel *in vitro* Sorting Assay

As outlined in the Introduction, endosomes have a central role in the endocytic pathway. They constantly receive material from the plasma membrane and the TGN that has to be sorted and targeted to different organelles within the cell. The endosome is thus a highly dynamic organelle which undergoes constant rounds of fusion, sorting and budding, and at the same time maintains its identity.

In contrast to fusion, it has been difficult to reconstitute sorting and budding from endosomes *in vitro*. Indeed, much of our present knowledge about homotypic fusion of endosomes emerged from *in vitro* assays which have been around for decades (Gruenberg and Howell, 1989). In most cases, these assays are based on monitoring interactions between endocytosed markers [such as antibody and antigen, biotin and avidin, or two fluorescent dyes, Brandhorst et al. (2006)] that are derived from separately labeled cell populations and mix upon endosome fusion. Compared to live cell approaches, *in vitro* assays allow direct biochemical access to the docking and fusion machineries. For instance, proteins can be depleted or perturbed using cell-impermeant inhibitors such as antibodies. Perturbations are usually acute, largely avoiding compensatory effects that may complicate the interpretation of knock-out or knock-down approaches. In contrast, sorting and formation of vesicular carriers from early endosomes has so far largely been studied in live cells using approaches such as electron microscopy (de Wit et al., 1999, 2001; Stoorvogel et al., 1996), an-

alyzing single endosomes by fluorescence microscopy (Sharma et al., 2004) or monitoring transferrin release from intact cells with either biotinylated (Altschuler et al., 1998; Damke et al., 1994) or radioactive (Martys et al., 1996; Spiro et al., 1996) transferrin. However, these are only indirect assays to investigate sorting and budding, since transferrin recycling is a multi-step process. Therefore, inhibition of transferrin recycling is no proof for a sorting or budding deficiency but could also be the result of dysfunctions in other parts of the recycling pathway.

There is, however, so far no convenient and sensitive assay available for monitoring these processes *in vitro*, although several lines of evidence document that cargo sorting and budding of vesicles from endosomes can occur under cell-free conditions:

- In permeabilized cells (“ghost” cells), newly budded small vesicles were shown to diffuse through holes in the membranes that could later be isolated from the medium (Pagano et al., 2004; Prekeris et al., 1998).
- Kelly and collaborators developed an *in vitro* budding assay which allowed to monitor formation of synaptic-like microvesicles (SLMVs) from labeled endosomal precursors of PC12 cells using size fractionation on glycerol velocity gradients (Clift-O’Grady et al., 1998; Desnos et al., 1995; Lichtenstein et al., 1998).
- A similar assay has been used to reconstitute the budding of GLUT4 and transferrin-containing vesicles from early endosomes by biochemical fractionation (de Wit et al., 2001; Lim et al., 2001).
- Electron microscopy was used to study budding of synaptic vesicles from neuronal early endosome-like organelles (Takei et al., 1996).
- Budding of fluorescent endosomes has been analyzed using flow cytometry (Chavrier et al., 1997).
- Recently, fluorescence microscopy was used to show that the transferrin receptor can be segregated from ASOR (asialoorosomuroid, a degradative marker) in single endocytic vesicles which are prepared from rat liver homogenates (Murray et al., 2008).

However, none of these assays is of comparable ease and versatility as the fusion assays.

In the present study I therefore developed a fluorescence based cell-free assay to reconstitute the cargo sorting of budding of recycling and retrograde vesicles from early endosomes, which was based on the labeling of organelles with differentially trafficking fluorescent endocytic markers. Due to its higher signal-to-noise ratio, it was more sensitive than biochemical assays (compare **Figure 3.8** and **Figure 3.14**) and allowed to identify some of the factors essential for this process. The finding that sorting and budding require physiological temperature, cytosol, and an energy source is in line with results from other *in vitro* budding and transport assays, like those reconstituting the formation of secretory granules from the TGN (Tooze and Huttner, 1990), late endosome to Golgi transport (Itin et al., 1997), or the formation of GLUT4 or transferrin receptor-containing endocytic small vesicles (ESVs) from early endosomes (Lim et al., 2001).

As expected, transferrin recycling proceeds through the formation of small vesicles from the endosomes. This is in agreement with previous biochemical *in vitro* budding assays performed in the same system (PC12 cells), in which either budding of recycling vesicles (Prekeris et al., 1998) or synaptic vesicles (Clift-O'Grady et al., 1998) was reconstituted. I found that the newly budded vesicles have a size of approximately 60-100 nm, as determined by STED and electron microscopy. This was in line with observations from Lim et al. (2001) who showed in a different *in vitro* system that endosomes bud transferrin-containing vesicles with a size of around 70-90 nm.

As basic requirements, I found that sorting and budding are dependent on GTPases, in agreement with previous findings (Lim et al., 2001; Shi et al., 1998). However, they require neither the cytoskeletal elements actin or microtubules, nor the presence of a pH gradient, calcium or the calcium-binding protein calmodulin. Some of these observations have been discussed controversially in the past:

- It has been shown that endosome sorting, tubule formation and budding in living cells require microtubules (Egami and Araki, 2008; Lakadamyali et al.,

2006) and motor proteins (Driskell et al., 2007; Wassmer et al., 2009). In contrast, Murray et al. (2008) show that the microtubule-inhibiting drug nocodazole has no direct effect on cargo separation *in vitro*, in line with my data. This discrepancy between the *in vivo* and *in vitro* data suggest that microtubules and motor proteins are not directly required for sorting and budding but come into play in the subsequent transport step.

- Calcium plays a critical role for endosome docking and fusion (Aballay et al., 1995; Geumann et al., 2008; Holroyd et al., 1999). Also calmodulin has been shown to be required for these processes (Colombo et al., 1997), most likely via interaction with EEA1 (Dumas et al., 2001; Lawe et al., 2003; Mills et al., 2001). Calmodulin was also shown to be required for the recycling of transferrin and its receptor (de Figueiredo and Brown, 1995). Furthermore, calcium has been reported to be required for COPI coat stabilization (Ahluwalia et al., 2001) but seems not to be involved in SLMV-formation from the endosome (Desnos et al., 1995).
- The endosome lumen is slightly acidic, with a pH of around 6.0. This is crucial for the dissociation of cargo from the receptors and is therefore an important aspect of early endosome sorting. However, in agreement with my data, cargo sorting was not affected by NH_4Cl in the assay of Wessling-Resnick and Braell (1990).

As summarized in **Figure 4.1**, the sorting and budding were also dependent on major players in membrane organization and identity such as PI(3)-kinases and Rab proteins, which have been shown to be crucial for homotypic early endosomal docking and fusion (Mills et al., 1999). Interestingly, the process was also dependent on the fusion cofactors NSF and α -SNAP, but not on the function of SNARE-proteins, the molecules that drive membrane fusion (Jahn and Scheller, 2006). Furthermore, efficient cargo separation required both carrier vesicle formation (of recycling or retrograde vesicles) and active maturation (for early to late endosome transition). The role of these molecules and processes will be discussed in detail in the following sections.

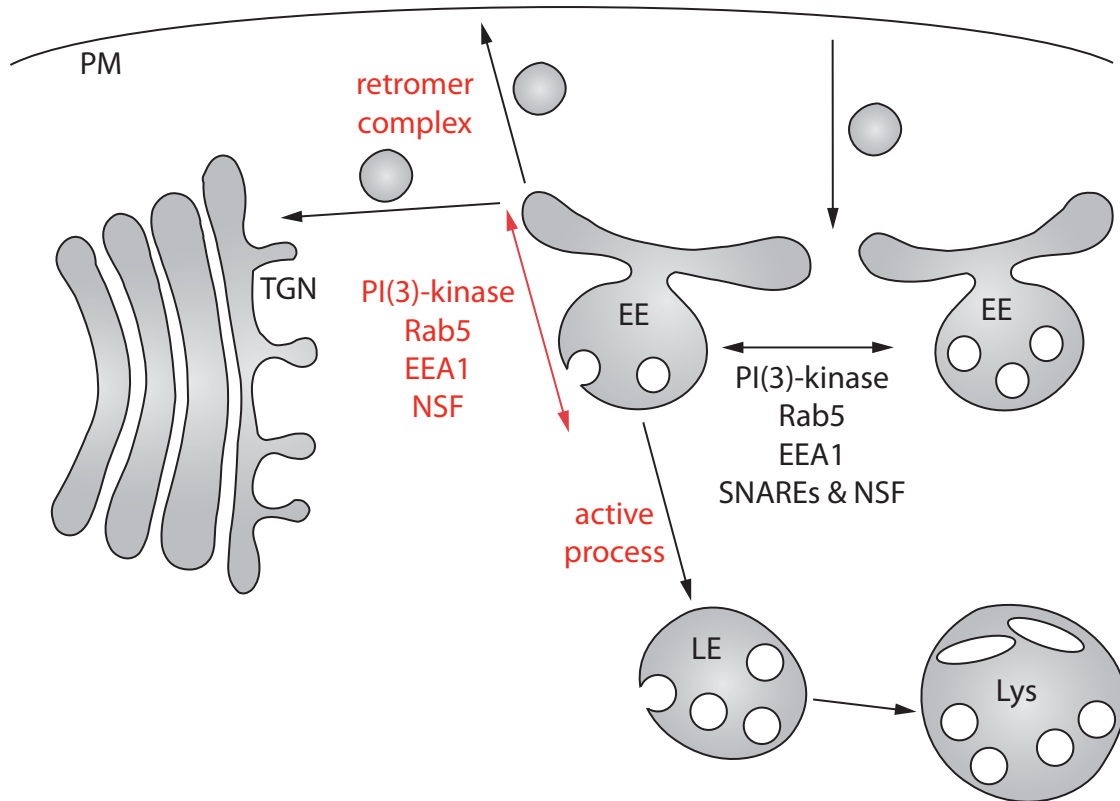


Figure 4.1: It is known that homotypic early endosomal docking and fusion require the PI(3)-kinase, Rab5 and the docking factor EEA1, as well as the cognate set of early endosomal SNAREs and NSF for their disassembly. Cargo sorting within the early endosome has not been studied before. This work shows that cargo sorting also requires the docking factors PI(3)-kinase, Rab5 and EEA1, as well as the fusion co-factor NSF. It does not require, however, direct SNARE function. Furthermore, the simultaneous action of vesicle budding and active maturation is needed for efficient cargo separation. Budding of recycling and retrograde vesicles involves the components of the retromer complex and maturation requires organelle acidification.

4.2 The Role of Docking and Fusion Factors in Early Endosomal Cargo Sorting

4.2.1 The Role of SNARE-disassembly in Sorting and Budding

SNARE proteins are the engines of membrane fusion. They are present in two opposing membranes and zipper together, forming a *trans* complex, which overcomes the energy barrier and drives the fusion of both membranes. After fusion the SNARE complex is present in a *cis*-configuration on one membrane. For new fusion rounds it is necessary to disassemble the SNARE complex, which is achieved by the AAA-ATPase NSF in cooperation with its cofactor α -SNAP. The inhibition of NSF by the drug NEM and by the dominant-negative NSF-cofactor α -SNAP as well as SNARE inhibition by soluble cytosolic SNARE fragments and specific antibodies leads to an efficient block in homotypic early endosomal fusion [see **Figure 3.19** and Brandhorst et al. (2006)]. Surprisingly, the inhibition of NSF by the same means also led to the inhibition of the sorting and budding reaction, while inhibition of SNARE proteins had no effect. One possible explanation might be that NSF is required in another context than the disassembly of SNARE complexes. Indeed, NSF has been reported to operate in various cellular contexts [reviewed in Whiteheart and Matveeva (2004)]. However, it appears that α -SNAP functions exclusively in SNARE disassembly, while all other processes seem to be independent of it. It is therefore unlikely that the inhibition of the sorting reaction by α -SNAP L294A (**Figure 3.19**) represents a NSF-effect other than the disassembly of SNAREs.

Also other lines of evidence have suggested that NSF function is important for different transport events within the cell. First, Itin et al. (1997) showed that α -SNAP and NSF facilitate the transport from late endosomes to the TGN. However, this assay measures a transport step including vesicle budding at the late endosome, transport and vesicle fusion at the TGN. It is therefore possible that this final fusion

step is the rate-limiting one in that assay, in which case addition of α -SNAP/NSF would lead to an increased availability of free SNAREs and an acceleration of fusion (and thus of the total readout of the reaction). Furthermore, [Prekeris et al. \(1998\)](#), as well as [Wessling-Resnick and Braell \(1990\)](#) have reported that NEM can block cargo separation and vesicle formation. These observations alone were, however, not conclusive since NEM is an unspecific drug with all cystine-linking proteins being possible targets.

α -SNAP-dependent NSF activity, but not SNARE-mediated endosome fusion, was required for cargo sorting and budding (**Figure 3.19**). Coupling this with the fact that the SNARE composition of transferrin-containing organelles changed after the reaction (**Figure 3.20**), one is tempted to conclude that SNARE separation and sorting into different compartments on the endosomal membrane are necessary for this process. This view is in agreement with previous findings different trafficking organelles contain only a subset of SNAREs which are required for their function ([Barlowe et al., 1994](#); [Takamori et al., 2006](#)). Furthermore, it has been reported that single SNARE molecules can interact with coat proteins, which is likely important for SNARE sorting. For example, single ER-Golgi SNAREs can interact directly with the Sec23/24 subcomplex of COPII ([Miller et al., 2003](#); [Mossessova et al., 2003](#)) or can be linked to the COPI coat via the ADP-ribosylation factor (Arf)-GTPase-activating protein (GAP) ([Rein et al., 2002](#)). Furthermore, late endosomal SNAREs such as Vti1b can interact with ENTH domain-containing clathrin adaptor proteins ([Chidambaram et al., 2008](#); [Miller et al., 2007](#)).

The present results suggest that SNAREs clustered in *cis*-complexes in the endosome membrane ([Bethani et al., 2007](#)) need to be first separated by NSF in order to interact productively with such sorting machineries, which might represent a control mechanism for the targeting of specific SNAREs (that are needed for subsequent fusion steps) into the newly budding vesicle on the level of the donor organelle. This finding thus introduces a novel function for NSF, other than the classical priming of SNAREs before fusion events: NSF functions as a SNARE separating enzyme, in order to allow for sorting to take place.

4.2.2 The Role of PI(3)-kinase, Rab Proteins and EEA1 in Sorting and Budding

The endosome constantly receives new material by fusion and distributes it again by budding of vesicles, which makes it a rather transient organelle with a high turnover rate. Despite this constant turnover, the endosome manages to maintain its identity with relatively constant sizes of around 100 to 300 nm in diameter and a fixed set of associated components. The PI(3)-phosphate, PI(3)-kinase, Rab5, EEA1, Rabenosyn-5, Rabaptin-5, Rabex-5, as well as syntaxin 13 and syntaxin 6 are clearly the key molecules present on the endosomal membrane which determine its specificity (Zerial and McBride, 2001).

All of these factors are required for endosomal docking and fusion (Mills et al., 1999), with EEA1 and the SNARE proteins syntaxin 13 and syntaxin 6 thought to function exclusively in these processes. Surprisingly, I found that PI(3)-phosphate, PI(3)-kinase, Rab5 and EEA1 are furthermore essential for endosomal cargo sorting and budding, suggesting an unexpected molecular link between the opposing processes of docking/fusion and sorting/budding. Is it possible that the molecular composition of the endosome directly affect or regulates its constant size (i.e. the balance between fusion and budding)? Indeed, it has been shown in the past that the disruption of some of the endosomal components leads to the domination of one process: for example docking and fusion are accelerated when Rab5 is constitutively active (Barbieri et al., 1996; Stenmark et al., 1994), causing a drastic increase in the endosome size. Furthermore, the disruption of PI(3)-kinase activity by wortmannin or other inhibitors leads to a phenotype in which endosomes seem to become “swollen”. These enlarged endosomes have always been discussed as the block in inward vesiculation for MVB formation (Futter et al., 2001), block in the pinching of those vesicles (Fernandez-Borja et al., 1999) or an inhibition of reformation of dense-core lysosomes from a late endosome-lysosome-hybrid organelle (Bright et al., 1997). The data from the present work now add the hypothesis that the fusion-budding balance is disrupted in such a way that while budding is blocked (**Figure 3.16**), fusion is not completely inhibited (**Figure 3.18**), leading to larger endosomes. The

relative maintenance of the endosome size and protein composition might thus be a hint for the regulatory coupling between the events of fusion and budding.

The Role of Rab Proteins

Rab proteins are the membrane organizers and important for organelle identity and function (Zerial and McBride, 2001). While they are generally implied in docking, fusion and different transport processes, some data also suggest their involvement in cargo selection and vesicle formation (Stenmark, 2009). One example is the late endosomal Rab9, which functions in the recycling of mannose-6-phosphate receptors (M6PRs) from late endosomes to TGN. The cytosolic tail of M6PRs is recognized by the sorting adaptor TIP47, an effector of Rab9 (Carroll et al., 2001; Itin et al., 1997). Also Rab5 has been implicated in cargo sequestration: Complexed with GDI, it was identified as an essential factor for assembly of clathrin-coated pits at the plasma membrane and for clathrin-mediated endocytosis of transferrin receptors (McLauchlan et al., 1998).

Rab proteins are generally localized to distinct organelles in eukaryotic cells where they occupy special domains (Miaczynska and Zerial, 2002). Early and recycling endosomes are comprised of multiple combinations of Rab4, Rab5 and Rab11 domains that are dynamic but do not significantly intermix over time. Similarly, late endosomes contain distinct membrane domains that are positive for Rab7 and Rab9, respectively. Due to this prominent role of Rab proteins in endosome function, the finding that Rab inactivation by GDI blocks endosomal cargo sorting (**Figure 3.18**), was thus not very surprising. Using a combination of *in vitro* and *in vivo* experiments, I found that Rab5 function is directly required for cargo sorting at the early endosome (**Figure 3.28** and **Figure 3.29**). In contrast, the early and late endosomal Rab proteins Rab4, Rab7, Rab9 or Rab11 (or their respective effectors) were neither required for cargo sorting, nor for direct vesicle formation (**Figure 3.29**). These data are partially in line with those from Pagano et al. (2004) who showed evidence for the involvement of the Rabaptin-5/Rabex-5 complex in the regulation of transferrin-vesicle formation. However, based on immunodepletion experiments

they suggested the involvement of Rab4 but not Rab5. Given that the Rab5 depletion in these experiments was extremely inefficient compared to that of Rab4, these results for Rab5 were not very conclusive.

Furthermore, I investigated the involvement of two other Rab proteins that have been associated with endosomes in the past: Rab22 has been shown to interact directly with EEA1 (Kauppi et al., 2002); Rab35 has been shown to function in cells of the immune system where they impaired the recycling of transferrin (Patino-Lopez et al., 2008). Moreover, Rab18 served as a negative control, since it has been shown to be involved in ER to Golgi transport (Dejgaard et al., 2008) and associates to lipid droplets (Martin and Parton, 2008). None of these proteins had an effect on endosomal sorting, which was surprising for Rab22 in view of its ability to interact with EEA1. The reported involvement of Rab35 in transferrin recycling, however, might be specific to cells of the immune system. Alternatively, the lack of an effect might be due to the fact that Rab35 has been shown (again in cells of the immune system) to localize to endosomes which are Arf6- and EHD1-positive (Walseng et al., 2008). These endosomes were suggested to be different from the Rab5-positive early/sorting endosomes (Donaldson et al., 2009). Another interesting candidate for future investigations is Rab21, which could not be purified in the course of this thesis (due to technical problems). It is mainly localized on early endosomes and seems to be implicated in endosome dynamics (Egami and Araki, 2008; Simpson et al., 2004). Furthermore, it also uses Rabex-5 as a GEF and shows similar binding affinities as Rab5/Rabex-5 (Delprato and Lambright, 2007; Delprato et al., 2004), even though a recent study has demonstrated that Varp functions as a Rab21 GEF and regulates endosome dynamics (Zhang et al., 2006).

The Role of the PI(3)-kinase

There are three classes of PI(3)-kinases, which have different substrates and products and which are all inhibited by the drug wortmannin (Backer, 2000; Wymann and Pirola, 1998): class I and class II utilize as substrates mainly PI(4,5)P₂, PI(4)P and PI(5)P, and only to lesser extends PI. The endosomal class III PI(3)-kinase Vps34 on the

other hand uses exclusively PI as a substrate, resulting in the generation of PI(3)P. PI(3)P is a phospholipid that is only present in the early endosome and in the intraluminal vesicles of MVBs (Di Paolo and De Camilli, 2006; Gillooly et al., 2003). Since this work focuses on early endosomes, it is therefore likely that the block by wortmannin represents a specific class III/Vps34 effect. However, further evidence came from the effects obtained from two other PI(3)-kinase inhibitors, LY 294,002 and 3-Methyladenine. LY 294,002 is widely used as “an inhibitor for all classes”. However, this is only an assumption, since a direct effect of LY 294,002 on Vps34 has not been shown so far (Fruman et al., 1998; Hawkins et al., 2006) and is therefore in line with my results that LY 294,002 does not strongly inhibit cargo sorting. The final evidence for the involvement of Vps34 came from the experiments with 3-Methyladenine, a drug that has originally been described to inhibit autophagy (Seglen and Gordon, 1982). However, recent evidence suggested that this drug specifically inhibits the class III PI3K (Petiot et al., 2000) and thereby can increase the tubulation in early endosomes (Egami and Araki, 2008) or block the retrograde early endosome to TGN transport of the CI-M6PR (Hirosako et al., 2004).

Taken together, the differential effects of the PI3K-inhibiting drugs wortmannin, LY 294,002 and 3-Methyladenine all point into the direction of a direct requirement of the class III PI(3)-kinase Vps34 and ultimately the endosomal lipid PI(3)P in cargo sorting.

The Role of Rab5 Effectors

One Rab5 effector is the PI(3)-kinase Vps34 whose function has been discussed above. The PI(3)P that is created by Vps34 acts together with Rab5 in a coincidence mechanism (Di Paolo and De Camilli, 2006) and leads to the recruitment of other downstream effectors such as EEA1 and Rabenosyn-5 (Backer, 2000, 2008).

EEA1 is a long coiled coil protein that acts as a docking factor in early endosomes (Christoforidis et al., 1999a). The fact that an antibody against EEA1 strongly blocks budding (even stronger than it blocks fusion) is difficult to reconcile with

an exclusive function for this molecule in tethering endosomes prior to fusion, although it is in line with a recent observation that EEA1 knock-down perturbs transferrin dynamics and EGF processing (Leonard et al., 2008). Since EEA1 is structurally not adapted to function directly as a budding factor, its role is most likely based on the interaction with other molecules. Apart from Rab5 and PI(3)P, EEA1 can also directly interact with calmodulin (Dumas et al., 2001; Lawe et al., 2003; Mills et al., 2001). Combining this with the facts that calmodulin leads to enlarged endosomes and inhibits recycling of transferrin and its receptor in living cells (de Figueiredo and Brown, 1995), it was surprising that the calmodulin inhibitor W-7 had no effect on the sorting reaction (**Figure 3.16**). Furthermore, EEA1 can interact with SNAREs, such as syntaxin 13 (McBride et al., 1999) or syntaxin 6 (Simonsen et al., 1999) and could thus be required for SNARE selection prior to endosomal budding.

Rabenosyn-5 is another Rab5 effector whose exact function is less well characterized. Given that the disruption of other molecules from the Rab5 machinery (such as Rab5 directly, PI(3)-kinase and EEA1) blocked the sorting reaction, it is likely that also Rabenosyn-5 is required. Indeed, Rabenosyn-5 might possibly represent a linking molecule between the Rab5 machinery and a budding factor. It has been suggested to interact with the dynamin-like EHD proteins and promote endosomal recycling to the plasma membrane (Naslavsky et al., 2004).

4.2.3 Possible Links Between Budding and Fusion

As mentioned above, one possible explanation is that coats, as budding factors, directly interact with the fusion factors such as the “correct” SNAREs for the following fusion step. It could thus be possible that docking factors such as Rab5, EEA1 or other Rab5 effectors can interact with sorting or budding factors: the interactions of Rabaptin-5/Rabex-5 with GGA proteins (Kawasaki et al., 2005) or Rabenosyn-5 with EHD proteins (Naslavsky et al., 2004) represent the most likely ones to our current knowledge.

This would lead to the view that the processes of endosome docking/fusion and sorting/budding are linked, being performed by macromolecular machineries which contain components involved in both processes. This is in line with observations on yeast vacuoles (the equivalent of mammalian late endosomes), where dynamin appears to be required not just for budding, but also for fusion (Peters et al., 2004). Other proteins, such as the vacuolar proton pump, V-ATPase (Baars et al., 2007), are also involved at different steps in both fusion and budding in this system. It is even possible that EEA1 perturbation results in a poorer activity of NSF (which would in itself block sorting), as a multiprotein machinery containing EEA1, NSF, and also Rab5 and endosomal SNAREs (syntaxin 6 or 13) may function in the endosome membrane (McBride et al., 1999; Mills et al., 2001; Simonsen et al., 1999). Thus, our results point into the direction of multifunctional (and multiprotein) domains existing on the early endosomal membrane (Gruenberg, 2001; Miaczynska and Zerial, 2002), which may act in more than just one trafficking pathway. Support of this may be found in Sharma et al. (2004), where sorting of transferrin from LacCer requires special endosomal domains.

While membrane organizers such as the Rab proteins have been suspected for some time to be involved in basically all organelle trafficking processes (Pfeffer, 2007), it is indeed surprising that some of the effector molecules, such as EEA1, are so strongly involved in reactions for which they seem structurally not adapted. Taken together, our results are in line with a fairly novel view of endosomal traffic in which the opposing events of docking, fusion and budding are tightly connected on a molecular level, as multiple “faces” of the same paradigm - the flow of molecules through the organelle.

4.3 Factors Required for Budding of Transferrin and Cholera Toxin

The results from **Figure 3.23** suggest that in addition to the formation of carrier vesicles, successful cargo separation also requires active endosome maturation

(i.e. acidification), although from a mechanistic standpoint it may have been more intuitive to see the maturation process as only passive.

Even though the nature of the molecules involved in carrier vesicle formation is still an open issue, I was able to identify the retromer complex as one player. This is in agreement with results from the groups of Bonifacino ([Arighi et al., 2004](#)) and Johannes ([Popoff et al., 2007](#)), who showed that small vesicles destined to the TGN bud from the early endosome through retromer-dependent processes. Nevertheless, my results suggest a further involvement of the retromer complex also in budding of transferrin-containing recycling vesicles, which was largely unexpected. The factors that link different cargo molecules to the retromer complex (and possibly also to other coats) are sorting nexins (SNXs) ([Cullen, 2008](#)). Indeed, of the 33 different isoforms of SNXs only few are characterized: while SNX1 and 2 function in cargo selection for the retrograde route ([Carlton et al., 2004](#); [Rojas et al., 2007](#)), SNX9 is involved in different modes of endocytosis ([Yarar et al., 2007](#)), and SNX4 in the recycling of transferrin receptor ([Carlton et al., 2004](#); [Traer et al., 2007](#)). Thus, it might be possible that the retromer complex is required for both transferrin recycling and the retrograde transport of cholera toxin, with the specificity being defined and regulated by different sorting nexins ([Carlton et al., 2005](#)). However, this hypothesis still needs to be tested.

In contrast, COPI coats [which were reported to be present on early endosomes ([Aniento et al., 1996](#); [Whitney et al., 1995](#))] and the clathrin-dynamin machinery were not needed for budding of transferrin and cholera toxin. Indeed the role of clathrin and dynamin on early endosomes has been discussed controversially:

- It has been suggested that the recycling of transferrin is dependent on clathrin and dynamin ([Pagano et al., 2004](#); [van Dam and Stoorvogel, 2002](#); [Wetley et al., 2002](#)), while [Damke et al. \(1994\)](#) found this process to be independent of dynamin. Furthermore, [van Dam et al. \(2002\)](#) have proposed the existence of two distinct recycling pathways: one that involves the transfer from the early to the recycling endosome from which clathrin-coated vesicles bud, and a clathrin-independent (but PI(3)-kinase-dependent) one which transports material di-

rectly from the early endosome to the plasma membrane, a concept which is in line with my data.

- [Lauvrak et al. \(2004\)](#) and [Popoff et al. \(2007\)](#) have shown that shiga toxin may not only use the retromer complex, but also clathrin for the retrograde endosome to TGN transport.
- The budding of SLMVs from the early endosomes was suggested to function independent of clathrin ([Faundez et al., 1997](#)).
- The PI(3)P-binding protein Hrs recruits clathrin to early endosomes, which is required for early- to late endosome transition ([Raiborg et al., 2002, 2001](#)).

Thus, even though clathrin seems to be present on early endosomes (at least in some cells), its function in endosomal trafficking is still not clear.

Finally, a number of known sorting/budding factors from other systems, such as the adaptor proteins AP1 and AP3 or COPII coats, as well as Hrs ([Hanyaloglu et al., 2005](#); [Raiborg et al., 2001](#)), Arf-proteins ([Donaldson and Honda, 2005](#)), phospholipases ([de Figueiredo et al., 2000](#); [Jovanovic et al., 2006](#); [Padron et al., 2006](#)), EHD-proteins ([Grant and Caplan, 2008](#)), or different sorting nexins ([Cullen, 2008](#)) still remain to be tested.

4.4 The Cell-based Sorting Assay

The cell-based sorting assay presented in [Figure 3.27](#) and [Figure 3.28](#) is a powerful tool that allows to investigate sorting on the level of single endosomes. At the same time it enables the quantification of larger data sets, in contrast to live cell imaging approaches of single organelles. In this thesis I have used the assay to investigate the requirement of Rab5 in endosomal sorting. In agreement with the data obtained from the the *in vitro* assay, it is needed for cargo sorting and transferrin recycling.

In future experiments, this assay can be used for investigating different aspects of endosomal cargo sorting, for example it is possible to study other Rab proteins.

Additionally, one can validate the role of EEA1 in endosomal sorting, possibly by the expression of the dominant-negative C-terminal fragment (Lawe et al., 2002; Stenmark et al., 1996). Furthermore, RNA interference could be used to gain further insights into the processes of sorting and budding. The downregulation of retromer components has been used in the past to dissect its role in endosome to TGN transport (Arighi et al., 2004; Popoff et al., 2007) and might be an interesting starting point for further investigations.

4.5 Conclusions

This thesis describes the establishment and use of a new fluorescence-based *in vitro* assay for early endosomal cargo sorting and vesicle budding. Interestingly, it appears that cargo sorting requires at least two active processes: first, vesiculation of small recycling or retrograde vesicles, with the retromer complex being involved, and second, active maturation of LDL-containing early endosomes into late endosomes by acidification of the organelles. Moreover, this work strongly suggests that cargo sorting and budding require molecules which have so far been thought to be exclusively involved in endosomal docking and fusion: the endosomal docking factors Rab5, PI(3)-kinase and EEA1 seem to play a crucial role. While Rab proteins as membrane organizers have been proposed to be required for basically all organelle trafficking processes (Stenmark, 2009), it is surprising that some of their effector molecules, such as EEA1, are involved in cargo sorting and budding reactions for which they seem structurally not adapted. Although the exact molecular mechanism, e.g. the link between Rab5 and its effectors to a classical budding machinery, still remains to be solved, this work shows an unexpected connection between the “opposing” events of docking/fusion and sorting/budding on the molecular level.

“Science... never solves a problem
without creating ten more.”

(George Bernard Shaw)

5

Summary and Outlook

Early endosomes are an entry point for internalized molecules, and serve as the first sorting station within the endocytic pathway. They are involved in both recycling and degradation pathways and are connected to several other compartments within the cell such as the plasma membrane, the TGN and late endosomes and lysosomes. Therefore, the early endosome has a central role within the endocytic pathway, and its ability for efficient and specific protein sorting is essential for proper cellular function, growth and differentiation. Trafficking between the early endosome and its different target compartments is mediated by vesicles. Formation of these vesicles requires cargo sorting, enrichment and budding from the early endosome. However, the molecular mechanisms underlying these processes are largely unknown. Does budding of differently targeted vesicles differ in the mechanisms and pathways involved - e.g. do recycling vesicles and other types of vesicles such as those targeted to the TGN differ in their formation? Which molecules are involved? How are the different budding events regulated? Are fusion and budding events mechanistically coupled? These are only some of the remaining open questions that could not be answered due to a lack of specific assays which would allow a direct manipulation of the system.

The present study shows the development of a novel cell-free assay for early endosomal segregation of cargo. I took advantage of the fact that transferrin (as a recycling marker) and the low-density-lipoprotein LDL (as a marker for the degradative pathway) are differentially sorted within early endosomes. Transferrin, which remains

bound to its receptor, is sorted into vesicles that bud off from early endosome precursors. The majority of transferrin is directly recycled to the plasma membrane by means of small carrier vesicles whereas another fraction is first transported to recycling endosomes before returning to the plasma membrane. In contrast, LDL is destined for lysosomal degradation. Thus, it remains in early endosomes during their maturation to late endosomes. I show here that isolated endosomes double labeled with fluorescent transferrin, cholera toxin and LDL efficiently separated these markers *in vitro*, a process that turned out to be rather easy to monitor and quantify. As expected, cargo segregation requires physiological temperature, cytosol and an energy source. Interestingly, I found that cargo sorting and budding are dependent on Rab5 and some of its effectors, the phosphatidylinositol-(3)-kinase and the docking factor EEA1. It seems as if the endosome consists of some complex multi-protein domains which are involved in more than just one endosomal function. However, it is not clear at this stage what the exact underlying molecular mechanisms are.

- What is the composition and morphology of possible “multi-tasking” domains on the endosome?
- Is there an unknown molecular link to a known budding machinery (such as clathrin, COPI, COPII or retromer)?
- Does the disruption of “typical” early endosomal proteins such as Rab5, EEA1 and PI(3)-kinase lead to the loss of the endosomal identity? If yes, how is the presence or absence of these factors sensed?
- Are other Rab5-effectors such as Vps45, Rabenosyn-5 or Rabaptin-5 required?

Surprisingly, I also found that the ATPase NSF, a fusion cofactor which disassembles SNARE complexes is required for efficient cargo segregation. However, perturbation of the SNARE-driven fusion machinery itself did not have any effects. This suggests that while SNARE function seems not to be required for sorting and budding, they need to be sorted and disassembled for the proper packing into the budding vesicle.

- How is the assembly or disassembly sensed: from the cytosolic or from the luminal side of the endosome? Which molecules are required?

-
- Is there a molecular interaction between the single “correct” SNAREs and possible budding factors?
 - Which SNAREs need to be sorted, i.e. which SNARE is targeted into which budding vesicle?

Moreover, transferrin and LDL are separated from the early endosome by two active processes. First, carrier vesicle formation of recycling vesicles and those destined to the TGN requires the function of the retromer complex, but not clathrin, dynamin or COPI action. Second, early to late endosome maturation is an active process with effective acidification clearly being involved.

- What is the exact role of the retromer complex? If both endosome-to-Golgi and endosome-to-plasma membrane budding events are dependent on the retromer complex, how are both events regulated to ensure their proper functioning?
- Are other budding factors required, such as adaptor proteins (AP1, AP2, AP3 or AP4), COPII, different sorting nexins, Arf-proteins, GGA-proteins or EHD proteins?

Taken together, the *in vitro* assay presented in this thesis provides a powerful tool for early endosomal cargo sorting. It can therefore be used in the future for deeper investigations of other molecular components in the differential sorting of the presented cargo molecules, with HRS, phosphatases, phospholipases being some of the potential candidates.

However, the assay also has the potential to be and could be extended to study for example the differential sorting of internalized lipids from each other and from different cargoes. Similar to cholera toxin, one could internalize fluorescent lipids such as phosphatidylethanolamine, phosphatidylcholine, phosphatidylserine and glycosylphosphatidylinositol.

Another interesting aspect would be the full reconstitution of the system. To ultimately remove all the cytosolic factors that might be present in the PNS, a crude purification step could be useful. The proteins that one would have to purify up to now are Rab5, PI(3)-kinase, EEA1, α -SNAP and NSF. With cytosol fractions

that contain only a subset of all cytosolic proteins, one would therefore be able to identify new factors.

Finally, to obtain further insight into the exact requirements of Rab proteins in the differential sorting of transferrin and LDL in early endosomes, one can use the *in vivo* assay (single endosome assay) to investigate the role of different Rab mutants. Furthermore, RNA-interference could be used in combination with this assay to expand its application.

Bibliography

- ABALLAY A, SARROUF MN, COLOMBO MI, STAHL PD and MAYORGA LS. Zn²⁺ depletion blocks endosome fusion. *Biochem J*, 312 (Pt 3):919–23, 1995.
- AHLUWALIA JP, TOPP JD, WEIRATHER K, ZIMMERMAN M and STAMNES M. A role for calcium in stabilizing transport vesicle coats. *J Biol Chem*, 276(36):34148–55, 2001.
- ALTSCHULER Y, BARBAS SM, TERLECKY LJ, TANG K, HARDY S, MOSTOV KE and SCHMID SL. Redundant and distinct functions for dynamin-1 and dynamin-2 isoforms. *J Cell Biol*, 143(7):1871–81, 1998.
- ANGGONO V and ROBINSON PJ. Syndapin I and endophilin I bind overlapping proline-rich regions of dynamin I: role in synaptic vesicle endocytosis. *J Neurochem*, 102(3):931–43, 2007.
- ANIENITO F, GU F, PARTON RG and GRUENBERG J. An endosomal beta COP is involved in the pH-dependent formation of transport vesicles destined for late endosomes. *J Cell Biol*, 133(1):29–41, 1996.
- ANTONIN W, FASSHAUER D, BECKER S, JAHN R and SCHNEIDER TR. Crystal structure of the endosomal SNARE complex reveals common structural principles of all SNAREs. *Nat Struct Biol*, 9(2):107–11, 2002.
- ARIGHI CN, HARTNELL LM, AGUILAR RC, HAFT CR and BONIFACINO JS. Role of the mammalian retromer in sorting of the cation-independent mannose 6-phosphate receptor. *J Cell Biol*, 165(1):123–33, 2004.

- BAARS TL, PETRI S, PETERS C and MAYER A. Role of the V-ATPase in regulation of the vacuolar fission-fusion equilibrium. *Mol Biol Cell*, 18(10):3873–82, 2007.
- BACKER JM. Phosphoinositide 3-kinases and the regulation of vesicular trafficking. *Mol Cell Biol Res Commun*, 3(4):193–204, 2000.
- BACKER JM. The regulation and function of Class III PI3Ks: novel roles for Vps34. *Biochem J*, 410(1):1–17, 2008.
- BALCH WE and ROTHMAN JE. Characterization of protein transport between successive compartments of the Golgi apparatus: asymmetric properties of donor and acceptor activities in a cell-free system. *Arch Biochem Biophys*, 240(1):413–25, 1985.
- BARBIERI MA, LI G, MAYORGA LS and STAHL PD. Characterization of Rab5:Q79L-stimulated endosome fusion. *Arch Biochem Biophys*, 326(1):64–72, 1996.
- BARLOWE C, ORCI L, YEUNG T, HOSOBUCHI M, HAMAMOTO S, SALAMA N, REXACH MF, RAVAZZOLA M, AMHERDT M and SCHEKMAN R. COPII: a membrane coat formed by Sec proteins that drive vesicle budding from the endoplasmic reticulum. *Cell*, 77(6):895–907, 1994.
- BARNARD RJ, MORGAN A and BURGOYNE RD. Domains of alpha-SNAP required for the stimulation of exocytosis and for N-ethylmaleimide-sensitive fusion protein (NSF) binding and activation. *Mol Biol Cell*, 7(5):693–701, 1996.
- BARR FA and SHORT B. Golgins in the structure and dynamics of the Golgi apparatus. *Curr Opin Cell Biol*, 15(4):405–13, 2003.
- BETHANI I, LANG T, GEUMANN U, SIEBER JJ, JAHN R and RIZZOLI SO. The specificity of SNARE pairing in biological membranes is mediated by both proof-reading and spatial segregation. *Embo J*, 26(17):3981–92, 2007.

- BETHANI I, WERNER A, KADIAN C, GEUMANN U, JAHN R and RIZZOLI SO. Endosomal Fusion upon SNARE Knockdown is Maintained by Residual SNARE Activity and Enhanced Docking. *Traffic*, 2009.
- BLOCK MR, GLICK BS, WILCOX CA, WIELAND FT and ROTHMAN JE. Purification of an N-ethylmaleimide-sensitive protein catalyzing vesicular transport. *Proc Natl Acad Sci U S A*, 85(21):7852–6, 1988.
- BLUMSTEIN J, FAUNDEZ V, NAKATSU F, SAITO T, OHNO H and KELLY RB. The neuronal form of adaptor protein-3 is required for synaptic vesicle formation from endosomes. *J Neurosci*, 21(20):8034–42, 2001.
- BOCK JB, MATERN HT, PEDEN AA and SCHELLER RH. A genomic perspective on membrane compartment organization. *Nature*, 409(6822):839–41, 2001.
- BOEHM M and BONIFACINO JS. Adaptins: the final recount. *Mol Biol Cell*, 12(10):2907–20, 2001.
- BOMAN AL. GGA proteins: new players in the sorting game. *J Cell Sci*, 114(Pt 19):3413–8, 2001.
- BOMAN AL, ZHANG C, ZHU X and KAHN RA. A family of ADP-ribosylation factor effectors that can alter membrane transport through the trans-Golgi. *Mol Biol Cell*, 11(4):1241–55, 2000.
- BONIFACINO JS and GLICK BS. The mechanisms of vesicle budding and fusion. *Cell*, 116(2):153–66, 2004.
- BONIFACINO JS and HURLEY JH. Retromer. *Curr Opin Cell Biol*, 20(4):427–36, 2008.
- BONIFACINO JS and LIPPINCOTT-SCHWARTZ J. Coat proteins: shaping membrane transport. *Nat Rev Mol Cell Biol*, 4(5):409–14, 2003.
- BONIFACINO JS and ROJAS R. Retrograde transport from endosomes to the trans-Golgi network. *Nat Rev Mol Cell Biol*, 7(8):568–79, 2006.

- BRACHET V, PEHAU-ARNAUDET G, DESAYMARD C, RAPOSO G and AMIGORENA S. Early endosomes are required for major histocompatibility complex class II transport to peptide-loading compartments. *Mol Biol Cell*, 10(9):2891–904, 1999.
- BRADFORD MM. A rapid and sensitive method for the quantitation of microgram quantities of protein utilizing the principle of protein-dye binding. *Anal Biochem*, 72:248–54, 1976.
- BRANDHORST D, ZWILLING D, RIZZOLI SO, LIPPERT U, LANG T and JAHN R. Homotypic fusion of early endosomes: SNAREs do not determine fusion specificity. *Proc Natl Acad Sci U S A*, 103(8):2701–6, 2006.
- BRIGHT NA, REAVES BJ, MULLOCK BM and LUZIO JP. Dense core lysosomes can fuse with late endosomes and are re-formed from the resultant hybrid organelles. *J Cell Sci*, 110 (Pt 17):2027–40, 1997.
- BURGUETE AS, FENN TD, BRUNGER AT and PFEFFER SR. Rab and Arl GTPase family members cooperate in the localization of the golgin GCC185. *Cell*, 132(2):286–98, 2008.
- CAI H, REINISCH K and FERRO-NOVICK S. Coats, tethers, Rabs, and SNAREs work together to mediate the intracellular destination of a transport vesicle. *Dev Cell*, 12(5):671–82, 2007.
- CARLTON J, BUJNY M, PETER BJ, OORSCHOT VM, RUTHERFORD A, MELLOR H, KLUMPERMAN J, MCMAHON HT and CULLEN PJ. Sorting nexin-1 mediates tubular endosome-to-TGN transport through coincidence sensing of high-curvature membranes and 3-phosphoinositides. *Curr Biol*, 14(20):1791–800, 2004.
- CARLTON J, BUJNY M, RUTHERFORD A and CULLEN P. Sorting nexins—unifying trends and new perspectives. *Traffic*, 6(2):75–82, 2005.
- CARROLL KS, HANNA J, SIMON I, KRISE J, BARBERO P and PFEFFER SR. Role of Rab9 GTPase in facilitating receptor recruitment by TIP47. *Science*, 292(5520):1373–6, 2001.

- CHAVRIER P, VAN DER SLUIJS P, MISHAL Z, NAGELKERKEN B and GORVEL JP. Early endosome membrane dynamics characterized by flow cytometry. *Cytometry*, 29(1):41–9, 1997.
- CHIDAMBARAM S, ZIMMERMANN J and VON MOLLARD GF. ENTH domain proteins are cargo adaptors for multiple SNARE proteins at the TGN endosome. *J Cell Sci*, 121(Pt 3):329–38, 2008.
- CHRISTOFORIDIS S, MCBRIDE HM, BURGOYNE RD and ZERIAL M. The Rab5 effector EEA1 is a core component of endosome docking. *Nature*, 397(6720):621–5, 1999a.
- CHRISTOFORIDIS S, MIACZYNSKA M, ASHMAN K, WILM M, ZHAO L, YIP SC, WATERFIELD MD, BACKER JM and ZERIAL M. Phosphatidylinositol-3-OH kinases are Rab5 effectors. *Nat Cell Biol*, 1(4):249–52, 1999b.
- CLAGUE MJ. Molecular aspects of the endocytic pathway. *Biochem J*, 336 (Pt 2):271–82, 1998.
- CLIFT-O'GRADY L, DESNOS C, LICHTENSTEIN Y, FAUNDEZ V, HORNG JT and KELLY RB. Reconstitution of synaptic vesicle biogenesis from PC12 cell membranes. *Methods*, 16(2):150–9, 1998.
- COLLINS BM. The structure and function of the retromer protein complex. *Traffic*, 9(11):1811–22, 2008.
- COLOMBO MI, BERON W and STAHL PD. Calmodulin regulates endosome fusion. *J Biol Chem*, 272(12):7707–12, 1997.
- CONNER SD and SCHMID SL. Regulated portals of entry into the cell. *Nature*, 422(6927):37–44, 2003.
- CULLEN PJ. Endosomal sorting and signalling: an emerging role for sorting nexins. *Nat Rev Mol Cell Biol*, 9(7):574–82, 2008.

- DAMKE H, BABA T, WARNOCK DE and SCHMID SL. Induction of mutant dynamin specifically blocks endocytic coated vesicle formation. *J Cell Biol*, 127(4):915–34, 1994.
- DE FIGUEIREDO P and BROWN WJ. A role for calmodulin in organelle membrane tubulation. *Mol Biol Cell*, 6(7):871–87, 1995.
- DE FIGUEIREDO P, DRECKTRAH D, POLIZOTTO RS, COLE NB, LIPPINCOTT-SCHWARTZ J and BROWN WJ. Phospholipase A2 antagonists inhibit constitutive retrograde membrane traffic to the endoplasmic reticulum. *Traffic*, 1(6):504–11, 2000.
- DE WIT H, LICHTENSTEIN Y, GEUZE HJ, KELLY RB, VAN DER SLUIJS P and KLUMPERMAN J. Synaptic vesicles form by budding from tubular extensions of sorting endosomes in PC12 cells. *Mol Biol Cell*, 10(12):4163–76, 1999.
- DE WIT H, LICHTENSTEIN Y, KELLY RB, GEUZE HJ, KLUMPERMAN J and VAN DER SLUIJS P. Rab4 regulates formation of synaptic-like microvesicles from early endosomes in PC12 cells. *Mol Biol Cell*, 12(11):3703–15, 2001.
- DEJGAARD SY, MURSHID A, ERMAN A, KIZILAY O, VERBICH D, LODGE R, DEJGAARD K, LY-HARTIG TB, PEPPERKOK R, SIMPSON JC and PRESLEY JF. Rab18 and Rab43 have key roles in ER-Golgi trafficking. *J Cell Sci*, 121(Pt 16):2768–81, 2008.
- DELL'ANGELICA EC, PUERTOLLANO R, MULLINS C, AGUILAR RC, VARGAS JD, HARTNELL LM and BONIFACINO JS. GGAs: a family of ADP ribosylation factor-binding proteins related to adaptors and associated with the Golgi complex. *J Cell Biol*, 149(1):81–94, 2000.
- DELPRATO A and LAMBRIGHT DG. Structural basis for Rab GTPase activation by VPS9 domain exchange factors. *Nat Struct Mol Biol*, 14(5):406–12, 2007.
- DELPRATO A, MERITHEW E and LAMBRIGHT DG. Structure, exchange determinants, and family-wide rab specificity of the tandem helical bundle and Vps9 domains of Rabex-5. *Cell*, 118(5):607–17, 2004.

- DENKER A, KROHNERT K and RIZZOLI SO. Revisiting synaptic vesicle pool localization in the Drosophila neuromuscular junction. *J Physiol*, 587(Pt 12):2919–26, 2009.
- DESNOS C, CLIFT-O’GRADY L and KELLY RB. Biogenesis of synaptic vesicles in vitro. *J Cell Biol*, 130(5):1041–9, 1995.
- DI PAOLO G and DE CAMILLI P. Phosphoinositides in cell regulation and membrane dynamics. *Nature*, 443(7112):651–7, 2006.
- DONALDSON JG and HONDA A. Localization and function of Arf family GTPases. *Biochem Soc Trans*, 33(Pt 4):639–42, 2005.
- DONALDSON JG, PORAT-SHLIOM N and COHEN LA. Clathrin-independent endocytosis: a unique platform for cell signaling and PM remodeling. *Cell Signal*, 21(1):1–6, 2009.
- DONNERT G, KELLER J, MEDDA R, ANDREI MA, RIZZOLI SO, LUHRMANN R, JAHN R, EGGELING C and HELL SW. Macromolecular-scale resolution in biological fluorescence microscopy. *Proc Natl Acad Sci U S A*, 103(31):11440–5, 2006.
- DRISKELL OJ, MIRONOV A, ALLAN VJ and WOODMAN PG. Dynein is required for receptor sorting and the morphogenesis of early endosomes. *Nat Cell Biol*, 9(1):113–20, 2007.
- DUDEN R, GRIFFITHS G, FRANK R, ARGOS P and KREIS TE. Beta-COP, a 110 kd protein associated with non-clathrin-coated vesicles and the Golgi complex, shows homology to beta-adaptin. *Cell*, 64(3):649–65, 1991.
- DUMAS JJ, MERITHEW E, SUDHARSHAN E, RAJAMANI D, HAYES S, LAWE D, CORVERA S and LAMBRIGHT DG. Multivalent endosome targeting by homodimeric EEA1. *Mol Cell*, 8(5):947–58, 2001.
- EGAMI Y and ARAKI N. Characterization of Rab21-positive tubular endosomes induced by PI3K inhibitors. *Exp Cell Res*, 314(4):729–37, 2008.

- FASSHAUER D, SUTTON RB, BRUNGER AT and JAHN R. Conserved structural features of the synaptic fusion complex: SNARE proteins reclassified as Q- and R-SNAREs. *Proc Natl Acad Sci U S A*, 95(26):15781–6, 1998.
- FAUNDEZ V, HORNG JT and KELLY RB. ADP ribosylation factor 1 is required for synaptic vesicle budding in PC12 cells. *J Cell Biol*, 138(3):505–15, 1997.
- FAUNDEZ V, HORNG JT and KELLY RB. A function for the AP3 coat complex in synaptic vesicle formation from endosomes. *Cell*, 93(3):423–32, 1998.
- FERNANDEZ-BORJA M, WUBBOLTS R, CALAFAT J, JANSSEN H, DIVECHA N, DUSSELJEE S and NEEFJES J. Multivesicular body morphogenesis requires phosphatidylinositol 3-kinase activity. *Curr Biol*, 9(1):55–8, 1999.
- FRUMAN DA, MEYERS RE and CANTLEY LC. Phosphoinositide kinases. *Annu Rev Biochem*, 67:481–507, 1998.
- FUTTER CE, COLLINSON LM, BACKER JM and HOPKINS CR. Human VPS34 is required for internal vesicle formation within multivesicular endosomes. *J Cell Biol*, 155(7):1251–64, 2001.
- GEUMANN U, BARYSCH SV, HOOPMANN P, JAHN R and RIZZOLI SO. SNARE Function Is Not Involved in Early Endosome Docking. *Mol Biol Cell*, 2008.
- GEUZE HJ, SLOT JW, STROUS GJ, LODISH HF and SCHWARTZ AL. Intracellular site of asialoglycoprotein receptor-ligand uncoupling: double-label immunoelectron microscopy during receptor-mediated endocytosis. *Cell*, 32(1):277–87, 1983.
- GILLOOLY DJ, RAIBORG C and STENMARK H. Phosphatidylinositol 3-phosphate is found in microdomains of early endosomes. *Histochem Cell Biol*, 120(6):445–53, 2003.
- GLICK BS and ROTHMAN JE. Possible role for fatty acyl-coenzyme A in intracellular protein transport. *Nature*, 326(6110):309–12, 1987.

- GORVEL JP, CHAVRIER P, ZERIAL M and GRUENBERG J. rab5 controls early endosome fusion in vitro. *Cell*, 64(5):915–25, 1991.
- GRANT BD and CAPLAN S. Mechanisms of EHD/RME-1 Protein Function in Endocytic Transport. *Traffic*, 2008.
- GRUENBERG J. The endocytic pathway: a mosaic of domains. *Nat Rev Mol Cell Biol*, 2(10):721–30, 2001.
- GRUENBERG J, GRIFFITHS G and HOWELL KE. Characterization of the early endosome and putative endocytic carrier vesicles in vivo and with an assay of vesicle fusion in vitro. *J Cell Biol*, 108(4):1301–16, 1989.
- GRUENBERG J and HOWELL KE. Membrane traffic in endocytosis: insights from cell-free assays. *Annu Rev Cell Biol*, 5:453–81, 1989.
- GURKAN C, STAGG SM, LAPOINTE P and BALCH WE. The COPII cage: unifying principles of vesicle coat assembly. *Nat Rev Mol Cell Biol*, 7(10):727–38, 2006.
- HAFT CR, DE LA LUZ SIERRA M, BAFFORD R, LESNIAK MA, BARR VA and TAYLOR SI. Human orthologs of yeast vacuolar protein sorting proteins Vps26, 29, and 35: assembly into multimeric complexes. *Mol Biol Cell*, 11(12):4105–16, 2000.
- HANSON PI, HEUSER JE and JAHN R. Neurotransmitter release - four years of SNARE complexes. *Curr Opin Neurobiol*, 7(3):310–5, 1997.
- HANYALOGLU AC, MCCULLAGH E and VON ZASTROW M. Essential role of Hrs in a recycling mechanism mediating functional resensitization of cell signaling. *EMBO J*, 24(13):2265–83, 2005.
- HARTER C and WIELAND F. The secretory pathway: mechanisms of protein sorting and transport. *Biochim Biophys Acta*, 1286(2):75–93, 1996.
- HAWKINS PT, ANDERSON KE, DAVIDSON K and STEPHENS LR. Signalling through Class I PI3Ks in mammalian cells. *Biochem Soc Trans*, 34(Pt 5):647–62, 2006.

- HENLEY JR, KRUEGER EW, OSWALD BJ and MCNIVEN MA. Dynamin-mediated internalization of caveolae. *J Cell Biol*, 141(1):85–99, 1998.
- HEUMANN R, KACHEL V and THOENEN H. Relationship between NGF-mediated volume increase and "priming effect" in fast and slow reacting clones of PC12 pheochromocytoma cells. Role of cAMP. *Exp Cell Res*, 145(1):179–90, 1983.
- HINSHAW JE. Dynamin and its role in membrane fission. *Annu Rev Cell Dev Biol*, 16:483–519, 2000.
- HIROSAKO K, IMASATO H, HIROTA Y, KURONITA T, MASUYAMA N, NISHIOKA M, UMEDA A, FUJITA H, HIMENO M and TANAKA Y. 3-Methyladenine specifically inhibits retrograde transport of cation-independent mannose 6-phosphate/insulin-like growth factor II receptor from the early endosome to the TGN. *Biochem Biophys Res Commun*, 316(3):845–52, 2004.
- HIRST J, LUI WW, BRIGHT NA, TOTTY N, SEAMAN MN and ROBINSON MS. A family of proteins with gamma-adaptin and VHS domains that facilitate trafficking between the trans-Golgi network and the vacuole/lysosome. *J Cell Biol*, 149(1):67–80, 2000.
- HOLROYD C, KISTNER U, ANNAERT W and JAHN R. Fusion of endosomes involved in synaptic vesicle recycling. *Mol Biol Cell*, 10(9):3035–44, 1999.
- HORIUCHI H, LIPPE R, MCBRIDE HM, RUBINO M, WOODMAN P, STENMARK H, RYBIN V, WILM M, ASHMAN K, MANN M and ZERIAL M. A novel Rab5 GDP/GTP exchange factor complexed to Rabaptin-5 links nucleotide exchange to effector recruitment and function. *Cell*, 90(6):1149–59, 1997.
- HUTTNER WB, SCHIEBLER W, GREENGARD P and DE CAMILLI P. Synapsin I (protein I), a nerve terminal-specific phosphoprotein. III. Its association with synaptic vesicles studied in a highly purified synaptic vesicle preparation. *J Cell Biol*, 96(5):1374–88, 1983.

- ITIN C, RANCANO C, NAKAJIMA Y and PFEFFER SR. A novel assay reveals a role for soluble N-ethylmaleimide-sensitive fusion attachment protein in mannose 6-phosphate receptor transport from endosomes to the trans Golgi network. *J Biol Chem*, 272(44):27737–44, 1997.
- JAHN R, LANG T and SUDHOF TC. Membrane fusion. *Cell*, 112(4):519–33, 2003.
- JAHN R and SCHELLER RH. SNAREs—engines for membrane fusion. *Nat Rev Mol Cell Biol*, 7(9):631–43, 2006.
- JAHN R, SCHIEBLER W and GREENGARD P. A quantitative dot-immunobinding assay for proteins using nitrocellulose membrane filters. *Proc Natl Acad Sci U S A*, 81(6):1684–7, 1984.
- JOCKUSCH WJ, PRAEFCKE GJ, MCMAHON HT and LAGNADO L. Clathrin-dependent and clathrin-independent retrieval of synaptic vesicles in retinal bipolar cells. *Neuron*, 46(6):869–78, 2005.
- JOVANOVIĆ OA, BROWN FD and DONALDSON JG. An effector domain mutant of Arf6 implicates phospholipase D in endosomal membrane recycling. *Mol Biol Cell*, 17(1):327–35, 2006.
- KAECH S and BANKER G. Culturing hippocampal neurons. *Nat Protoc*, 1(5):2406–15, 2006.
- KARYLOWSKI O, ZEIGERER A, COHEN A and MCGRAW TE. GLUT4 is retained by an intracellular cycle of vesicle formation and fusion with endosomes. *Mol Biol Cell*, 15(2):870–82, 2004.
- KAUPPI M, SIMONSEN A, BREMNES B, VIEIRA A, CALLAGHAN J, STENMARK H and OLKKONEN VM. The small GTPase Rab22 interacts with EEA1 and controls endosomal membrane trafficking. *J Cell Sci*, 115(Pt 5):899–911, 2002.
- KAWASAKI M, NAKAYAMA K and WAKATSUKI S. Membrane recruitment of effector proteins by Arf and Rab GTPases. *Curr Opin Struct Biol*, 15(6):681–9, 2005.

- KIRCHHAUSEN T. Three ways to make a vesicle. *Nat Rev Mol Cell Biol*, 1(3):187–98, 2000.
- KLOEPPER TH, KIENLE CN and FASSHAUER D. An elaborate classification of SNARE proteins sheds light on the conservation of the eukaryotic endomembrane system. *Mol Biol Cell*, 18(9):3463–71, 2007.
- KLOEPPER TH, KIENLE CN and FASSHAUER D. SNAREing the basis of multicellularity: consequences of protein family expansion during evolution. *Mol Biol Evol*, 25(9):2055–68, 2008.
- LAJOIE P, GOETZ JG, DENNIS JW and NABI IR. Lattices, rafts, and scaffolds: domain regulation of receptor signaling at the plasma membrane. *J Cell Biol*, 185(3):381–5, 2009.
- LAKADAMYALI M, RUST MJ and ZHUANG X. Ligands for clathrin-mediated endocytosis are differentially sorted into distinct populations of early endosomes. *Cell*, 124(5):997–1009, 2006.
- LAUVRAK SU, TORGERSEN ML and SANDVIG K. Efficient endosome-to-Golgi transport of Shiga toxin is dependent on dynamin and clathrin. *J Cell Sci*, 117(Pt 11):2321–31, 2004.
- LAW DC, CHAWLA A, MERITHEW E, DUMAS J, CARRINGTON W, FOGARTY K, LIFSHITZ L, TUFT R, LAMBRIGHT D and CORVERA S. Sequential roles for phosphatidylinositol 3-phosphate and Rab5 in tethering and fusion of early endosomes via their interaction with EEA1. *J Biol Chem*, 277(10):8611–7, 2002.
- LAW DC, SITOUAH N, HAYES S, CHAWLA A, VIRBASIVS JV, TUFT R, FOGARTY K, LIFSHITZ L, LAMBRIGHT D and CORVERA S. Essential role of Ca²⁺/calmodulin in Early Endosome Antigen-1 localization. *Mol Biol Cell*, 14(7):2935–45, 2003.
- LEONARD D, HAYAKAWA A, LAW DC, LAMBRIGHT D, BELLVE KD, STANDLEY C, LIFSHITZ LM, FOGARTY KE and CORVERA S. Sorting of EGF and trans-

- ferrin at the plasma membrane and by cargo-specific signaling to EEA1-enriched endosomes. *J Cell Sci*, 121(Pt 20):3445–58, 2008.
- LICHTENSTEIN Y, DESNOS C, FAUNDEZ V, KELLY RB and CLIFT-O'GRADY L. Vesiculation and sorting from PC12-derived endosomes in vitro. *Proc Natl Acad Sci U S A*, 95(19):11223–8, 1998.
- LIM SN, BONZELIUS F, LOW SH, WILLE H, WEIMBS T and HERMAN GA. Identification of discrete classes of endosome-derived small vesicles as a major cellular pool for recycling membrane proteins. *Mol Biol Cell*, 12(4):981–95, 2001.
- LIPPE R, MIACZYNSKA M, RYBIN V, RUNGE A and ZERIAL M. Functional synergy between Rab5 effector Rabaptin-5 and exchange factor Rabex-5 when physically associated in a complex. *Mol Biol Cell*, 12(7):2219–28, 2001.
- MACIA E, EHRLICH M, MASSOL R, BOUCROT E, BRUNNER C and KIRCHHAUSEN T. Dynasore, a cell-permeable inhibitor of dynamin. *Dev Cell*, 10(6):839–50, 2006.
- MANNEVILLE JB, CASELLA JF, AMBROGGIO E, GOUNON P, BERTHERAT J, BASSEREAU P, CARTAUD J, ANTONNY B and GOUD B. COPI coat assembly occurs on liquid-disordered domains and the associated membrane deformations are limited by membrane tension. *Proc Natl Acad Sci U S A*, 105(44):16946–51, 2008.
- MARKGRAF DF, PEPLowska K and UNGERMANN C. Rab cascades and tethering factors in the endomembrane system. *FEBS Lett*, 581(11):2125–30, 2007.
- MARTIN S and PARTON RG. Characterization of Rab18, a lipid droplet-associated small GTPase. *Methods Enzymol*, 438:109–29, 2008.
- MARTYS JL, WJASOW C, GANGI DM, KIELIAN MC, MCGRAW TE and BACKER JM. Wortmannin-sensitive trafficking pathways in Chinese hamster ovary cells. Differential effects on endocytosis and lysosomal sorting. *J Biol Chem*, 271(18):10953–62, 1996.

- MATSUDA H, TANAKA H, BLAS BL, NOSENAS JS, TOKAWA T and OHSAWA S. Evaluation of ELISA with ABTS, 2-2'-azino-di-(3-ethylbenzthiazoline sulfonic acid), as the substrate of peroxidase and its application to the diagnosis of schistosomiasis. *Jpn J Exp Med*, 54(3):131–8, 1984.
- MATSUOKA K, ORCI L, AMHERDT M, BEDNAREK SY, HAMAMOTO S, SCHEKMAN R and YEUNG T. COPII-coated vesicle formation reconstituted with purified coat proteins and chemically defined liposomes. *Cell*, 93(2):263–75, 1998.
- MAXFIELD FR and MCGRAW TE. Endocytic recycling. *Nat Rev Mol Cell Biol*, 5(2):121–32, 2004.
- MCBRIDE HM, RYBIN V, MURPHY C, GINER A, TEASDALE R and ZERIAL M. Oligomeric complexes link Rab5 effectors with NSF and drive membrane fusion via interactions between EEA1 and syntaxin 13. *Cell*, 98(3):377–86, 1999.
- MCLAUCHLAN H, NEWELL J, MORRICE N, OSBORNE A, WEST M and SMYTHE E. A novel role for Rab5-GDI in ligand sequestration into clathrin-coated pits. *Curr Biol*, 8(1):34–45, 1998.
- MCMAHON HT and MILLS IG. COP and clathrin-coated vesicle budding: different pathways, common approaches. *Curr Opin Cell Biol*, 16(4):379–91, 2004.
- MIACZYNSKA M and ZERIAL M. Mosaic organization of the endocytic pathway. *Exp Cell Res*, 272(1):8–14, 2002.
- MILLER EA, BEILHARZ TH, MALKUS PN, LEE MC, HAMAMOTO S, ORCI L and SCHEKMAN R. Multiple cargo binding sites on the COPII subunit Sec24p ensure capture of diverse membrane proteins into transport vesicles. *Cell*, 114(4):497–509, 2003.
- MILLER SE, COLLINS BM, MCCOY AJ, ROBINSON MS and OWEN DJ. A SNARE-adaptor interaction is a new mode of cargo recognition in clathrin-coated vesicles. *Nature*, 450(7169):570–4, 2007.

- MILLS IG, JONES AT and CLAGUE MJ. Regulation of endosome fusion. *Mol Membr Biol*, 16(1):73–9, 1999.
- MILLS IG, URBE S and CLAGUE MJ. Relationships between EEA1 binding partners and their role in endosome fusion. *J Cell Sci*, 114(Pt 10):1959–65, 2001.
- MORGAN JR, ZHAO X, WOMACK M, PRASAD K, AUGUSTINE GJ and LAFER EM. A role for the clathrin assembly domain of AP180 in synaptic vesicle endocytosis. *J Neurosci*, 19(23):10201–12, 1999.
- MOSSESOVA E, BICKFORD LC and GOLDBERG J. SNARE selectivity of the COPII coat. *Cell*, 114(4):483–95, 2003.
- MOSTOV K. Protein traffic in polarized epithelial cells: the polymeric immunoglobulin receptor as a model system. *J Cell Sci Suppl*, 17:21–6, 1993.
- MURRAY JW, SARKAR S and WOLKOFF AW. Single vesicle analysis of endocytic fission on microtubules in vitro. *Traffic*, 9(5):833–47, 2008.
- MURRAY JW and WOLKOFF AW. Roles of the cytoskeleton and motor proteins in endocytic sorting. *Adv Drug Deliv Rev*, 55(11):1385–403, 2003.
- NASLAVSKY N, BOEHM M, BACKLUND J P S and CAPLAN S. Rabenosyn-5 and EHD1 interact and sequentially regulate protein recycling to the plasma membrane. *Mol Biol Cell*, 15(5):2410–22, 2004.
- NEWELL-LITWA K, SEONG E, BURMEISTER M and FAUNDEZ V. Neuronal and non-neuronal functions of the AP-3 sorting machinery. *J Cell Sci*, 120(Pt 4):531–41, 2007.
- NIELSEN E, CHRISTOFORIDIS S, UTTENWEILER-JOSEPH S, MIACZYNSKA M, DEWITTE F, WILM M, HOFACK B and ZERIAL M. Rabenosyn-5, a novel Rab5 effector, is complexed with hVPS45 and recruited to endosomes through a FYVE finger domain. *J Cell Biol*, 151(3):601–12, 2000.

- NONET ML, HOLGADO AM, BREWER F, SERPE CJ, NORBECK BA, HOLLERAN J, WEI L, HARTWIEG E, JORGENSEN EM and ALFONSO A. UNC-11, a *Caenorhabditis elegans* AP180 homologue, regulates the size and protein composition of synaptic vesicles. *Mol Biol Cell*, 10(7):2343–60, 1999.
- NORKIN LC and ANDERSON HA. Multiple stages of virus-receptor interactions as shown by simian virus 40. *Adv Exp Med Biol*, 408:159–67, 1996.
- ORCI L, TAGAYA M, AMHERDT M, PERRELET A, DONALDSON JG, LIPPINCOTT-SCHWARTZ J, KLAUSNER RD and ROTHMAN JE. Brefeldin A, a drug that blocks secretion, prevents the assembly of non-clathrin-coated buds on Golgi cisternae. *Cell*, 64(6):1183–95, 1991.
- PADRON D, TALL RD and ROTH MG. Phospholipase D2 is required for efficient endocytic recycling of transferrin receptors. *Mol Biol Cell*, 17(2):598–606, 2006.
- PAGANO A, CROTTET P, PRESCIANNOTTO-BASCHONG C and SPIESS M. In vitro formation of recycling vesicles from endosomes requires adaptor protein-1/clathrin and is regulated by rab4 and the connector rabaptin-5. *Mol Biol Cell*, 15(11):4990–5000, 2004.
- PALADE G. Intracellular Aspects of the Process of Protein Synthesis. *Science*, 189(4206):867, 1975.
- PARTON RG and SIMONS K. The multiple faces of caveolae. *Nat Rev Mol Cell Biol*, 8(3):185–94, 2007.
- PATINO-LOPEZ G, DONG X, BEN-AISSA K, BERNOT KM, ITOH T, FUKUDA M, KRUHLAK MJ, SAMELSON LE and SHAW S. Rab35 and its GAP EPI64C in T cells regulate receptor recycling and immunological synapse formation. *J Biol Chem*, 283(26):18323–30, 2008.
- PELKMANS L and HELENIUS A. Endocytosis via caveolae. *Traffic*, 3(5):311–20, 2002.

- PELKMANS L, KARTENBECK J and HELENIUS A. Caveolar endocytosis of simian virus 40 reveals a new two-step vesicular-transport pathway to the ER. *Nat Cell Biol*, 3(5):473–83, 2001.
- PEPLOWSKA K, MARKGRAF DF, OSTROWICZ CW, BANGE G and UNGERMANN C. The CORVET tethering complex interacts with the yeast Rab5 homolog Vps21 and is involved in endo-lysosomal biogenesis. *Dev Cell*, 12(5):739–50, 2007.
- PEPPERKOK R, SCHEEL J, HORSTMANN H, HAURI HP, GRIFFITHS G and KREIS TE. Beta-COP is essential for biosynthetic membrane transport from the endoplasmic reticulum to the Golgi complex in vivo. *Cell*, 74(1):71–82, 1993.
- PETERS C, BAARS TL, BUHLER S and MAYER A. Mutual control of membrane fission and fusion proteins. *Cell*, 119(5):667–78, 2004.
- PETIOT A, OGIER-DENIS E, BLOMMAART EF, MEIJER AJ and CODOGNO P. Distinct classes of phosphatidylinositol 3'-kinases are involved in signaling pathways that control macroautophagy in HT-29 cells. *J Biol Chem*, 275(2):992–8, 2000.
- PFEFFER SR. Unsolved mysteries in membrane traffic. *Annu Rev Biochem*, 76:629–45, 2007.
- POPOFF V, MARDONES GA, TENZA D, ROJAS R, LAMAZE C, BONIFACINO JS, RAPOSO G and JOHANNES L. The retromer complex and clathrin define an early endosomal retrograde exit site. *J Cell Sci*, 120(Pt 12):2022–31, 2007.
- POUSSU A, LOHI O and LEHTO VP. Vear, a novel Golgi-associated protein with VHS and gamma-adaptin "ear" domains. *J Biol Chem*, 275(10):7176–83, 2000.
- PRAEFCKE GJ, FORD MG, SCHMID EM, OLESEN LE, GALLOP JL, PEAK-CHEW SY, VALLIS Y, BABU MM, MILLS IG and MCMAHON HT. Evolving nature of the AP2 alpha-appendage hub during clathrin-coated vesicle endocytosis. *Embo J*, 23(22):4371–83, 2004.

- PRAEFCKE GJ and MCMAHON HT. The dynamin superfamily: universal membrane tubulation and fission molecules? *Nat Rev Mol Cell Biol*, 5(2):133–47, 2004.
- PREKERIS R, KLUMPERMAN J, CHEN YA and SCHELLER RH. Syntaxin 13 mediates cycling of plasma membrane proteins via tubulovesicular recycling endosomes. *J Cell Biol*, 143(4):957–71, 1998.
- PUCADYIL TJ and SCHMID SL. Real-time visualization of dynamin-catalyzed membrane fission and vesicle release. *Cell*, 135(7):1263–75, 2008.
- PUCADYIL TJ and SCHMID SL. Conserved functions of membrane active GTPases in coated vesicle formation. *Science*, 325(5945):1217–20, 2009.
- RAIBORG C, BACHE KG, GILLOOLY DJ, MADSHUS IH, STANG E and STENMARK H. Hrs sorts ubiquitinated proteins into clathrin-coated microdomains of early endosomes. *Nat Cell Biol*, 4(5):394–8, 2002.
- RAIBORG C, BACHE KG, MEHLUM A and STENMARK H. Function of Hrs in endocytic trafficking and signalling. *Biochem Soc Trans*, 29(Pt 4):472–5, 2001.
- RAIBORG C and STENMARK H. The ESCRT machinery in endosomal sorting of ubiquitylated membrane proteins. *Nature*, 458(7237):445–52, 2009.
- RAPOPORT I, BOLL W, YU A, BOCKING T and KIRCHHAUSEN T. A motif in the clathrin heavy chain required for the Hsc70/auxilin uncoating reaction. *Mol Biol Cell*, 19(1):405–13, 2008.
- REIN U, ANDAG U, DUDEN R, SCHMITT HD and SPANG A. ARF-GAP-mediated interaction between the ER-Golgi v-SNAREs and the COPI coat. *J Cell Biol*, 157(3):395–404, 2002.
- RIZZOLI SO, BETHANI I, ZWILLING D, WENZEL D, SIDDIQUI TJ, BRANDHORST D and JAHN R. Evidence for early endosome-like fusion of recently endocytosed synaptic vesicles. *Traffic*, 7(9):1163–76, 2006.

- RIZZOLI SO and BETZ WJ. The structural organization of the readily releasable pool of synaptic vesicles. *Science*, 303(5666):2037–9, 2004.
- ROBINSON MS. Adaptable adaptors for coated vesicles. *Trends Cell Biol*, 14(4):167–74, 2004.
- ROJAS R, KAMETAKA S, HAFT CR and BONIFACINO JS. Interchangeable but essential functions of SNX1 and SNX2 in the association of retromer with endosomes and the trafficking of mannose 6-phosphate receptors. *Mol Cell Biol*, 27(3):1112–24, 2007.
- ROUX A, UYHAZI K, FROST A and DE CAMILLI P. GTP-dependent twisting of dynamin implicates constriction and tension in membrane fission. *Nature*, 441(7092):528–31, 2006.
- SAKSENA S, SUN J, CHU T and EMR SD. ESCRTing proteins in the endocytic pathway. *Trends Biochem Sci*, 32(12):561–73, 2007.
- SAMBROOK J and RUSSELL D. *Molecular cloning: a laboratory manual*, vol. 1-3. Cold Spring Harbor Laboratory Press, 3rd ed., 2001.
- SCHAGGER H. Tricine-SDS-PAGE. *Nat Protoc*, 1(1):16–22, 2006.
- SCHAGGER H and VON JAGOW G. Tricine-sodium dodecyl sulfate-polyacrylamide gel electrophoresis for the separation of proteins in the range from 1 to 100 kDa. *Anal Biochem*, 166(2):368–79, 1987.
- SCHMIDT A, HANNAH MJ and HUTTNER WB. Synaptic-like microvesicles of neuroendocrine cells originate from a novel compartment that is continuous with the plasma membrane and devoid of transferrin receptor. *J Cell Biol*, 137(2):445–58, 1997.
- SCHNATWINKEL C, CHRISTOFORIDIS S, LINDSAY MR, UTTENWEILER-JOSEPH S, WILM M, PARTON RG and ZERIAL M. The Rab5 effector Rabankyrin-5 regulates and coordinates different endocytic mechanisms. *PLoS Biol*, 2(9):E261, 2004.

- SEAMAN MN. Recycle your receptors with retromer. *Trends Cell Biol*, 15(2):68–75, 2005.
- SEGLÉN PO and GORDON PB. 3-Methyladenine: specific inhibitor of autophagic/lysosomal protein degradation in isolated rat hepatocytes. *Proc Natl Acad Sci U S A*, 79(6):1889–92, 1982.
- SHARMA DK, BROWN JC, CHOUDHURY A, PETERSON TE, HOLICKY E, MARKS DL, SIMARI R, PARTON RG and PAGANO RE. Selective stimulation of caveolar endocytosis by glycosphingolipids and cholesterol. *Mol Biol Cell*, 15(7):3114–22, 2004.
- SHARMA M, NASLAVSKY N and CAPLAN S. A role for EHD4 in the regulation of early endosomal transport. *Traffic*, 9(6):995–1018, 2008.
- SHI G, FAUNDEZ V, ROOS J, DELL’ANGELICA EC and KELLY RB. Neuroendocrine synaptic vesicles are formed in vitro by both clathrin-dependent and clathrin-independent pathways. *J Cell Biol*, 143(4):947–55, 1998.
- SIMONSEN A, GAULLIER JM, D’ARRIGO A and STENMARK H. The Rab5 effector EEA1 interacts directly with syntaxin-6. *J Biol Chem*, 274(41):28857–60, 1999.
- SIMPSON JC, GRIFFITHS G, WESSLING-RESNICK M, FRANSEN JA, BENNETT H and JONES AT. A role for the small GTPase Rab21 in the early endocytic pathway. *J Cell Sci*, 117(Pt 26):6297–311, 2004.
- SMITH PD, LIESEGANG GW, BERGER RL, CZERLINSKI G and PODOLSKY RJ. A stopped-flow investigation of calcium ion binding by ethylene glycol bis(beta-aminoethyl ether)-N,N'-tetraacetic acid. *Anal Biochem*, 143(1):188–95, 1984.
- SOLLNER T, WHITEHEART SW, BRUNNER M, ERDJUMENT-BROMAGE H, GEROMANOS S, TEMPST P and ROTHMAN JE. SNAP receptors implicated in vesicle targeting and fusion. *Nature*, 362(6418):318–24, 1993.

- SONNICHSEN B, LOWE M, LEVINE T, JAMSA E, DIRAC-SVEJSTRUP B and WARREN G. A role for giantin in docking COPI vesicles to Golgi membranes. *J Cell Biol*, 140(5):1013–21, 1998.
- SORKIN A. Cargo recognition during clathrin-mediated endocytosis: a team effort. *Curr Opin Cell Biol*, 16(4):392–9, 2004.
- SORRE B, CALLAN-JONES A, MANNEVILLE JB, NASSOY P, JOANNY JF, PROST J, GOUD B and BASSEREAU P. Curvature-driven lipid sorting needs proximity to a demixing point and is aided by proteins. *Proc Natl Acad Sci U S A*, 106(14):5622–6, 2009.
- SPIRO DJ, BOLL W, KIRCHHAUSEN T and WESSLING-RESNICK M. Wortmannin alters the transferrin receptor endocytic pathway in vivo and in vitro. *Mol Biol Cell*, 7(3):355–67, 1996.
- STAGG SM, GURKAN C, FOWLER DM, LAPOINTE P, FOSS TR, POTTER CS, CARRAGHER B and BALCH WE. Structure of the Sec13/31 COPII coat cage. *Nature*, 439(7073):234–8, 2006.
- STAGG SM, LAPOINTE P and BALCH WE. Structural design of cage and coat scaffolds that direct membrane traffic. *Curr Opin Struct Biol*, 17(2):221–8, 2007.
- STAGG SM, LAPOINTE P, RAZVI A, GURKAN C, POTTER CS, CARRAGHER B and BALCH WE. Structural basis for cargo regulation of COPII coat assembly. *Cell*, 134(3):474–84, 2008.
- STAMNES M. Regulating the actin cytoskeleton during vesicular transport. *Curr Opin Cell Biol*, 14(4):428–33, 2002.
- STEIN A, WEBER G, WAHL MC and JAHN R. Helical extension of the neuronal SNARE complex into the membrane. *Nature*, 460(7254):525–8, 2009.
- STENMARK H. Rab GTPases as coordinators of vesicle traffic. *Nat Rev Mol Cell Biol*, 10(8):513–25, 2009.

- STENMARK H, AASLAND R, TOH BH and D'ARRIGO A. Endosomal localization of the autoantigen EEA1 is mediated by a zinc-binding FYVE finger. *J Biol Chem*, 271(39):24048–54, 1996.
- STENMARK H, BUCCI C and ZERIAL M. Expression of Rab GTPases using recombinant vaccinia viruses. *Methods Enzymol*, 257:155–64, 1995.
- STENMARK H, PARTON RG, STEELE-MORTIMER O, LUTCKE A, GRUENBERG J and ZERIAL M. Inhibition of rab5 GTPase activity stimulates membrane fusion in endocytosis. *EMBO J*, 13(6):1287–96, 1994.
- STOORVOGEL W, OORSCHOT V and GEUZE HJ. A novel class of clathrin-coated vesicles budding from endosomes. *J Cell Biol*, 132(1-2):21–33, 1996.
- STOORVOGEL W, STROUS GJ, GEUZE HJ, OORSCHOT V and SCHWARTZ AL. Late endosomes derive from early endosomes by maturation. *Cell*, 65(3):417–27, 1991.
- STOWELL MH, MARKS B, WIGGE P and MCMAHON HT. Nucleotide-dependent conformational changes in dynamin: evidence for a mechanochemical molecular spring. *Nat Cell Biol*, 1(1):27–32, 1999.
- STROP P, KAISER SE, VRLJIC M and BRUNGER AT. The structure of the yeast plasma membrane SNARE complex reveals destabilizing water-filled cavities. *J Biol Chem*, 283(2):1113–9, 2008.
- SUTTON RB, FASSHAUER D, JAHN R and BRUNGER AT. Crystal structure of a SNARE complex involved in synaptic exocytosis at 2.4 Å resolution. *Nature*, 395(6700):347–53, 1998.
- SWEITZER SM and HINSHAW JE. Dynamin undergoes a GTP-dependent conformational change causing vesiculation. *Cell*, 93(6):1021–9, 1998.
- TAKAMORI S, HOLT M, STENIUS K, LEMKE EA, GRONBORG M, RIEDEL D, URLAUB H, SCHENCK S, BRUGGER B, RINGLER P, MULLER SA, RAMMNER B, GRATER F, HUB JS, DE GROOT BL, MIESKES G, MORIYAMA Y, KLINGAUF

- J, GRUBMULLER H, HEUSER J, WIELAND F and JAHN R. Molecular anatomy of a trafficking organelle. *Cell*, 127(4):831–46, 2006.
- TAKEI K, MUNDIGL O, DANIELL L and DE CAMILLI P. The synaptic vesicle cycle: a single vesicle budding step involving clathrin and dynamin. *J Cell Biol*, 133(6):1237–50, 1996.
- TOOZE SA and HUTTNER WB. Cell-free protein sorting to the regulated and constitutive secretory pathways. *Cell*, 60(5):837–47, 1990.
- TOWBIN H, STAEBELIN T and GORDON J. Immunoblotting in the clinical laboratory. *J Clin Chem Clin Biochem*, 27(8):495–501, 1989.
- TRAER CJ, RUTHERFORD AC, PALMER KJ, WASSMER T, OAKLEY J, ATTAR N, CARLTON JG, KREMERKOTHEN J, STEPHENS DJ and CULLEN PJ. SNX4 coordinates endosomal sorting of TfnR with dynein-mediated transport into the endocytic recycling compartment. *Nat Cell Biol*, 9(12):1370–80, 2007.
- TUCKER J, SCZAKIEL G, FEUERSTEIN J, JOHN J, GOODY RS and WITTINGHOFER A. Expression of p21 proteins in Escherichia coli and stereochemistry of the nucleotide-binding site. *EMBO J*, 5(6):1351–8, 1986.
- ULLRICH O, HORIUCHI H, BUCCI C and ZERIAL M. Membrane association of Rab5 mediated by GDP-dissociation inhibitor and accompanied by GDP/GTP exchange. *Nature*, 368(6467):157–60, 1994.
- UNGEWICKELL EJ and HINRICHSEN L. Endocytosis: clathrin-mediated membrane budding. *Curr Opin Cell Biol*, 19(4):417–25, 2007.
- VAN DAM EM and STOORVOGEL W. Dynamin-dependent transferrin receptor recycling by endosome-derived clathrin-coated vesicles. *Mol Biol Cell*, 13(1):169–82, 2002.
- VAN DAM EM, TEN BROEKE T, JANSEN K, SPIJKERS P and STOORVOGEL W. Endocytosed transferrin receptors recycle via distinct dynamin and phosphatidylinositol 3-kinase-dependent pathways. *J Biol Chem*, 277(50):48876–83, 2002.

- WALSENG E, BAKKE O and ROCHE PA. Major histocompatibility complex class II-peptide complexes internalize using a clathrin- and dynamin-independent endocytosis pathway. *J Biol Chem*, 283(21):14717–27, 2008.
- WASSMER T, ATTAR N, HARTERINK M, VAN WEERING JR, TRAER CJ, OAKLEY J, GOUD B, STEPHENS DJ, VERKADE P, KORSWAGEN HC and CULLEN PJ. The retromer coat complex coordinates endosomal sorting and dynein-mediated transport, with carrier recognition by the trans-Golgi network. *Dev Cell*, 17(1):110–22, 2009.
- WESSLING-RESNICK M and BRAELL WA. Characterization of the mechanism of endocytic vesicle fusion in vitro. *J Biol Chem*, 265(28):16751–9, 1990.
- WETTEY FR, HAWKINS SF, STEWART A, LUZIO JP, HOWARD JC and JACKSON AP. Controlled elimination of clathrin heavy-chain expression in DT40 lymphocytes. *Science*, 297(5586):1521–5, 2002.
- WHITEHEART SW and MATVEEVA EA. Multiple binding proteins suggest diverse functions for the N-ethylmaleimide sensitive factor. *J Struct Biol*, 146(1-2):32–43, 2004.
- WHITNEY JA, GOMEZ M, SHEFF D, KREIS TE and MELLMAN I. Cytoplasmic coat proteins involved in endosome function. *Cell*, 83(5):703–13, 1995.
- WHYTE JR and MUNRO S. Vesicle tethering complexes in membrane traffic. *J Cell Sci*, 115(Pt 13):2627–37, 2002.
- WILLIG KI, RIZZOLI SO, WESTPHAL V, JAHN R and HELL SW. STED microscopy reveals that synaptotagmin remains clustered after synaptic vesicle exocytosis. *Nature*, 440(7086):935–9, 2006.
- WYMAN MP and PIROLA L. Structure and function of phosphoinositide 3-kinases. *Biochim Biophys Acta*, 1436(1-2):127–50, 1998.

- YAO Q, CHEN J, CAO H, ORTH JD, MCCAFFERY JM, STAN RV and MCNIVEN MA. Caveolin-1 interacts directly with dynamin-2. *J Mol Biol*, 348(2):491–501, 2005.
- YARAR D, WATERMAN-STORER CM and SCHMID SL. SNX9 couples actin assembly to phosphoinositide signals and is required for membrane remodeling during endocytosis. *Dev Cell*, 13(1):43–56, 2007.
- ZERIAL M and MCBRIDE H. Rab proteins as membrane organizers. *Nat Rev Mol Cell Biol*, 2(2):107–17, 2001.
- ZHANG B, KOH YH, BECKSTEAD RB, BUDNIK V, GANETZKY B and BELLEN HJ. Synaptic vesicle size and number are regulated by a clathrin adaptor protein required for endocytosis. *Neuron*, 21(6):1465–75, 1998.
- ZHANG X, HE X, FU XY and CHANG Z. Varp is a Rab21 guanine nucleotide exchange factor and regulates endosome dynamics. *J Cell Sci*, 119(Pt 6):1053–62, 2006.
- ZWILLING D, CYPIONKA A, POHL WH, FASSHAUER D, WALLA PJ, WAHL MC and JAHN R. Early endosomal SNAREs form a structurally conserved SNARE complex and fuse liposomes with multiple topologies. *Embo J*, 26(1):9–18, 2007.

Appendix

The following program was written using Matlab (The Mathworks Inc., Natick, MA, USA) and was used to calculate the number of colocalized (double labeled/fused) or closely apposed (docked) organelles in the *in vitro* sorting/budding and docking/fusion assays and the *in vivo* colocalization assay in COS-7 cells (described in the section 2.2.7). The variables listed in the first lines are specific for the experimental conditions (such as the use of endosomes or cells, labeling efficiency of the endosomes, microscopy settings etc.) employed in this thesis. Comments explaining every programming part are indicated by the symbol “%”.

```
1 fusion_cutoff=100; %for COS7 cells:125
  filterRadiusGreen=15; %for COS7 cells:25
3 filterRadiusOrange=15; %for COS7 cells:25
  threshGreen=20; %for COS7 cells:25
5 threshOrange=18; %for COS7 cells:30
  threshBlue=15; %for COS7 cells:15
7 pixelSize=68;
  imageSizeY=1317;
9 ExclusionRadius=25;

11 root='P:\2009\sorting-and-budding';
  cellb={'ice', '37C'};
13
  % start folder loop
15 for iFolder=1:numel(cellb);
    cd(strcat(root, '\', cellb{iFolder}));
17    disp(['folder ', num2str(cellb{iFolder})]);
```

```

19     percentage = [];
        shift = [];
21     distOrange2Green = [];
        distGreen2Orange = [];
23
        % figuring out how many images are there
25     greenParam=dir('green*.tif');
        orangeParam=dir('red*.tif');
27     blueParam=dir('blue*.tif');

29     % start images loop
        for iImage=1:numel(blueParam)
31         disp(['image ', num2str(iImage)]);

33         % read images
            greenimg_orig=imread(greenParam(iImage).name);
35             orangeimg_orig=imread(orangeParam(iImage).name);
                blueimg_orig=imread(blueParam(iImage).name);
37

            % background subtraction
39             background=imopen(greenimg_orig, strel('disk',
                filterRadiusGreen));
41             greenimg=imsubtract(greenimg_orig, background);
                background=imopen(orangeimg_orig, strel('disk',
43                 filterRadiusOrange));
                    orangeimg=imsubtract(orangeimg_orig, background);
45

            % thresholding
47             green_cutoff=round(mean(mean(greenimg)))+threshGreen;
                orange_cutoff=round(mean(mean(orangeimg)))+threshOrange;
49             blue_cutoff=round(mean(mean(blueimg_orig)))+threshBlue;
                idxCutOffGreen=find(greenimg<green_cutoff);
51             greenimg(idxCutOffGreen)=0;
                idxCutOffOrange=find(orangeimg<orange_cutoff);
53             orangeimg(idxCutOffOrange)=0;
                idxCutOffBlue=find(blueimg_orig<blue_cutoff);
55             blueimg_orig(idxCutOffBlue)=0;

```

```

57  % finding the spots
    greenbwRaw=bwlabel(greenimg);
59  greenbw=bwlabel(bwmorph(greenbwRaw, 'clean'));
    orangebwRaw=bwlabel(orangeimg);
61  orangebw=bwlabel(bwmorph(orangebwRaw, 'clean'));
    bluebwRaw=bwlabel(blueimg_orig);
63  bluebw=bwlabel(bwmorph(bluebwRaw, 'clean'));

65  % determining the spot-centers
    bluex=[]; bluey=[];
67  for i=max(max(bluebw)):-1:1
        pxIdx=find(bluebw==i);
69  [y,x]=ind2sub(size(bluebw),pxIdx);
        pxIntensity=double(blueimg_orig(pxIdx));
71  bluex(i)=sum(x.*pxIntensity)/sum(pxIntensity);
        bluey(i)=sum(y.*pxIntensity)/sum(pxIntensity);
73  end;
    greenx=[]; greeny=[];
75  if (max(max(greenbw))<3000) && (max(max(greenbw))>1)
        for i=max(max(greenbw)):-1:1
77  pxIdx=find(greenbw==i);
            [y,x]=ind2sub(size(greenbw),pxIdx);
79  pxIntensity=double(greenimg(pxIdx));
            greenx(i)=sum(x.*pxIntensity)/sum(pxIntensity);
81  greeny(i)=sum(y.*pxIntensity)/sum(pxIntensity);
        end;
83  else
        continue
85  end;
    orangex=[]; orangey=[];
87  if (max(max(orangebw))<3000) && (max(max(orangebw))>1)
        for i=max(max(orangebw)):-1:1
89  pxIdx=find(orangebw==i);
            [y,x]=ind2sub(size(orangebw),pxIdx);
91  pxIntensity=double(orangeimg(pxIdx));
            orangex(i)=sum(x.*pxIntensity)/sum(pxIntensity);

```

```

93         orangey(i)=sum(y.*pxIntensity)/sum(pxIntensity);
           end;
95     else
           continue
97     end;

99     % determine bead-shift
           minDistOrangeBead_px=[]; beadIdxOrange=[];
101    orangeBeadx=[]; orangeBeady=[];
           minDistGreenBead_px=[]; beadIdxGreen=[];
103    greenBeadx=[]; greenBeady=[];
           distGreen2OrangeBeads=[];
105    if length(blueX)>=1
           nBeads=0;
107        for iBeads=1:length(blueX)
           x=blueX(iBeads);
109           y=blueY(iBeads);
           % bead distance to orange and green spots
111           distOrange=sqrt((orangex-x).^2+(orangey-y).^2);
           distGreen=sqrt((greenx-x).^2+(greeny-y).^2);
113           if (length(find(distOrange<ExclusionRadius))>1) ||
              (length(find(distGreen<ExclusionRadius))>1)
115               continue % too many spots around blue bead (within
                           ExclusionRadius) --> excluded
           end
117           nBeads=nBeads+1;
           blueXValid(nBeads)=blueX(iBeads);
119           blueYValid(nBeads)=blueY(iBeads);
           minDistOrangeBead_px(nBeads)=min(min(distOrange));
121           beadIdxOrange(nBeads)=find(distOrange==
              minDistOrangeBead_px(nBeads));
           orangeBeadx(nBeads)=orangex(beadIdxOrange(nBeads));
123           orangeBeady(nBeads)=orangey(beadIdxOrange(nBeads));
           % bead distance to green spots
125           minDistGreenBead_px(nBeads)=min(min(distGreen));
           beadIdxGreen(nBeads)=find(distGreen==
              minDistGreenBead_px(nBeads));

```

```

127         greenBeadx(nBeads)=greenx ( beadIdxGreen (nBeads) );
        greenBeady(nBeads)=greeny ( beadIdxGreen (nBeads) );
129     % distance between green and orange beads
        distGreen2OrangeBeads(nBeads)=sqrt (( greenBeadx(nBeads)-
            orangeBeadx(nBeads) ).^2+( greenBeady(nBeads)-
            orangeBeady(nBeads) ).^2 );
131     end

133     distGreen2OrangeBeadsAV=distGreen2OrangeBeads-
        mean( distGreen2OrangeBeads );
135     ChosenBead=find ( distGreen2OrangeBeadsAV<3 &
        distGreen2OrangeBeads<25 );
137     if ~isempty( ChosenBead )
        ChosenBead=ChosenBead(1); % if more beads fulfill the
            requirements
139     else
        continue
141     end

143     shiftx=greenBeadx( ChosenBead)-orangeBeadx( ChosenBead );
        shifty=greenBeady( ChosenBead)-orangeBeady( ChosenBead );
145     shiftBx=greenBeadx( ChosenBead)-bluexValid( ChosenBead );
        shiftBy=greenBeady( ChosenBead)-blueyValid( ChosenBead );
147     abs_shift=sqrt( shiftx^2 + shifty^2 );
        disp( [ 'shift: ', num2str( abs_shift ), 'px' ] );
149     shift(end+1,:)=[shiftx , shifty , abs_shift ];
        orangex=orangex+shiftx ;
151     orangey=orangey+shifty ;
        minDistOrangeBead_px2 = []; beadIdxOrange2 = [];
153     minDistGreenBead_px2 = []; beadIdxGreen2 = [];
        for iBeads=length( bluex ): -1:1
155         x=bluex( iBeads );
            y=bluey( iBeads );
157         % bead distance to orange and green spots
            distOrange=sqrt (( orangex-x-shiftBx ).^2+
159                 ( orangey-y-shiftBy ).^2 );
            distGreen=sqrt (( greenx-x-shiftBx ).^2+

```

```

161         (greeny-y-shiftBy).^2);
        minDistOrangeBead_px2(iBeads)=min(min(distOrange));
163         beadIdxOrange2(iBeads)=find(distOrange==
            minDistOrangeBead_px2(iBeads));
        minDistGreenBead_px2(iBeads)=min(min(distGreen));
165         beadIdxGreen2(iBeads)=find(distGreen==
            minDistGreenBead_px2(iBeads));

        end

167         orangex(beadIdxOrange2) = [];
        orangey(beadIdxOrange2) = [];
169         greenx(beadIdxGreen2) = [];
        greeny(beadIdxGreen2) = [];

171     else
        continue
173     end

175     % create mirror images
        greenxMirror=greenx;
177         greenyMirror=imageSizeY-greeny;
        orangexMirror=orangex;
179         orangeyMirror=imageSizeY-orangey;

181     % distance green to orange
        minDistGreen_px = []; minDistGreenMirror_px = [];
183     for iSpots=length(greenx):-1:1
        x=greenx(iSpots);
185         y=greeny(iSpots);
        dist=sqrt((orangex-x).^2+(orangey-y).^2);
187         distMirror=sqrt((orangexMirror-x).^2+
            (orangeyMirror-y).^2);
189         minDistGreen_px(iSpots)=min(min(dist));
        minDistGreenMirror_px(iSpots)=min(min(distMirror));
191     end;
        minDistGreen_nm=minDistGreen_px*pixelSize;
193         minDistGreenMirror_nm=minDistGreenMirror_px*pixelSize;
        siz=size(distGreen2Orange,1);

```



```

195     distGreen2Orange ( siz +1: siz+length (minDistGreen_nm) ,1)=
        minDistGreen_nm ;
    distGreen2Orange ( siz +1: siz+length (minDistGreen_nm) ,2)=iImage ;
197     % fusion detection green to orange
    idxFusionGreen=find (minDistGreen_nm<fusion_cutoff) ;
199     percentage (end+1,1)=length (idxFusionGreen) *100/
        (length (minDistGreen_nm) ) ;
201     idxFusionGreenMirror=find (minDistGreenMirror_nm<fusion_cutoff) ;
    percentage (end,2)=length (idxFusionGreenMirror) *100/
203         (length (minDistGreenMirror_nm) ) ;

205     % distance orange to green
    minDistOrange_px = [] ; minDistOrangeMirror_px = [] ;
207     for iSpots=length (orangex) : -1:1
        x=orangex (iSpots) ;
209         y=orangey (iSpots) ;
        dist=sqrt (( greenx-x) .^2+(greeny-y) .^2) ;
211         distMirror=sqrt (( greenxMirror-x) .^2+(greenyMirror-y) .^2) ;
        minDistOrange_px (iSpots)=min (min (dist) ) ;
213         minDistOrangeMirror_px (iSpots)=min (min (distMirror) ) ;
    end ;
215     minDistOrange_nm=minDistOrange_px *pixelSize ;
    minDistOrangeMirror_nm=minDistOrangeMirror_px *pixelSize ;
217     siz=size (distOrange2Green ,1) ;
    distOrange2Green ( siz +1: siz+length (minDistOrange_nm) ,1)=
219         minDistOrange_nm ;
    distOrange2Green ( siz +1: siz+length (minDistOrange_nm) ,2)=
221         iImage ;
    % fusion detection orange to green
223     idxFusionOrange=find (minDistOrange_nm<fusion_cutoff) ;
    percentage (end,3)=length (idxFusionOrange) *100/
225         (length (minDistOrange_nm) ) ;
    idxFusionOrangeMirror=find (minDistOrangeMirror_nm<
227         fusion_cutoff) ;
    percentage (end,4)=length (idxFusionOrangeMirror) *100/
229         (length (minDistOrangeMirror_nm) ) ;

```

```

231 end; %images loop (iImage)

233 % output files
percnames={'Green_to_Orange', 'Green_to_Orange_Mirror',
235 'Orange_to_Green', 'Orange_to_Green_Mirror'};
xlswrite(strcat(num2str(fusion_cutoff), 'percentages.xls'),
237 percnames, 1, 'A1');
xlswrite(strcat(num2str(fusion_cutoff), 'percentages.xls'),
239 percentage, 1, 'A2');
dlmwrite('all_distances_from_green.txt', distGreen2Orange);
241 dlmwrite('all_distances_from_orange.txt', distOrange2Green);
shiftnames={'x_shift [px]', 'y_shift [px]', 'abs_shift [px]'};
243 xlswrite(strcat(num2str(fusion_cutoff), 'shift_new.xls'),
shiftnames, 1, 'A1');
245 xlswrite(strcat(num2str(fusion_cutoff), 'shift.xls'), shift, 1, 'A2');

247 % histograms
x=0:25:10000;
249 histograms(:,3)=hist(distOrange2Green(:,1),x)*100/
length(distOrange2Green(:,1));
251 histograms(:,2)=hist(distGreen2Orange(:,1),x)*100/
length(distGreen2Orange(:,1));
253 histograms(:,1)=x';
dlmwrite('all_histograms.txt', histograms);
255 histnames={'x', 'Green_to_Orange', 'Orange_to_Green'};
xlswrite('all_histograms.xls', histnames, 1, 'A1');
257 xlswrite('all_histograms.xls', histograms, 1, 'A2');

259 end %iFolder

```

Acknowledgements

First of all, I want to thank my supervisor Prof. Reinhard Jahn for his support and his trust in my abilities. It was an honor to be part of the excellent working environment in his lab and I greatly enjoyed to be involved in the “academic life”, such as teaching activities and many conferences.

I am deeply grateful to Dr. Silvio Rizzoli for his endless support and care - at any time throughout the past three years. He taught me everything that is required for being a good scientist, not only experimentally, but also in writing manuscripts and reviewing papers. Thank you Silvio, it was a real pleasure to have worked with you!

I thank Prof. Brose and Prof. Thumm for being part of my thesis committee and for their comments and ideas during the committee meetings.

Many thanks to Dr. Steffen Burkhardt, Ivana Bacakova and Kerstin Grüniger from the “Molecular Biology” Program for their support and the excellent environment they created for the PhD students.

I want to thank all my colleagues from the department of Neurobiology for creating an enjoyable working atmosphere. Special thanks to Gottfried for his daily help in the lab.

During my time at the lab I met people who influenced me, not only scientifically, but also personally - Matias, Nickias, Pawel, Nathan and Dagmar, thank you for your friendship! And to my dear friend Ioanna who had a special role throughout this time: thank you so much for always being there for me - inside and outside the lab. I will never forget our endless conversations at lunch, in the cell culture and during felting and Greek cooking sessions!

Many thanks to my labrotation students Shweta, Jenny, Caroline and Julia for their commitment and good work.

I thank the Society of General Physiologists, the FEBS Organization, the Protein Society and the EMBO Organization for financially supporting interesting and inspiring meetings in Woods Hole, Pavia, Boston and Cargèse.

I am grateful to my parents for their support and love. They accompanied my way from the beginning and made me to what I am.

Finally, I want to thank my wonderful husband Christian who was there for me whenever I needed him. Thank you so much for supporting - and extending upon - my dreams, for your constant belief and trust in me - and for your love during all those years!

Curriculum Vitae

Personal Information

Sina-Victoria Barysch
Adress Karolinenweg 31
37075 Göttingen
Germany
Email sbarysc@gwdg.de
Date of Birth January 5, 1983
Nationality German

Education

Max-Planck-Institute for Biophysical Chemistry
2006 - 2009 PhD in the Department of Neurobiology
Thesis: "Investigation of early endosomal sorting and budding"
Georg August University Göttingen, Germany
2005 - 2006 Molecular Biology (MSc/PhD program - International Max
Planck Research School)
Dresden University of Technology, Germany
2002 - 2005 Molecular Biotechnology (BSc)
Thesis: "Characterization of estrogen responsiveness of the
mammary epithelial cell line HC11 during different stages of dif-
ferentiation"

Teaching

Tutor of Lectures

2007 - 2009 “Protein Sorting and Processing”, “Vesicular Transport” and “Organelle Biosynthesis” within the International MSc/PhD Programs “Molecular Biology” and “Neurosciences”

Supervisor of Labrotations

2008 - 2009 Shweta Aggarwal, Caroline von Spee and Julia Cajan within the International MSc/PhD Program “Molecular Biology”
Jennifer Seefeldt within her BSc studies in Biology

Tutor of Methods Courses

2008 - 2009 “Subcellular Fractionation and Centrifugation” within the International MSc/PhD Program “Molecular Biology”

Honors and Awards

2005 - present Max Planck Society (MSc and PhD stipend)

2009 Protein Science Young Investigator Travel Grant / The Protein Society Finn Wold Travel Award (travel stipend)

2009 EMBO grant (travel stipend)

2008 FEBS YTF grant (travel stipend)

2007 Society of General Physiologists (travel stipend)

2004 German Academic Exchange Service (DAAD) (undergraduate travel stipend)

Conferences

- 2009 “Proteins in Motion” - 23rd Symposium of The Protein Society, Boston, MA, USA (invited talk)
- 2009 FEBS-EMBO Advanced Lecture Course “Molecular and Cellular Membrane Biology”, Cargèse, France (poster)
- 2008 The Golgi meeting: “Membrane trafficking in global cellular responses”, Pavia, Italy (poster)
- 2008 6th Life Science Day, Weizmann Institute, Rehovot, Israel (poster)
- 2008 SFB Symposium: “Intracellular Transport and Trafficking”, Göttingen, Germany (poster)
- 2007 61st Annual Meeting of the Society of General Physiologists: “Membrane Biophysics of Fusion, Fission, and Rafts in Health and Disease”, Woods Hole, MA, USA (poster)

Extracurricular Activities

Student representative

- 2007 - 2009 International MSc/PhD Program “Molecular Biology”, Georg August University Göttingen, Germany

Co-Organizer

- 2007 - 2009 4th and 5th International PhD Student Symposium: “Horizons in Molecular Biology”, Göttingen, Germany